論文 / 著書情報
Article / Book Information

題目(和文)	
Title(English)	Use of Seasonal Streamflow Forecast to Support Reservoir Operation for Flood Mitigation in the Chao Phraya River Basin
著者(和文)	KOMPORWONGNARIN
Author(English)	Wongnarin Kompor
出典(和文)	学位:博士(学術), 学位授与機関:東京工業大学, 報告番号:甲第12014号, 授与年月日:2021年3月26日, 学位の種別:課程博士, 審査員:鼎 信次郎,竹村 次朗,吉村 千洋,藤井 学,木内 豪
Citation(English)	Degree:Doctor (Academic), Conferring organization: Tokyo Institute of Technology, Report number:甲第12014号, Conferred date:2021/3/26, Degree Type:Course doctor, Examiner:,,,,
学位種別(和文)	博士論文
Type(English)	Doctoral Thesis

Use of Seasonal Streamflow Forecast to Support Reservoir Operation for Flood Mitigation in the Chao Phraya River Basin

Wongnarin Kompor

February 2021

Summary

In 2011, catastrophic flooding occurred in Thailand. From May until October 2011 the country experienced heavy rainfall as a result of five typhoons. This rainfall was estimated to total 1439 mm or about 143% of the average rainy season rainfall from 1982 to 2002. This flood caused substantial damage to the Thai economy and society. The capital city, Bangkok, and industrial areas were inundated from August until December, which caused the Thai economy to lose about USD 45 billion. Because of a lack of information on future rainfall, there was no plan for this unexpectedly severe rainfall event, which affected the Chao Phraya River Basin (CPRB). Thus, two large reservoirs located behind the Bhumibol and Sirikit dams were unable to mitigate the flooding.

A previous study by Mateo et al. [Mateo et al., 2014] proposed a useful operation scheme for flood mitigation. However, they still did not consider seasonal streamflow prediction. The simulated results of their study show that flood mitigation in 2011 could be achieved by proposing an alternative reservoir operation. Their alternative reservoir operation was different by controlling the storage of the target dams. In reality, water managers cannot set target storage levels at the beginning of the wet season without predictive information and water demand; in addition, climatic factors are uncertain. Therefore, to predict seasonal streamflow while accounting for reservoir operation, this study aims to update and develop a method for using seasonal streamflow predictive data to support adaptive reservoir operation. Thus, the objective of this study is to demonstrate the use of streamflow predictive information for adaptive reservoir operation with the aim of mitigating the flood in the CPRB, especially the 2011 flood year. This thesis consists of 5 chapters as follows.

Chapter 1 presents the introduction of this study. Background, research motivation, literature reviews, and research objectives are presented in this chapter.

Chapter 2 presents the details of the study area, hydrological model, and data in this study. Furthermore, two major reservoirs that have an impact on the Chap Phraya River Basin are shown in this chapter. Next, this chapter shows the details of the hydrological model that used in this study. Lastly, the details of observed meteorological data and

predictive data that are used as input data in the H08 model are shown in this chapter.

Chapter 3 and chapter 4 presents the method and results using seasonal predictive data to support reservoir operation in this study. There are two main methods for using seasonal predictive data. The model H08, a distributed hydrological model with a reservoir module, was used to obtain predictions of river discharge and reservoir storage for both methods with a 6-month prediction period.

Chapter 3, the first method is to select the reservoir operation from the streamflow prediction at the beginning of the wet season. There are three alternative operations for the first method, which was presented in the previous study [Mateo et al., 2014]. Seasonal hydrological predictions were carried out by using European Centre for Medium - Range Weather Forecasts (ECMWF) seasonal precipitation predictive data with two different bias correction techniques. Most of the results of streamflow prediction lead to select the 2011 operation as the reservoir operation scheme in 2011, which cannot mitigate flood in 2011. However, one simulation by quantile mapping, out of 25 ensemble members, that selected the alternative operation that could mitigate flooding during the peak period in October with a lesser peak amount of about 18 percent.

Chapter 4, the second method was updated from the first method, which can be considered as an adaptive reservoir operation. The 6-month ECMWF prediction period was used to support the operation plan for mitigating flooding in the 2011 flood year around each reservoir during the wet season. Decision-making for reservoir operation based on seasonal predictions was conducted on a monthly time scale. There are two different operating plans to compare river discharge results for this method. The first (PlanU) was simply to follow the 2011 operation schedule, which followed the 2011 rule curve. The second (PlanM) resembled reservoir operations described in a previous study, in which the maximum target storage in 2011 was reduced. The results for river discharge based on seasonal predictions obtained using PlanU showed that seasonal predictive information could be useful for flood mitigation and slightly decreased the peak river discharge, by about 4%, for 2011. In contrast, the results for PlanM showed that peak river discharge was reduced by about 20% relative to the observed 2011 river discharge. The reservoir operation under PlanM, which set target storage levels for each reservoir, tended to make each reservoir release its storage earlier than those under PlanU. That is, a combination of seasonal prediction and PlanM best-mitigated flooding. In addition, the use of seasonal predictive data for adaptive reservoir operation in 1995 and the use of past rainfall data for adaptive reservoir operation in 2011 was investigated in this study. The results show that both cases could mitigate floods in 1995 and 2011.

Chapter 5 presents the conclusion of this study. As a whole, the simulation results of the second method of using predictive data in this study show that the prediction data could mitigate flood in 2011. However, there is some aspect that needs to point out in this study, which needs to be further study in the future. First, the current method needs to investigate whether the seasonal predictive data could mitigate for a drought year. Second, the current parameters were calibrated from the previous study to well represent the hydrological process in the Chao Phraya River Basin, especially at station C2. However, the accuracy of river discharge at station N1 (Nan basin) was still not satisfactory, which is also mentioned in the previous study [Mateo et al., 2014]. Finally, the high accuracy of seasonal predictive data, especially at the beginning of the wets season, is still necessary for reservoir operation in order to give the most benefit to society. Most of the results show that the release rate was increased during August in both reservoirs. In reality, the river channel capacity was not allowed to increase the rate of release during August in Nan river.

Table of Contents

Summary i

Table of Contents iv

List of Figures vi

List of Tables xiii

Chapter 1 Introduction 1

Chapter 2 Study Area, Hydrological model and Data...10

2.1 Study Area 10

2.2 Hydrological model 18

2.2.1 Overview of the H08 model 18

2.2.2 Land surface model 21

2.2.3 River model 23

2.2.4 Reservoir operation model 25

2.2.5 General setting...27

2.3 Data...33

2.3.1 Observed dataset...33

2.3.2 Predictive data 36

Chapter 3 Selecting Reservoir Operation Scheme from Seasonal Streamflow Prediction..39

3.1 Model calibration and verification 39

3.2 Bias correction...52

3.3 Setting the criteria to select reservoir scheme 53

3.4 Result and discussion 58

3.4.1 Using the bias correction method to improve the accuracy of rainfall prediction...58

3.4.2 Simulation of streamflow prediction in 2011..60

3.4.3 Impact of seasonal streamflow prediction on reservoir operation.............61

3.5 Conclusion 64

Chapter 4 Use of Seasonal Streamflow Forecasts for Flood Mitigation with Adaptive Reservoir Operation 67

4.1 Methodology for using predictive data to support reservoir operation 68

4.1.1 Hydrological model and data 68

4.1.2 Adaptation of reservoir operation based on predictive data 69

4.2 Results and discussion 75

4.2.1 Reliability of the predictive data 75

4.2.2 Adaptive operation using predictive data 79

4.2.3 Adaptive operation using predictive data based on PlanM operation 85

4.2.4 Sensitivity test on adaptive operation using predictive data 90

4.2.5 Adaptive reservoir operation on flood mitigation 96

4.3 Conclusion 106

Chapter 5 Conclusions 108

Appendix A 114

Appendix B 123

Appendix C 136

Appendix D 139

Reference 158

List of Figures

1.1 Number of natural disasters in the world..2

1.2 Global reported natural disasters by type from 1970 to 2019 3

1.3 Characteristic of Thailand climates (a) and Track of Tropical cyclone in 2011 (b) 4

1.4 Water storage at Bhumibol dam (a) and Sirikit dam (b) in 2011 6

2.1.1 Chao Phraya River Basin...13

2.1.2 River diagram of the Chao Phraya River Basin 14

2.1.3 Average 30-year (1981-2010) river discharge at station C2 and rainfall................15

2.2.1 The six model in the H08 model 19

2.2.2 Schematic diagram of the land processes model in the H08 model 23

2.2.3 Schematic diagram of the river model in the H08 model.......................................24

2.2.4 Algorithms used for reservoir storage constraints and reservoir releases for the locally adapted and alternative reservoir operation schemes 26

2.2.5.1 Sensitivity test of bulk transfer coefficient...31

2.2.5.2 Sensitivity test of soil depth 32

2.2.5.3 Sensitivity test of daily maximum surface runoff 32

2.2.5.4 Sensitivity test of shape parameter 32

2.3.1 Scatter plot of T12 rainfall data and observed rainfall (in mm/month) from rain gauge station in the Chao Phraya River Basin from 1981 to 2011 (a) Comparison of T12 rainfall and observed rainfall...35

3.1.1 Comparison of the naturalized river discharge (a) and scatter plot (b) between observation and simulation at C2 station on monthly scale from 1981 to 2004 42

3.1.2 Comparison of the monthly river discharge (a) and scatter plot (b) between observation and simulation at station C2 from 1981 to 2004...43

3.1.3 Comparison of the daily river discharge (a) and scatter plot (b) between observation and simulation at station C2 from 2010 to 2011...44

3.1.4 Comparison of the daily river discharge (a) and scatter plot (b) between observation and simulation at station C2 from 2010 to 2011...45

3.1.5 Comparison of the monthly river discharge (a) and scatter plot (b) between observation and simulation at station P1 from 1981 to 2004 46

3.1.6 Comparison of the monthly river discharge (a) and scatter plot (b) between observation and simulation at station P1 from 1981 to 2004 47

3.1.7 Comparison of daily outflow at station P2A (a) and station N12A (b) between observation data (black line) and simulation data (red line) 49

3.1.8 Comparison of daily dam storage at Bhumibol (a) and Sirikit reservoir (b) between observation (black line) and simulation (red line)..50

3.1.9 Comparison of daily inflow at station P1 (a) and station N1 (b) between observation data (black line) and simulation data (red line) 51

3.2.1 Conceptual image of quantile mapping technique 53

3.3.1 Algorithms used for reservoir storage constraints for an alternative reservoir scheme 54

3.3.2 Example of selecting reservoir operation from streamflow prediction 57

3.3.3 Example of river discharge with selecting reservoir operation from streamflow prediction (red line) and without setting the criteria to select reservoir operation (green line)..57

3.4.1.1 Average seasonal rainfall prediction during August, September, and October from 1993 to 2016 (a) raw (b) bias-corrected by quantile mapping rainfall prediction compares with average observed rainfall. The red box represents the range of standard deviation of prediction data, and blue triangle shows observed rainfall data. Each point represents the average rainfall data from August to October 59

3.4.2.1 Streamflow prediction in 2011. The red box shows the deviation of prediction results. Blue line shows the observed river discharge in 2011. Black line shows the 30-year average of natural flow during August, September, and October in CPRB. Dot red color represents each 25-predictions results..61

3.4.3.1 Dam storage of (a) Bhumibol and (b) Sirikit reservoir in 2011 by PlanU (Red line), Rev0.5Jul (Blue line) and Rev0.25Jul (Green line) scheme..63

3.4.3.2 Comparison of daily river discharge at C2 station in 2011 be-tween observed river discharge (Black line), simulation using PlanU (Red line), Rev0.5Jul (Blue line) and Rev0.25Jul (Green line) scheme..64

3.4.3.3 Comparison of daily outflow at Bhumibol reservoir in 2011 between observed river discharge (Black line), simulation using PlanU (Red line), Rev0.5Jul (Blue line) and Rev0.25Jul (Green line) scheme..64

3.4.3.4 Comparison of daily outflow at Sirikit reservoir in 2011 between observed river discharge (Black line), simulation using PlanU (Red line), Rev0.5Jul (Blue line) and Rev0.25Jul (Green line) scheme..65

4.1.2.1 Reservoir operation that used in this chapter; PlanU (red line), and PlanM (yellow line)..70

4.1.2.2 Image of operation plan setting in this chapter.. 72-73

4.1.2.3 Method of using predictive information to support operation in this chapter.....74

4.2.1.1 Comparison of daily discharge at station C2 between observations (black line), simulation results (red line), simulation results using ensemble predicted rainfall data (light blue dotted line), and the median of simulation data using ensemble predicted rainfall data (blue line). Simulation results using (a) the original European Centre for Medium - Range Weather Forecasts (ECMWF) System 5 ensemble predicted data and (b) bias-corrected ensemble predictions 77

4.2.1.2 Scatter plot of accuracy indices between simulated daily discharge using the original predicted data (x-axis) and simulated daily discharge using quantile mapping (y-axis). (a) Root mean square error (RMSE); (b) coefficient of variation of the RMSE (CV); (c) relative mean error (RME); (d) Nash–Sutcliffe model efficiency coefficient (NSE); (e) coefficient of determination (R2); (f) correlation coefficient (CC)................................78

4.2.2.1 River discharge at station C2 (a) and reservoir storage predictions (green line) from June until December at the Bhumibol (b) and Sirikit (c) reservoir. Blue line represents simulation using observed meteorological data (hindcast). Black dashed line represents rule curve. Dash-point black line represents maximum storage capacity......81

4.2.2.2 River discharge predictions at station C2 (a) and storage predictions from July until December at the Bhumibol (b) and Sirikit (c) reservoir, shown with the green line, and river discharge and storage prediction after adaptive operation with predictive data from July until December (red dashed line)..82

4.2.2.3 River discharge predictions at C2 station (a) and storage predictions from August until December at the Bhumibol (b) and Sirikit (c) reservoir, shown with the green line, and river discharge and storage predictions after adaptive operation with predictive data from August until December (red dashed line) 83

4.2.2.4 River discharge predictions at C2 station (a) and storage predictions from September until December at the Bhumibol (b) and Sirikit (c) reservoir, shown with the green line, and river discharge and storage predictions after adaptive operation with predictive data from September until December (red dashed line)................................84

4.2.3.1 River discharge predictions at station C2 (a) and storage predictions from July until December at the Bhumibol (b) and Sirikit (c) reservoir, shown with the green line, and river discharge and storage predictions after adaptive operation with predictive data from July until December (orange dashed line) 87

4.2.3.2 River discharge predictions at station C2 (a) and storage predictions from August until December at the Bhumibol (b) and Sirikit (c) reservoir, shown with the green line, and river discharge and storage prediction after adaptive operation with prediction data from August until December (orange dashed line)...88

4.2.3.3 River discharge prediction at station C2 (a) and storage prediction from September until December at the Bhumibol (b) and Sirikit (c) reservoir, shown with the green line, and river discharge and storage prediction after adaptive operation with predictive data from September until December (orange dashed line) 89

4.2.4.1.1 River discharge prediction at station C2 (a) and storage prediction from August until December at the Bhumibol (b) and Sirikit (c) reservoir, shown with the green line, and river discharge and storage prediction after adaptive operation with predictive data from August until December (red dashed line) 91

4.2.4.1.2 River discharge prediction at station C2 (a) and storage prediction from September until December at the Bhumibol (b) and Sirikit (c) reservoir, shown with the green line, and river discharge and storage prediction after adaptive operation with predictive data from September until December (red dashed line) 92

4.2.4.2.1 River discharge prediction at station C2 (a) and storage prediction from August until December at the Bhumibol (b) and Sirikit (c) reservoir, shown with the green line, and river discharge and storage prediction after adaptive operation with predictive data from August until December (red dashed line) 94

4.2.4.2.2 River discharge prediction at station C2 (a) and storage prediction from September until December at the Bhumibol (b) and Sirikit (c) reservoir, shown with the green line, and river discharge and storage prediction after adaptive operation with predictive data from September until December (red dashed line) 95

4.2.5.1 Comparison of river discharge, showing simulated discharge with PlanU operation in 2011 (green line), simulated discharge with PlanM operation in 2011 (blue line), and simulated discharge: (1) after adaptive operation based on 2011 operations using seasonal predictive data (red line) and (2) after adaptive operation based on PlanM using predictive data (orange line) 98

4.2.5.2 Comparison of peak discharge (blue bar color) and percentage of peak discharge different from simulation (red bar color) between peak simulated discharge using PlanU operation and simulated discharge using PlanM operation in 2011 and simulated discharge: (1) after adaptive operation using predictive data and (2) after adaptive operation using predictive data by PlanM 98

4.2.5.3 Comparison of outflow, showing simulated outflow using PlanU operation in 2011 (green line) and simulated discharge using PlanM operation in 2011 (blue line): (1) after adaptive operation using predictive data based on 2011 operations (red line) and (2) after adaptive operation using predictive data based on PlanM (yellow line).......................100

4.2.5.4 Comparison of outflow between simulated discharge using PlanU operation in 2011 (green line) and simulated discharge using PlanM operation in 2011 (blue line): (1) after adaptive operation using predictive data based on 2011 operations (red line): and (2) after adaptive operation using predictive data based on PlanM (yellow line). The yellow dash line shows the target storage of PlanM in this study..101

4.2.5.5 Comparison of daily discharge at P12C (a) and N8 station (b), showing simulated daily discharge using PlanU operation in 2011 (green line) and simulated discharge using PlanM operation in 2011 (blue line): (1) after adaptive operation using predictive data based on 2011 operations (red line) and (2) after adaptive operation using predictive data based on PlanM (yellow line)...102

4.2.5.6 Comparison of river discharge, showing simulated discharge with PlanU operation in 2011 (green line), simulated discharge with PlanU with 40% operation in 2011 (orange line), and simulated discharge with PlanU with 60% operation in 2011 (blue line). 103

4.2.5.7 Comparison of outflow at Bhumibol and Sirikit reservoir, showing simulated outflow with PlanU operation in 2011 (green line), simulated discharge with PlanU with 40% operation in 2011 (orange line), and simulated discharge with PlanU with 60% operation in 2011 (blue line).. 104

4.2.5.8 Comparison of dam storage at Bhumibol and Sirikit reservoir, showing simulated dam storage with PlanU operation in 2011 (green line), simulated dam storage with PlanU with 40% operation in 2011 (orange line), and simulated discharge with PlanU with 60% operation in 2011 (blue line).. 105

A1 The accuracy of raw seasonal rainfall prediction for each initial month (a) February (b) May (c) August and (d) November as initial month 116

A2 The accuracy of bias-corrected seasonal rainfall prediction for each initial month (a) February (b) May (c) August and (d) November as initial month........................ 117

A3 The accuracy of river discharge prediction for each initial month (a) February (b) May (c) August and (d) November as initial month 119

A4 Difference accuracy of river discharge prediction between K10 and seasonal rainfall prediction as input data to H08 mode for each initial month (a) February (b) May (c) August and (d) November as initial month 119-120

A5 River discharge simulation using bias-corrected rainfall prediction of 1 to 3 months lead time as input data from 1982 to 2004 121

A6 The accuracy of river discharge simulation using bias-corrected rainfall as input after postprocessing (a) February (b) May (c) August and (d) November as an initial month for prediction.. 122

A7 River discharge simulation for each initial month.. 122-123

B1 Anomalies of original ECMWF rainfall prediction from June to December (1993-2016); rainfall prediction on June (a); July(b); August (c); September (d); October (e); November (f); December (g) 124

B2 Anomalies of bias-corrected (quantile mapping) ECMWF rainfall prediction from June to December (1993-2016); rainfall prediction on June (a); July(b); August (c); September (d); October (e); November (f); December (g).. 125

B3 Anomalies of original ECMWF rainfall prediction from July to January (1993-2016); rainfall prediction on July(a); August (b); September (c); October (d); November (e); December (f); January (g).. 126

B4 Anomalies of bias-corrected (quantile mapping) ECMWF rainfall prediction from July to January (1993-2016); rainfall prediction on July(a); August (b); September (c); October (d); November (e); December (f); January (g) 127

B5 Anomalies of original ECMWF rainfall prediction from August to February (1993-2016); rainfall prediction on August (a); September (b); October (c); November (d); December (e); January (f); February (g)..128

B6 Anomalies of bias-corrected (quantile mapping) ECMWF rainfall prediction from August to February (1993-2016); rainfall prediction on August (a); September (b); October (c); November (d); December (e); January (f); February (g) 129

B7 Anomalies of original ECMWF rainfall prediction from September to March (1993-2016); rainfall prediction on September (a); October (b); November (c); December (d); January (e); February (f); March (g) 130

B8 Anomalies of bias-corrected (quantile mapping) ECMWF rainfall prediction from September to March (1993-2016); rainfall prediction on September (a); October (b); November (c); December (d); January (e); February (f); March (g)............................131

B9 Anomalies of original ECMWF rainfall prediction from October to April (1993-2016); rainfall prediction on October (a); November (b); December (c); January (d); February (e); March (f); April (g) 132

B10 Anomalies of bias-corrected (quantile mapping) ECMWF rainfall prediction from October to April (1993-2016); rainfall prediction on October (a); November (b); December (c); January (d); February (e); March (f); April (g).....................................133

C1 Comparison of daily rainfall data, showing observed rainfall (blue line), ensemble seasonal rainfall predictions (light pink dashed line), and average ensemble seasonal rainfall prediction (pink line). Rainfall predictions from (a) June until December 2011, (b) July until December 2011, (c) August until December 2011, and (d) September until December 2011 137

C2 Scatter plot of monthly rainfall data, showing observed rainfall (y-axis) and average rainfall prediction (x-axis) with ensemble seasonal rainfall predictions (colored lines). Rainfall predictions for (a) June 2011, (b) July 2011, (c) August 2011, (d) September 2011, and (e) October 2011 138

D1 River discharge predictions at station C2 (a) and storage predictions from June until December at the Bhumibol (b) and Sirikit (c) reservoir, shown with the green line, and river discharge and storage prediction after adaptive operation with predictive data from June until December (red dashed line) 141

D2 River discharge predictions at station C2 (a) and storage predictions from July until December at the Bhumibol (b) and Sirikit (c) reservoir, shown with the green line, and river discharge and storage prediction after adaptive operation with predictive data from July until December (red dashed line)..142

D3 River discharge predictions at C2 station (a) and storage predictions from August until December at the Bhumibol (b) and Sirikit (c) reservoir, shown with the green line, and river discharge and storage predictions after adaptive operation with predictive data from August until December (red dashed line)...143

D4 River discharge predictions at C2 station (a) and storage predictions from September until December at the Bhumibol (b) and Sirikit (c) reservoir, shown with the green line, and river discharge and storage predictions after adaptive operation with predictive data from September until December (red dashed line)..144

D5 River discharge at station C2 (a) and reservoir storage predictions (green line) from June until December at the Bhumibol (b) and Sirikit (c) reservoir. Blue line represents simulation using observed meteorological data (hindcast). Black dashed line represents rule curve. Dash-point black line represents maximum storage capacity 146

D6 River discharge predictions at station C2 (a) and storage predictions from July until December at the Bhumibol (b) and Sirikit (c) reservoir, shown with the green line, and river discharge and storage prediction after adaptive operation with predictive data from July until December (red dashed line)..147

D7 River discharge predictions at C2 station (a) and storage predictions from August until December at the Bhumibol (b) and Sirikit (c) reservoir, shown with the green line, and river discharge and storage predictions after adaptive operation with predictive data from August until December (red dashed line) 148

D8 River discharge predictions at C2 station (a) and storage predictions from September until December at the Bhumibol (b) and Sirikit (c) reservoir, shown with the green line, and river discharge and storage predictions after adaptive operation with predictive data from September until December (red dashed line)...149

D9 Comparison of river discharge, showing simulated discharge with PlanU operation in 1995 (green line), and simulated discharge after adaptive operation based on rule curve using seasonal predictive data (red line)...150

D10 Comparison of outflow, showing simulated outflow using PlanU operation in 2011 (green line) and simulated discharge using PlanM operation in 2011 (blue line): (1) after adaptive operation using predictive data based on 2011 operations (red line) and (2) after adaptive operation using predictive data based on PlanM (yellow line).......................151

D11 Comparison of outflow between simulated discharge using PlanU operation in 1995 (green line) and simulated discharge after adaptive operation using predictive data based on 1995 operations (red line)...152

D12 Comparison of peak discharge (blue bar color) and percentage of peak discharge different from simulation (red bar color) between peak simulated discharge using PlanU and simulated discharge after adaptive operation using predictive data 153

D13 Comparison of river discharge, showing simulated discharge with PlanU operation in 2011 (green line), after adaptive operation based on 2011 operations using seasonal predictive data (red line) and past rainfall data (purple dash line), with Rev0.5Jul (blue dash line), and with Rev0.25Jul (yellow dash line)..154

D14 Comparison of outflow, showing simulated outflow using PlanU operation in 2011 (green line), after adaptive operation based on 2011 operations using seasonal predictive data (red line), and past rainfall data (purple dash line), with Rev0.5Jul (blue dash line), and with Rev0.25Jul (yellow dash line) 155

D15 Comparison of dam storage between simulated discharge using PlanU operation in 2011 (green line) and simulated discharge after adaptive operation using predictive data based on 2011 operations (red line), and past rainfall data (purple dash line), with Rev0.5Jul (blue dash line), and with Rev0.25Jul (yellow dash line) 156

D16 Comparison of river discharge, showing simulated discharge at station P12C (a) and N8 (b) with PlanU operation in 2011 (green line), after adaptive operation based on 2011 operations using seasonal predictive data (red line) and past rainfall data (purple dash line), with Rev0.5Jul (blue dash line), and with Rev0.25Jul (yellow dash line)...........157

List of Tables

2.1.1 Water demand in Chao Phraya River Basin 15

2.1.2 Bhumibol dam features and properties 16

2.1.3 Sirikit dam features and properties 17

2.2.1 Four parameters mainly affecting the land surface model 28

2.3.1 Detail of T12 data 35

2.3.2 Summary of data in this study 38

3.1.1 Location of the stations used for validation 42

3.3.1 Parameter values used in reservoir operation 56

3.4.3.1 Selecting operation scheme from streamflow prediction 64

B1 Pbias and root mean square error (RMSE) of original ECMWF rainfall prediction, bias-corrected by quantile mapping (BCQM) from June to December (1993-2016)....135

B2 Pbias and root mean square error (RMSE) of original ECMWF rainfall prediction, bias-corrected by quantile mapping (BCQM) from July to January (1993-2016) 135

B3 Pbias and root mean square error (RMSE) of original ECMWF rainfall prediction, bias-corrected by quantile mapping (BCQM) from August to February (1993-2016)..135

B4 Pbias and root mean square error (RMSE) of original ECMWF rainfall prediction, bias-corrected by quantile mapping (BCQM) from September to March (1993-2016) 136

B5 Pbias and root mean square error (RMSE) of original ECMWF rainfall prediction, bias-corrected by quantile mapping (BCQM) from October to April (1993-2016) 136

Chapter 1

Introduction

Water is crucial for all living life. The river is an important natural resource for mankind. River coming from the mountain and flow into the ocean through the river's canal. The amount of river's water increases by precipitation. Precipitation is regarded as the most influential climate variable on the catchment water resources. Drought and flood normally happened all around the world in a random year. Drought is a period of below-average precipitation while the flood is an overflow of water that submerges land due to excessive precipitation. However, humans can reduce the damage caused by disasters by developing advanced technologies such as dams [Mercer et al., 2009, Fadul et al., 2019, Tasseff et al., 2019]. The purpose of dam construction is to control water so that it provides the greatest possible benefit to society [Berhane et al., 2016, Ehteram et al., 2017]. Water management can be managed water to mitigate drought and flood that can have a substantial impact on the ecosystem and agriculture of the affected region [Mateo et al., 2014, Ehsani et al., 2017, Liu et al., 2018].

However, the number of natural disasters such as flood and drought have increased around the globe for the past decade. Figure 1.1 represents the number of natural disasters by comparing with the year from 1981-1990, 1991-2000, and 2001-2010. From this figure, the number of natural disasters was increased all over the globe, especially in Asia. Figure 1.2 shows the natural disaster by type. From Figure 1.2, floods have more chance to happen when compared with other natural disasters. Moreover, extreme weather was also increased. Besides, a report by the Intergovernmental Panel on Climate Change [Field et al., 2012] noted that the effects of climate change make extreme weather and climate events, such as extreme precipitation events and droughts, more frequent and severe globally. Due to this reason, drought and flood still exist and have been increasing even if manmade construction such as a dam, which aims to mitigate flood and drought disaster. The impact of flood and drought disasters has caused damage to the economy and society. In Asia, the impact of flood and drought disasters are more pronounced than in the American and European due to the characteristic of climatology and geographical locations. Thailand is a country located in South East Asia, where is a tropical area. The wet season in Thailand is started from May until October, which almost half a year. Thus, the characteristic of the wet and dry season is visible.

Figure 1.1 Number of natural disasters in the world (World Bank)

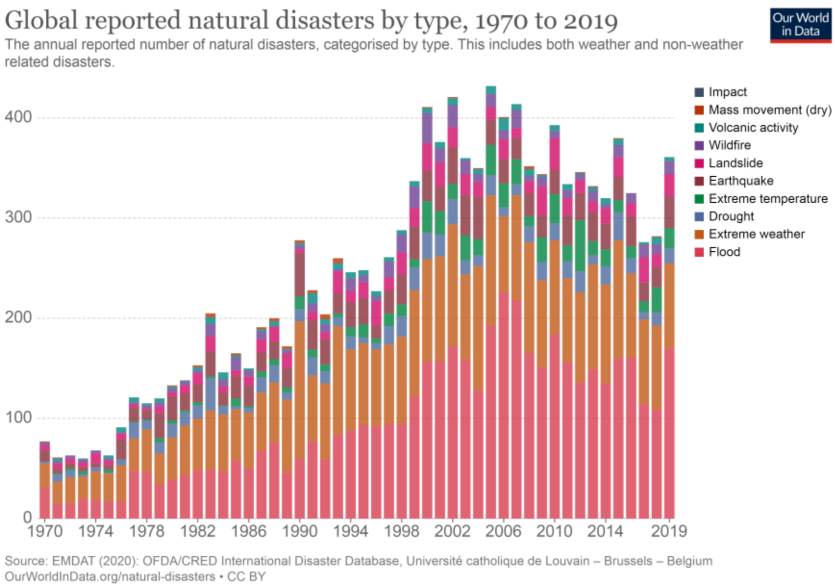

Figure 1.2 Global reported natural disasters by type from 1970 to 2019 (EMDAT, 2020)

Figure 1.3 shows the characteristic of Thailand's climate and track of tropical cyclones in 2011. From Figure 1.3, the tropical typhoon started from June to October in the north part of Thailand, which the Chao Phraya River Basin is located. Moreover, the South West (SW) monsoon started from May to October in the north part of Thailand. Due to this reason, the wet season of CPRB starts from May to October. However, catastrophic flooding occurred in Thailand in 2011. From May until October 2011 the country experienced heavy rainfall as a result of five typhoons. This rainfall was estimated to total 1439 mm or about 143% of the average rainy season rainfall from 1982 to 2002 [Komori et al., 2012, Gale et al., 2013]. Also, the cumulative rainfall in 2011 was higher about 35% when compared with the average cumulative rainfall from 1981 to 2010 as shown in Figure 1.4. Due to these reasons, this flood caused substantial damage to the Thai economy and society.

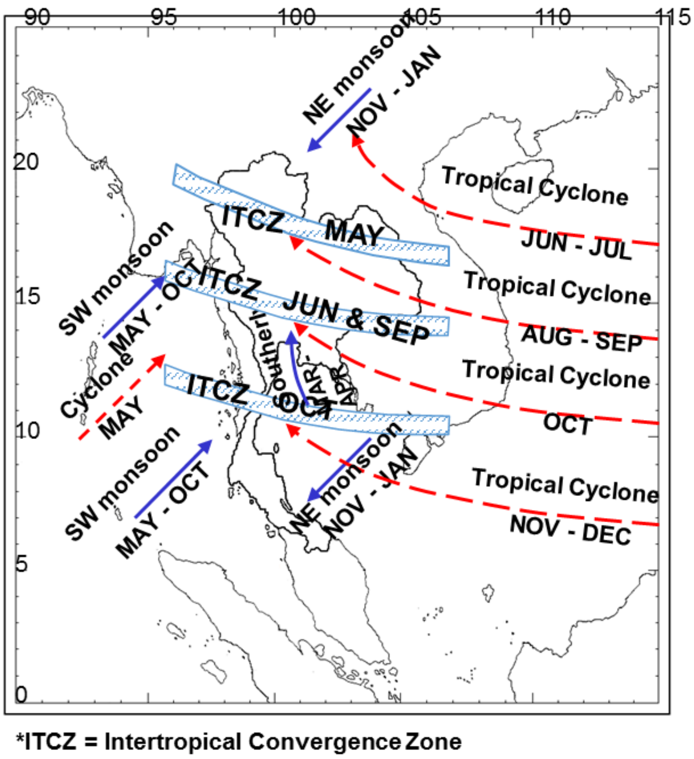

(a)

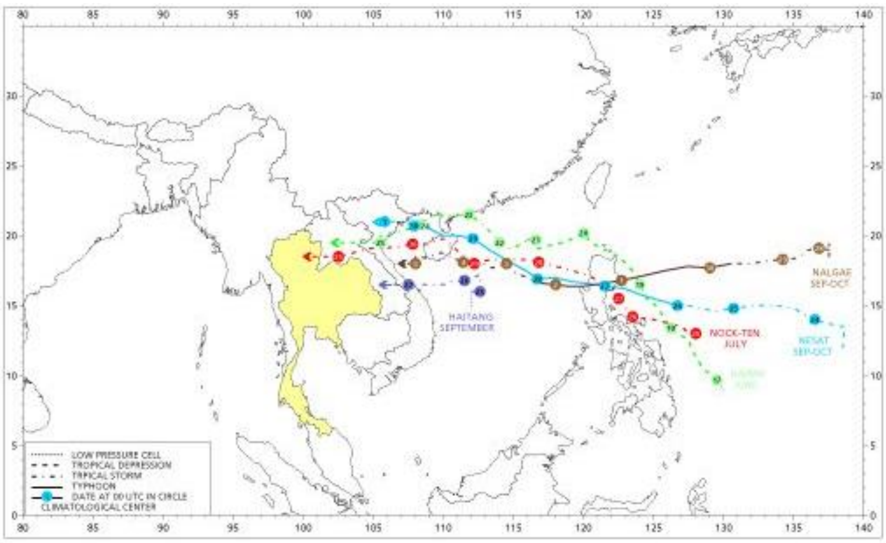

(b)

Figure 1.3 Characteristic of Thailand climates (a) and Track of Tropical cyclone in 2011 (b)

The capital city, Bangkok, and industrial areas were inundated from May until December, which caused the Thai economy to lose about USD 45 billion [World Bank, 2012]. Because of a lack of information on future rainfall, there was no plan for this unexpectedly severe rainfall event, which affected the Chao Phraya River Basin. Thus, two large-scale dams (Bhumibol and Sirikit dam), which are located in Chao Phraya River Basin, were unable to mitigate the flooding in 2011.

In Thailand, most reservoirs are operated using a rule curve. The rule curve is created by historical streamflow in the target area [Prasanchum et al., 2017]. The rule curve was purposed to guide the water manager to control the reservoir in Thailand. The rule curve has been analyzed using past streamflow since the records of streamflow have begun. The rule curve has two curves, which are called 1) upper rule curve and 2) lower rule curve. The upper rule curve is defined as the standard of water amount of reservoir in each month. It is important to maintain the water level in the reservoir not to exceed the upper control level. In order to reserve water between the upper water level and the maximum water level to prevent flooding. The lower rule curve is defined as the minimum water level in the reservoir of each month is set to a standard not lower than the control level below. This is to reserve the amount of water between the bottom water level and the lowest level of water for cultivation in order to prevent water shortage during the dry season [Kangrang et al., 2018]. Figure 1.4 shows the rule curve used for guiding the Bhumibol dam and Sirikit dam. In 2011, Bhumibol dam and Sirikit dam were operated using a rule curve (blue dash line), the water storage was lower than the rule curve at the beginning of the wet season and there is a lack of information on whether streamflow will increase or decrease for the next couple months. Additionally, the reservoirs might not be appropriately managed to mitigate flooding in 2011. Due to this reason, the water storage reached the maximum capacity in both dams in 2011. Because water storage reached the maximum capacity, Bhumibol and Sirikit dam were unable to keep water during the flooding in 2011. Thus, flood mitigation by reservoir operation was unable to mitigate flood in 2011.

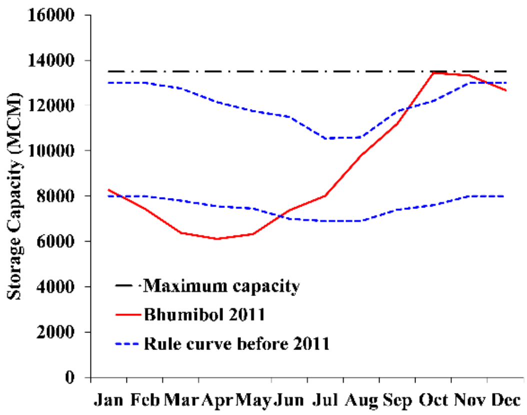

(a)

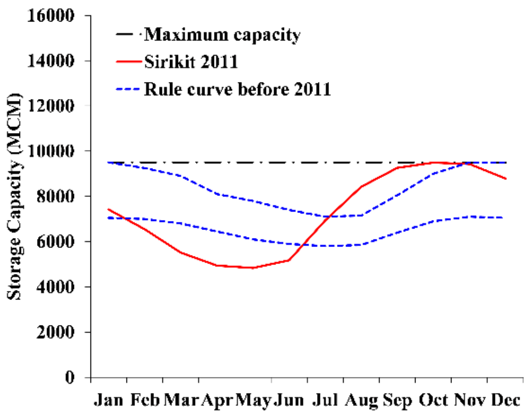

(b)

Figure 1.4 Water storage at Bhumibol dam (a) and Sirikit dam (b) in 2011

Two crucial aspects of effective water management are 1) a suitable plan for reservoir operation and 2) the seasonal streamflow prediction. Flood and drought mitigation can benefit from weather and streamflow forecasts at a seasonal scale such as when anticipating catastrophes and increasing the potential buffering capacity of water-storing facilities [Faber and Stedinger, 2001, Franz et al., 2003, Anghileri et al., 2016]. For example, if a flood is forecasted with sufficient lead time, reservoir outlets can be operated to reduce the peak flow rate [Saavedra Valeriano et al., 2010, Zhao and Zhao, 2014, Anghileri et al., 2016].

Most studies related to streamflow forecasts focused on improving the accuracy of seasonal streamflow forecasts. Two approaches are often used in seasonal streamflow forecasting, namely, statistical methods and dynamic methods [Li et al., 2018]. A mixed-method has been applied in recent studies. The hydrological model is forced with a range of probability in a seasonal climate forecast from general circulation models (GCMs), which is called the hydrological ensemble prediction system (HEPS) approach [Schaake et al., 2007]. HEPS has been widely used around the globe. However, GCM seasonal climate forecast generally produced bias, which can increase the uncertainty in the streamflow forecast. Besides, the spread of the GCM ensemble climate forecast may be too wide for a regional area such as CPRB [Fang et al., 2015]. Thus, these deficiencies need to be improved in terms of accuracy before GCM climate forecast information could be utilized in water management [Li et al., 2018]. Accordingly, an uncertainty of seasonal streamflow forecasts is induced from GCM outputs and hydrological model system. Recent studies on seasonal streamflow forecasts have been applied to preprocessing and postprocessing approach to reduce the uncertainty from GCM outputs [Lucatero et al., 2018]. Quantile mapping is a popular method for bias-corrected. Their studies show that an ensemble of GCM forecasts could be reduced the error in GCM outputs by applying linear scaling and quantile mapping method [Crochemore et al., 2016].

However, less attention has been paid to the use of seasonal streamflow forecasts to support water management. But still, there is some study that use of streamflow forecasts to support water management. Breckpot et al. and Wang et al. [Anghileri et al., 2016] use the streamflow forecasts at the short-term forecasts for flood control operation. A few studies have focused on the use of streamflow forecasts for irrigation or municipal supply [Georgakakos and Graham, 2008; You and Cai, 2008, Anghileri et al., 2016]. At a longer time scale, several studies have investigated the value of forecasts, and predictable inter-annual variability, for hydrogenation [Voisin et al., 2006, Alemu et al., 2010, Anghileri et al., 2016]. These studies used ensemble streamflow prediction to design reservoir operations in snow-dominated river basins. Nevertheless, there are no study use seasonal forecasts to support water management in Southeast Asia, particularly in Thailand. Because the major difference between Thailand's basin and those previous studies [Voisin et al., 2006, Alemu et al., 2010, Anghileri et al., 2016] is the river basin characteristics, because the Chao Phraya River Basin, which is located in Thailand, is not affected by snow. Besides, the rule curve is commonly used by Thai water managers to operate reservoirs.

Although there is no study on the use of streamflow forecast to support water management, particularly in Thailand. However, the previous study by Mateo et al. [Mateo et al., 2014] proposed a useful operation scheme to mitigate floods in 2011. This previous study [Mateo et al., 2014] showed promising results for successful mitigation of the 2011 flood without using predictive information. The authors showed the 2011 flood could have been mitigated by releasing stored water during the early wet season, thus giving reservoirs sufficient storage capacity to retain a greater volume of water during the peak period. Although they [Mateo et al., 2014] proposed a useful operation scheme, they did not consider seasonal streamflow prediction. Moreover, their research mitigated the 2011 flood by controlling the storage of the target dams. In reality, water managers cannot set target storage levels at the beginning of the wet season without predictive information and water demand; in addition, climatic factors are uncertain.

Therefore, to predict seasonal streamflow while accounting for reservoir operation, we updated and developed a method for using seasonal streamflow predictive data to support adaptive reservoir operation. The objective of this study is to demonstrate the use of streamflow predictive information for adaptive reservoir operation with the aim of mitigating the 2011 flood in the CPRB. This study presents a comparison of river discharge with and without the use of predictive information to support adaptive reservoir operation. In addition, the results of river discharge with the 2011 reservoir operation and river discharge with the alternative reservoir operation were compared in this study.

Chapter 2

Study area, Hydrological model and Data

<u>Abstract of this chapter</u>

This chapter presents study area of this study. The characteristic and the details of Chao Phraya River Basin is discussed in this chapter. There are two major reservoirs are located in Chao Phraya River Basin. The impact on river discharge from two major reservoirs are shown in this chapter. Next, this chapter shows the details of hydrological model that used in this study. The hydrological model (H08 model) is forced with observed meteorological data to simulate historical river discharge in this study. In this chapter, the details of observed meteorological data and predictive data that used as input data in the H08 model are shown in this study. The accuracy of the input data is discussed in this chapter.

2.1 Study area

The Chao Phraya River Basin is located in the central part of Thailand. The Chao Phraya River Basin (Figure 2.1.1) is one of the largest river basins in Thailand with an area of about 158,000 km² (30% of Thailand's area). The Chao Phraya River Basin has long supported the local community and economy. The Thai people have made use of the Chao Phraya River Basin for transport, drainage, recreation, fishing, agriculture (in particular, rice), and as a source of water for centuries. Table 2.1.1 shows the water demand in Chao Phraya River Basin. Bangkok is located downstream of the Chao Phraya River Basin. The total number of households in the Chao Phraya River Basin is 23.0 million (1996), and it accounts for 66% of Thailand's gross domestic product (GDP) [ONWRD 2003]. Given its importance, the impact of natural disasters on the Thai economy and society, in particular downstream of the Chao Phraya River Basin, is significant. There are two major reservoirs are located in the upper part of the Chao Phraya River Basin. The maximum dam storage capacity of the Bhumibol reservoir (13,500 million centimeters; MCM) is greater than that of the Sirikit reservoir (9700 MCM). The detail of Bhumibol and Sirikit reservoir are shown in Table 2.1.2 and Table 2.1.3 The representative discharge station for the Chao Phraya River Basin is station C2, where the four main river located in the upper part of the Chao Phraya River basin are confluence at this station. The river storage capacity at station C2, which is the lowest flow rate that indicates flooding, is 3590 m^3/s. While the river storage capacity at Ping River and Wang River (downstream of Bhumibol reservoir) is 1660 m^3/s and 890 m^3/s, respectively.

Ping, Wang, Yom, and Nan, which is the sub-basin of CPRB, are located in the upstream area. At the downstream area, Pasak, Thajean and Sakaekrang are located. Bhumibol and Sirikit reservoir located in the Ping and Nan river, respectively. Figure 2.1.2 shows the river diagram of the Chao Phraya River Basin (upper part). Four main river, Ping, Wang, Yom and Nan river flows from the north of Thailand. The water flows from the north of Thailand before covering at C2 station, which is located at Nakorn Sawan. The downstream of Chao Phraya River Basin is the Gulf of Thailand. Figure 2.1.2

shows the relationship between average observed river discharge at station C2 and observed rainfall from 1981 to 2010. From Figure 2.1.3, the rainy season start at May, where the highest average rainfall amount is found in September. The last month of rainy season is at October before the amount of rainfall start to decrease at November. Therefore, the dry season in Chao Phraya River Basin starts from November to April, where the wet season starts from May to October. In order to supply the water in the dry season and mitigate flood in the wet season, two large reservoirs were built, which have a storage capacity of 23 billion m^3. Bhumibol and Sirikit reservoirs are taken an essential role in water management. Due to the impact of two large reservoirs, river discharge is increased in the dry season and decreased in the wet season compared to the river discharge without reservoirs (Figure 2.1.3). The peak period of river discharge in Chao Phraya River Basin is from September to October where heavy rainfall normally happened from August to September. Thus, the outflow in the wet season from August to October from reservoirs is usually lower than the outflow from May to July.

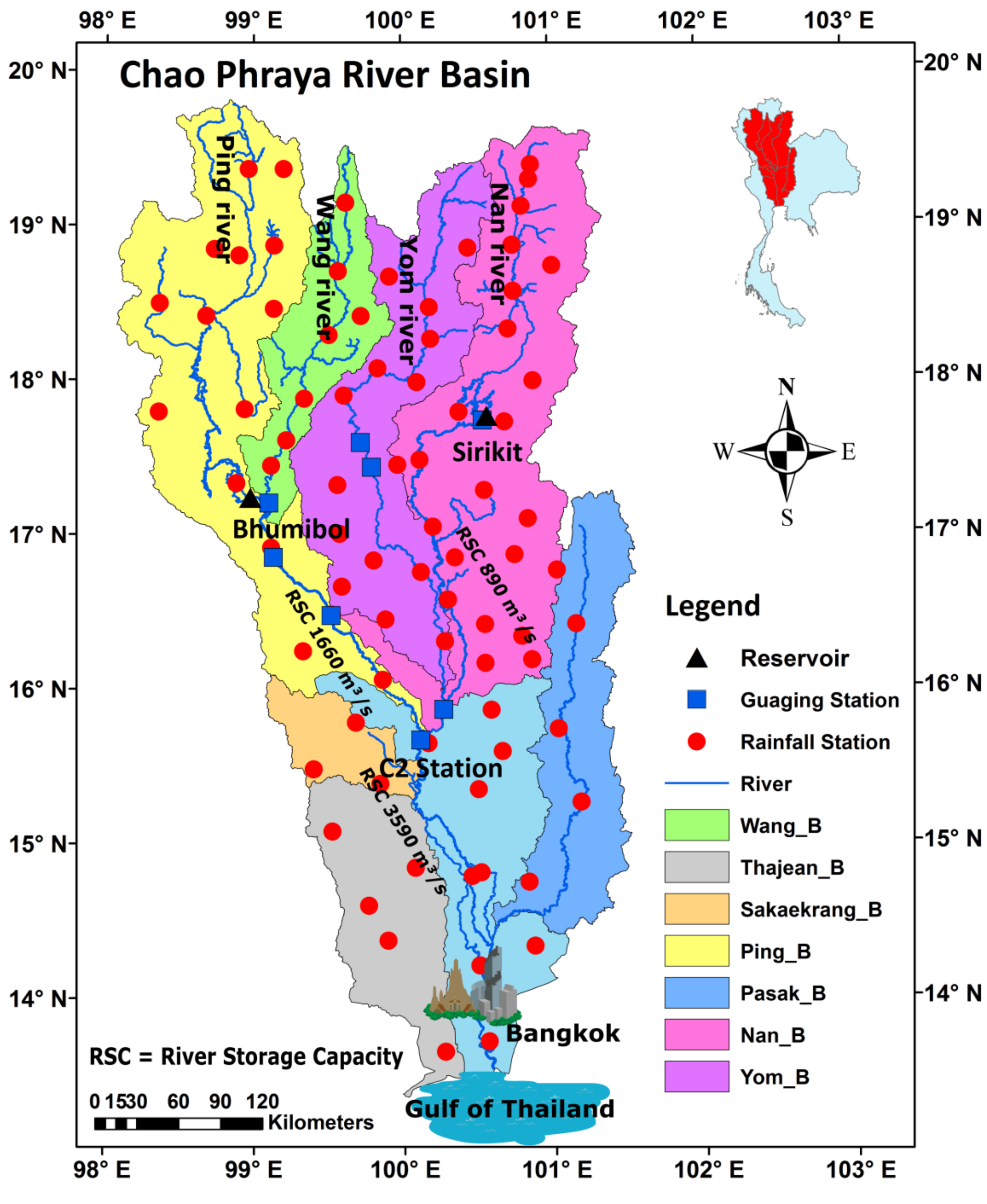

Figure 2.1.1 Chao Phraya River Basin

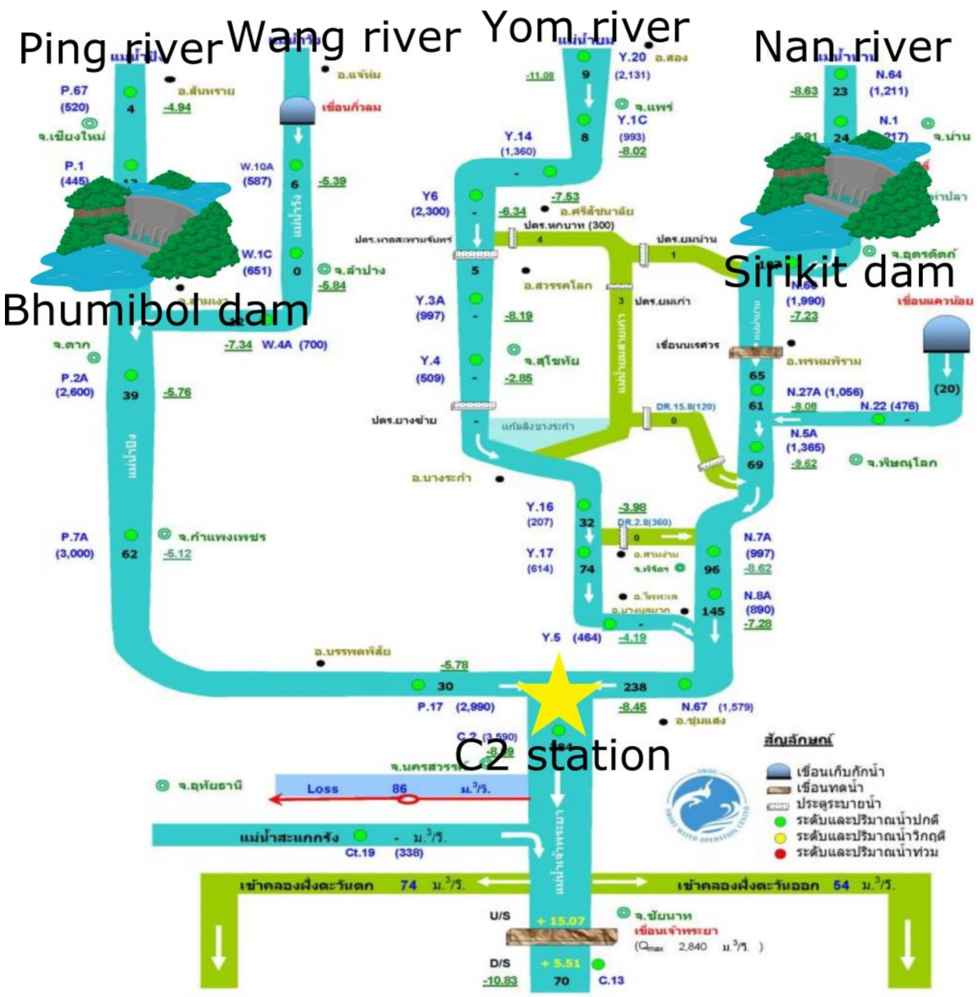

Figure 2.1.2 River diagram of the Chao Phraya River Basin

[Illustration Figures from the Thai Royal Irrigation Department]

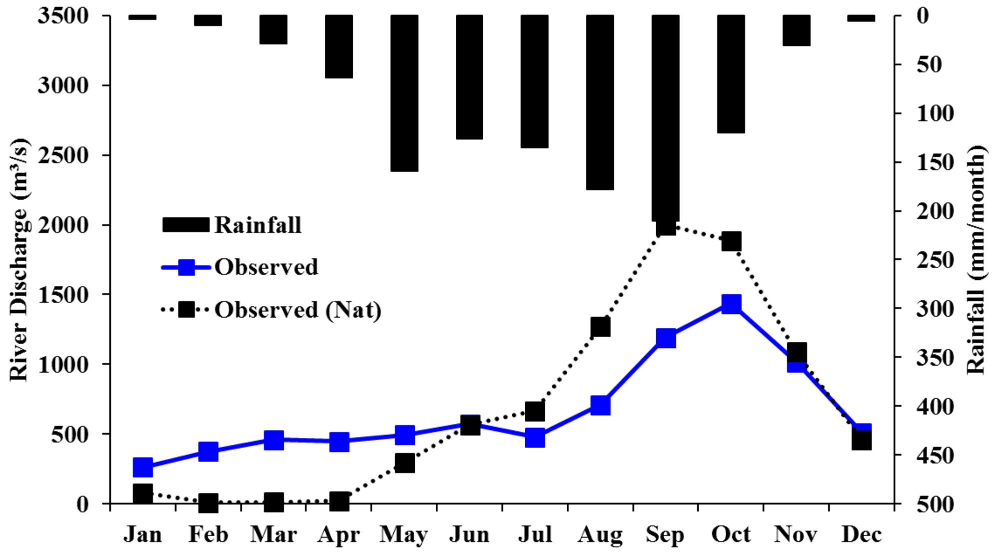

Figure 2.1.3 Average 30-year (1981-2010) river discharge at station C2 and rainfall [Source: Royal Irrigation Department, RID]

Table 2.1.1 Water demand in Chao Phraya River Basin [Thai water]

Order	Water demand in Chao Phraya River Basin	Amount of water demand (Million Centimeters)
1	Consume and tourism	236.42
2	Agriculture	7787.60
3	Industrial	931.95
4	Livestock	34.96
	Summation	8990.93
5	Conservation of ecosystems at downstream area	2386.41
	Overall water demand in the Chao Phraya River Basin	11377.34

Table 2.1.2 Bhumibol dam features and properties

(Source: Electricity Generation Authority of Thailand, EGAT)

Dam features	
Type	Concrete arch gravity
Height	154 meters
Crest elevation	+261 meters (MSL)
Crest length	486 meters
Crest width	6 meters
Maximum width (at base)	52.2 meters
Dam properties	
Catchment area of dam	26,400 square kilometers
Surface area	300 square kilometers
Total capacity of storage	13,462 million cubic meters
Active capacity of storage	9,762 million cubic meters
Average annual inflow (A.D. 1964-2018)	5,636 million cubic meters
Average annual outflow (A.D. 1964-2018)	6,146 million cubic meters

Table 2.1.3 Sirikit dam features and properties

(Source: Electricity Generation Authority of Thailand, EGAT)

Dam features	
Type	Concrete arch gravity
Height	154 meters
Crest elevation	+261 meters (MSL)
Crest length	486 meters
Crest width	6 meters
Maximum width (at base)	52.2 meters
Dam properties	
Catchment area of dam	13,130 square kilometers
Surface area	311 square kilometers
Total capacity of storage	9,510 million cubic meters
Active capacity of storage	6,600 million cubic meters
Average annual inflow (A.D. 1974-2018)	5,713 million cubic meters
Average annual outflow (A.D. 1974-2018)	6,045 million cubic meters

2.2 Hydrological model

2.2.1 Overview of the H08 model

Hydrological model is an important tool to evaluate water resources by simulation in hydrological basins. In the present study, the H08 model [Hanasaki et al., 2007a] is applied for simulating the hydrological process in Chao Phraya River Basin such as river discharge, inflow and outflow at reservoirs. The H08 model is a distributed global hydrological model. The model was developed by Hanasaki et al. The H08 model is one of the few models that were developed with an aim to reproduce the sub-annual variations in the water cycle. This model integrate anthropogenic (human influences) such as reservoir operation with the natural water cycle. The anthropogenic activities or human influences such as water withdrawal are usually driven by the seasonality of the lack of water. Therefore, a hydrological model that prefers to effectively simulate water resources along with human activity should be able to consider in a sub-annual scale [Hanasaki et al., 2007a]

The H08 model consists of six sub-models, which are 1) the land surface model, 2) river model, 3) Environmental flow model, 4) Withdrawal model, 5) Crop growth model and 6) Reservoir operation model. Figure 2.2.1 shows a diagram of the total six model in the H08 model. The land processes and river model are necessary to simulate natural hydrological processes. The reservoir operation model, which buffers the seasonality of water upstream. The anthropogenic water withdrawal model, which is driven by the industrial, domestic, and agricultural demands downstream. The crop growth model, which determines the water needs driven by agricultural demands. Lastly, the environmental flow model, which determines the water flow that need to maintain good river environment downstream [Hanasaki et al., 2007a]. The six models in H08 model can be run separately. However, all of the six model can be simultaneously run the processes in an integrated manner while coupled module. The features related to virtual water were later improved and expanded, and these changes are covered in the H08 model [Hanasaki et al., 2010] as shown in Figure 2.2.1. The details of each sub-model are explained in this section.

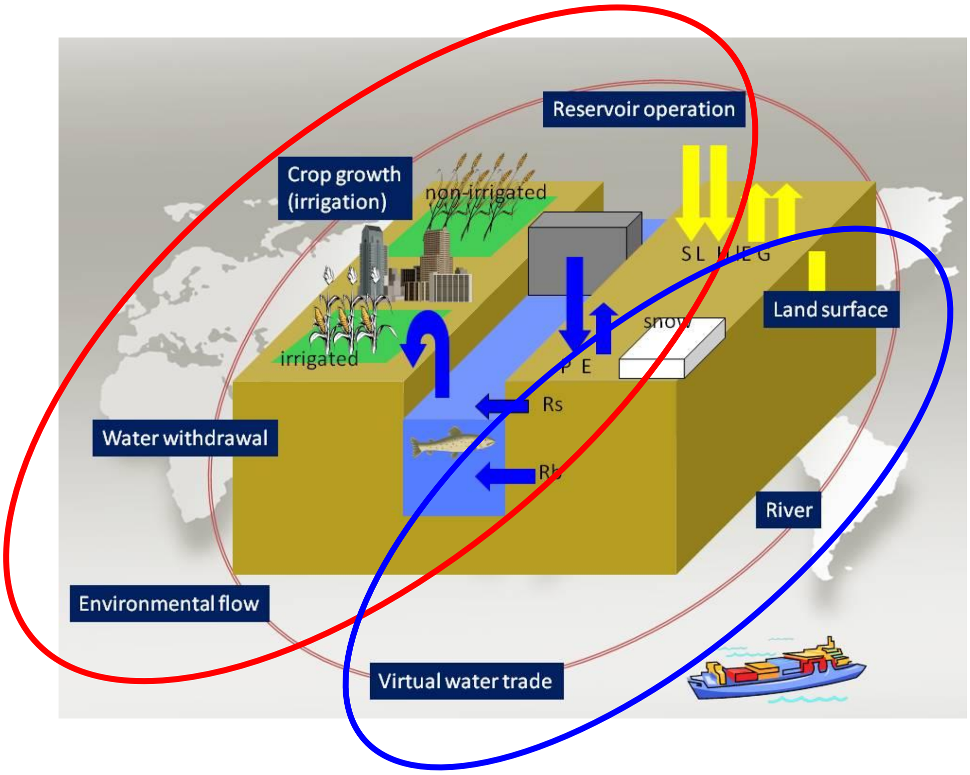

Figure 2.2.1 The six model in the H08 model
[Hanasaki et al., 2010]

The crop growth model in the H08 model is based on the Soil Water Integrated Model (SWIM) [Krysanova et al., 1998] that integrates vegetation, erosion, and erosion with hydrology at a watershed scale. Because of H08 model intends to use the model for estimating water for crop growth, so the parameters from SWIM was only adopted for crop vegetation [Hanasaki et al., 2007]. The crop growth model, sub-model in the H08 model, works under the assumption that agricultural water demand in irrigated fields is equal to the water needed to maintain soil moisture at 75 percentages of field capacity [Hanasaki et al., 2007]. Water below this threshold prevents the optimal growth of the plant biomass due to water stress.

Next sub-model in the H08 model is the environmental flow. The environmental flow model is based on the algorithm by previous studies [Shirakawa 2004, Shirakawa 2005]. This sub-model is based on an allocated amount, which concern flush streamflow during the rainy season, and the minimum stream flow, which has to be maintained in the channel. This sub-model algorithm was based on several case studies and field work in high density in populated regions or in semi-arid to arid regions. For several reasons, the algorithm (at this moment) does not required sufficient river flow for aquatic ecosystems at these stages. In addition, the algorithm of the current model also does not consider about the cultural and economic perspectives, which rather simply concern about natural hydrological conditions.

The anthropogenic water withdrawal model used the information from AQUASTAT database to estimate the demand for the domestic and industrial water. The anthropogenic water model withdraws water from the river channel for domestic, industrial, and agricultural purposes. The anthropogenic water withdrawal model is important for coupling the water fluxes in the other sub-models.

The other sub-models, which are the land surface model, river model, and reservoir operation model, were used in this study. Therefore, the details of the land surface model, river model, and reservoir operation model were explained in more details in Section 2.2.2, Section 2.2.3 and Section 2.2.4.

2.2.2 Land surface model

The land surface hydrology model in the H08 model is based on the leaky bucket model [Manabe 1969, Robock et al. 1995]. The leaky model expresses a single-layer bucket for all vegetation and soil types, soil moisture in a 15 cm deep. The soil moisture in the leaky model drains continuously in the bucket while the original bucket model generates runoff only when the bucket is overfilled. The runoff is generated when the bucket is overfilled in the leaky model. The soil water balance was expressed as equation (2.1) as follow:

$$\frac{dW}{dt} = \mathrm{Rainf} - \mathrm{E} - Q_s - Q_{sb} \tag{2.1}$$

where W is soil water content (kg m^{-2}), Rainf is the rainfall (kg m^{-2} s^{-1}), E is evaporation (kg m^{-2} s^{-1}), Q_s is surface runoff (kg m^{-2} s^{-1}) and and Q_{sb} is the subsurface runoff (kg m^{-2} s^{-1}). The total runoff (Q_{tot} (kg m^{-2} s^{-1})) is shown in equation (2.2) as follow:

$$Q_{tot} = Q_s + Q_{sb} \tag{2.2}$$

where Q_s is the surface runoff (kg m^{-2} s^{-1}) generated when soil water content (W (kg m^{-2})) exceeds the capacity of soil water ($W_f = 0.15 \times SD$), where SD is soil depth (m), as shown in equation (2.3).

$$Q_{sb} = \frac{W_f}{\tau \times 86400}\left(\frac{W}{W_f}\right)^{\gamma} \tag{2.3}$$

where τ and γ are two shape parameters for subsurface flow generation

Figure 2.2.2 shows a simplified diagram of the schematic diagram of the land processes model, which is sub-model in the H08 model. The red arrow color in Figure 2.2.2 shows the energy balance components, the equation governing the interaction drawn inside a red box. Whereas, the water balance components were drawn at the left hand side of Figure 2.2.2 with the blue arrows, with the governing equation written inside a blue box. On the right hand side of Figure 2.2.2, SWdown and SWup mean short wave downward and shortwave upward radiation, respectively. LWdown and LWup represents long wave downward and longwave upward radiation, respectively. Moreover, Tair means air temperature, Qair is specific humidity, Wind represents wind speed, Qh is sensible heat flux, Qle is latent heat flux, Qg is ground heat flux, AvgSurfT is the average surface temperature, and SoilTemp is soil temperature. On the left hand side of Figure 2.2.2 represents the water equation, Prcp is precipitation, SoilMoist means soil moisture, SWE is snow water equivalent, Evap is evaporation, and Qtot is total runoff. Arrows indicate fluxes while those in circle and those that were underlined are state variables. The first year is usually used to calculate in spinup mode until the state variables have stabilized or have reached a low difference compared with the previous spinup process.

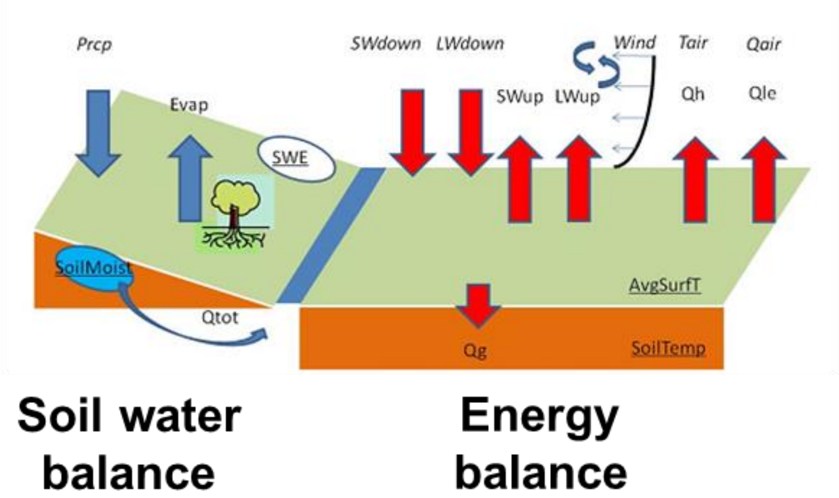

Soil water balance

$$\frac{dW}{dt} = Rainf + Q_{sm} - E - Q_s - Q_{sb}$$

Energy balance

$$SW_{down} + LW_{down} = SW_{up} + LW_{up} - Q_h - Q_{le} - Q_g$$

Figure 2.2.2 Schematic diagram of the land processes model in the H08 model [The H08 User's Manual by Hanasaki et al.]

2.2.3 River model

The river model in the H08 model, the Total Runoff Integrated Pathways model (TRIP) [Oki and Sud 1998] is an idealized global river channel network. In this model, the streamflow was calculated by accumulating the runoff from the land surface model and uses hydrologic routing to calculate. The river is depicted as straight lines without any cross-sectional component that flows at a constant velocity to the downstream cell. Flow directions were determined from digital elevation models that were manually corrected using atlases [Mateo et al. 2014]. The TRIP model does not consider lakes or swamps, reservoir operation, withdrawal, or evaporation loss from water surfaces.

Figure 2.2.3 illustrate the calculation of the river model. This figure shows the fluxes in arrows and the state variables underlined. From Figure 2.2.3, Qtot means the total runoff inflow from the land processes model comping from the upstream grid cell, RivInf is the river inflow from the upstream grid cells, RivOut is the river discharge or streamflow, and RivSto indicates the river storage. The total runoff can be calculated from total runoff Qtot multiplies with total Area A, both from the upstream cell. The red box in Figure 2.2.3 shows the equation used for calculating the river water balance.

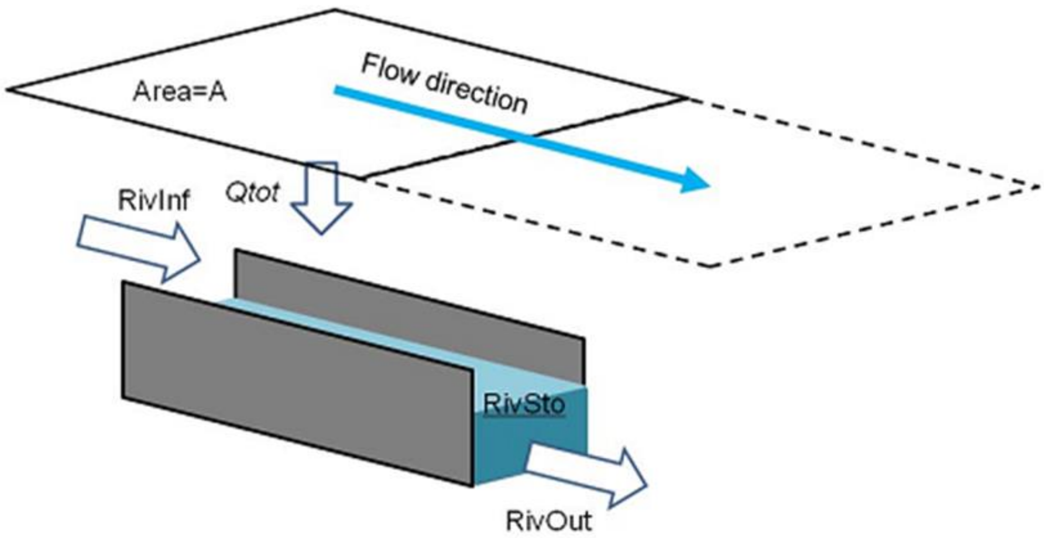

$$\Delta RivSto = (RivInf + Q_{tot}A - RivOut)\Delta t$$

Figure 2.2.3 Schematic diagram of the river model in the H08 model

[The H08 User's Manual by Hanasaki et al.]

2.2.4 Reservoir operation model

The large and medium scale reservoirs are considered in the reservoir operation model. Reservoir details that affect operation such as effective storage capacity, purpose in order of priority, surface area, and location are used as input. The reservoir operation model then sets the operating rules according to the purpose of the dam. For global calculations, reservoir operating rules are based on two types of reservoirs. One that is used for agricultural or irrigation supply purposes, which will be operated based on the irrigation water demands downstream. The second is to minimize interannual and subannual streamflow variation [Hanasaki et al., 2006]. For the regional application, the reservoir operating rules could be edited and adjusted to incorporate the actual or simplified rules, which could be a function of release, storage, or inflow in the reservoir.

Figure 2.2.4 represents the algorithms used for reservoir storage constraints and reservoir releases for the reservoir operation schemes from previous study [Mateo et al., 2013]. Because the two large scale reservoirs in the Chao Phraya River basin, which are the Bhumibol and Sirikit reservoirs, are not operated by a fixed set of rules. However, both reservoirs can be characterized from the historical operation by 1) high seasonal variation in reservoir outflows, and 2) the use of two storage guide curves. Representation of the seasonal variations in reservoir outlet is necessary to simulate the high flow during monsoon or rainfall season (the wet season) and the demand for water during the dry season [Mateo et al., 2013]. The upper and lower rule curves which serve as storage targets or limits can critically affect the simulated volume of water stored in the reservoirs [Mateo et al., 2013].

We can represent these two features in the reservoir operation model in the H08 model by following the parameters, which were included in the reservoir operation algorithm as shown in Figure 2.2.4. R_d (in m^3/s) is the outflow from dam in the dry season, R_w (in m^3/s) is the outflow from dam in the wet season, K_0 is the ration of the effective storage capacity, C (in m^3) represents water storage, $K_0 \cdot C$ means the target water storage limit level, and T_s is the storage limit target date. For simplicity, target storage limit level will be referred as "target level" and storage limit target date will be referred to as "target date" [Mateo et al., 2013].

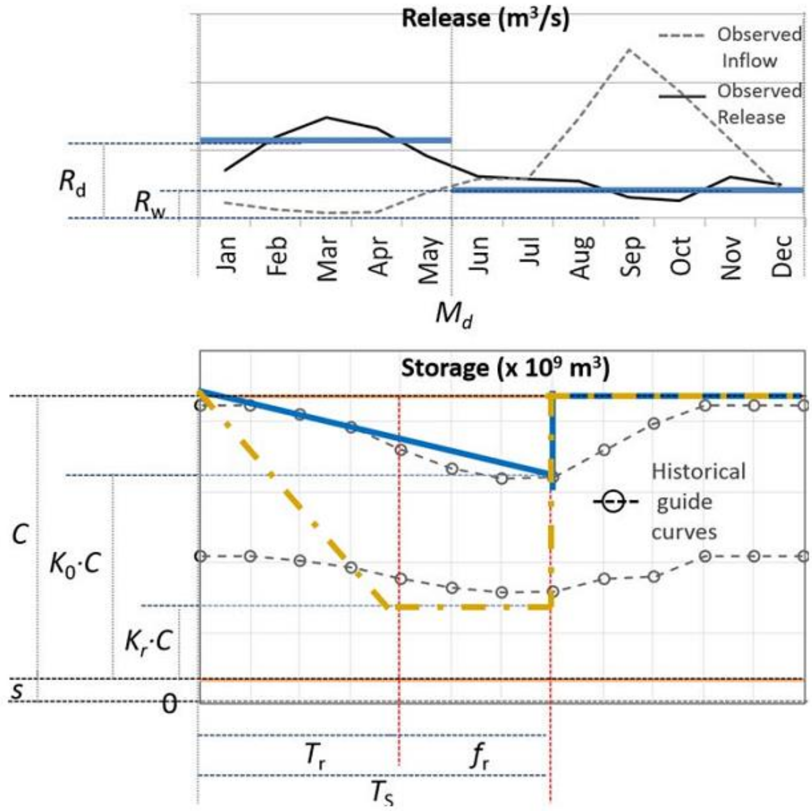

Figure 2.2.4 Algorithms used for reservoir storage constraints and reservoir releases for the locally adapted and alternative reservoir operation schemes

[Mateo et al., 2014]

2.2.5 General setting

In this study, the simulation was done at a spatial resolution of 5 min. (1/12º degree or about 25 kilometers) in both latitude and longitude on the Chao Phraya River Basin. The Chao Phraya River Basin is range from 97ºE to 102ºE in longitude and 13ºN to 20ºN latitude. Since the computation is at 5 minute resolution, so there are 60 grid cells in x-axis and 84 grid cells along the y-axis. Thus, the total grid cells in simulation are 5,040 grid cells (60*84 grid cells). The data format that used for handling data was Hformat2D, amethod wherein the data is divided into fixed elevation, time, experiment, and variable dimensions, and 2 flexible space dimensions (x,y) is followed previous study [The H08 User's Manual]

In this study, there are four parameters that mainly affecting the land surface model, which are the bulk transfer coefficient (C_D), soil depth (SD), time constant for daily maximum surface runoff (τ), and shape parameter which sets the relationship between subsurface flow and soil moisture (γ). The four parameters were followed the previous study by Mateo et al. [Mateo et al., 2013]. Table 2.2.1 shows the four parameters that have been adopted from previous study [Mateo et al., 2013], which compares with typical values in the tropical forests. The details of the methodology for calibration was already discussed in the previous study [Mateo 2012].

Table 2.2.1 Four parameters mainly affecting the land surface model

Parameter	Calibrated Value H08	Typical Values in Tropical Forests
Bulk transfer coefficient, C_D	0.007	0.006 in paddy fields; 0.007 in well-irrigated paddy fields
Soil depth (m), S_D	3.50	Not applicable
Time constant (d), τ	155	100
Shape parameter, γ	2.30	2.00

Relationship between four parameters and the hydrograph

In order to understand the relationship between four calibrated parameters, it is important to understand how changes in each parameter would affect the hydrograph and water balance in the Chao Phraya River Basin [Mateo 2012]. Therefore, this section discuss about the calibrated parameters that affect the hydrograph.

The first parameter is the bulk transfer coefficient (C_D). The bulk transfer coefficient greatly affects the potential evaporation, the sensible heat flux, the energy balance, and the soil water balance. Equation 2.4 shows the equation of the potential evaporation (E_p in $kgm^{-2}s^{-1}$).

$$E_p(T_S) = \rho C_D U(q_{sat}(T_S) - q_a \tag{2.4}$$

where ρ is the density of the air (in kgm^{-3}), U is the wind speed (in ms^{-1}), $q_{sat}(T_S)$ is the saturated specific humidity at surface temperature, and q_a is the specific temperature (both in kg/kg) [Hanasaki et al., 2007]. Equation 2.5 shows the equation of surface evaporation, which the potential evaporation affects the surface evaporation.

$$\mathrm{E} = \beta E_p(T_S) \tag{2.5}$$

where β is expressed in equation 2.6 as a function of the soil water content (W), and the soil water content at field capacity (W_f), which was fixed at 150 (both expressed in kgm^{-2}).

$$\beta = \begin{cases} 1, 0.75W_f \leq W \\ \frac{W}{W_c}, W < 0.75W_f \end{cases} \tag{2.6}$$

Equation 2.7 shows the equation of sensible heat flux (H), which expressed as a function of C_D. C_p^* is a specific hear of air (1005 J $kg^{-1}K^{-1}$). T_a represents air temperature (in K).

$$\mathrm{H} = C_p^* \rho C_D U(T_S - T_a) \tag{2.7}$$

According to Equation 2.4 to 2.7, it could be concluded that if C_D is increased then the potential evaporation (E_p), surface evaporation (E), and sensible heat flux (H) will be increased. On the other hand, if C_D is decreased then the potential evaporation (E_p), surface evaporation (E), and sensible heat flux (H) will be decreased. Examining equation 2.8, it further affects the soil water balance by decreasing the total runoff for a certain amount of rainfall. In the equation, Q_{sm} is the rate of snow melt (it is negligible in Thailand), Q_{sh} is the surface runoff, Q_{sb} is the subsurface runoff, Q_s is the surface runoff (all expressed in $kgm^{-2}s^{-1}$).

$$\frac{dW}{dt} = \text{Rainf} + Q_{sm} - \text{E} - Q_s - Q_{sb} \tag{2.8}$$

The next parameter is the soil depth (SD in m), which affects the hydrograph by increasing the soil water content at field capacity (W_f) as shown in Equation 2.9. An increase of soil depth causes a decreased in the surface runoff (Q_s) as shown in Equation 2.10. A higher soil depth also tends to delay the timing of the peak discharge as it tends to delay the saturation of the effective soil layer.

$$W_f = SD \cdot (\theta_{field\ capacity} - \theta_{witting\ point}) \tag{2.9}$$

$$Q_s = \begin{cases} W - W_f & W_f \leq W \\ 0 & W < W_f \end{cases} \tag{2.10}$$

Equation 2.11 shows the equation of subsurface runoff (Q_{sb}). From this equation, an increased in shape parameter (γ) increase the subsurface runoff, which then reduces the surface runoff at a constant precipitation and evaporation. From the same set of equations, it could be concluded that an increase in time constant for daily maximum subsurface runoff (τ) would results to a decrease in the subsurface runoff, thereby increasing the surface runoff (Q_{sb}) at a constant precipitation and evaporation [Mateo 2012]. The sensitivity test of each parameter was discussed in the previous study [Mateo 2012].

$$Q_{SB} = \frac{W_f}{\tau}\left(\frac{W}{W_f}\right)^{\gamma} \tag{2.11}$$

In order to better understanding the relationship of four parameter to the hydrograph. In this section, the sensitivity test was carried out. Figure 2.2.5.1 shows how the bulk transfer coefficient (C_D) changes. From Figure 2.2.5.1, the graph shows that when C_D increasing then the discharge is reduced as shown with red line. The results show that with the change of 0.001 in C_D results to a changes of around 4% when compared with peak discharge. Figure 2.2.5.2 shows the sensitivity test of soil depth. The results show that the increased of soil depth can decreased discharge. On the other hand, the decreased of soil depth can increased discharge as shown in Figure 2.2.5.2. The change of 0.01 m in soil depth can be changed in peak around 3%. Figure 2.2.5.3 and Figure 2.2.5.4 shows the sensitivity test of daily maximum surface runoff and shape parameter. The results from Figure 2.2.5.3 and Figure 2.2.5.4 show that aside from increasing peak discharge, increasing daily maximum surface runoff and shape parameter reduce fluctuations, reduces discharge volume, and shortens the time of peaking.

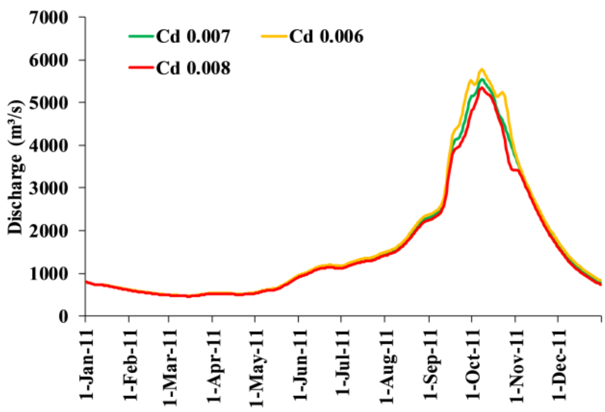

Figure 2.2.5.1 Sensitivity test of bulk transfer coefficient

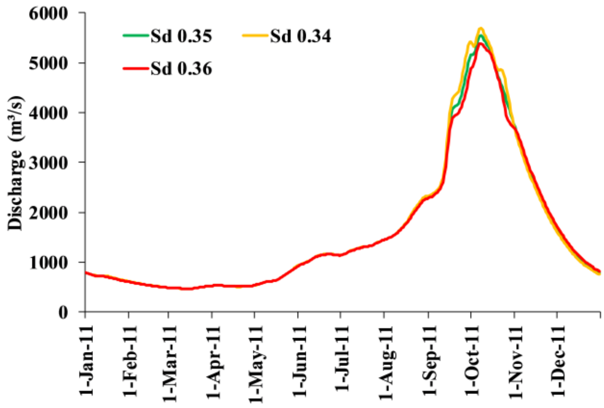

Figure 2.2.5.2 Sensitivity test of soil depth

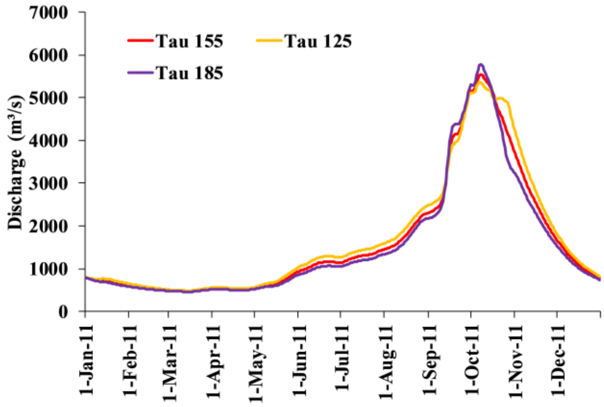

Figure 2.2.5.3 Sensitivity test of daily maximum surface runoff

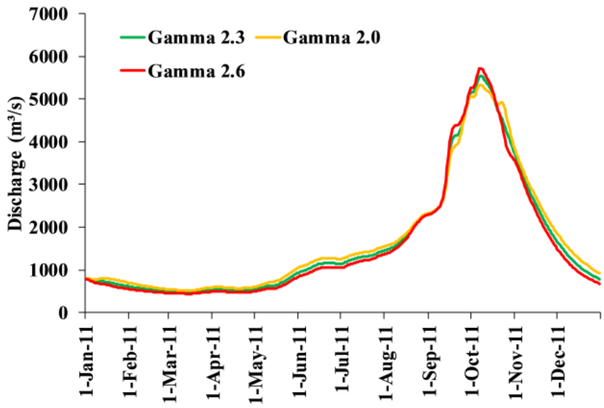

Figure 2.2.5.4 Sensitivity test of shape parameter

2.3 Data

There are two types of input data to the H08 model in this study. The first data is based on the observation such as rainfall (from rain-gauge station), temperature, relative humidity, wind speed, wave radiation, and surface air pressure. The second data is based on the prediction, which is the seasonal precipitation data (generated by European Centre for Medium – Range Weather Forecasts).

2.3.1 Observed data set

The meteorological forcing data is from the previous study by Tanaka et al. [Tanaka et al., 2012], which called T12 dataset. Tanaka et al. developed a new set of accurate precipitation data, which the forcing data available from 1981 to 2011. T12 dataset is based from precipitation observation points, which provides by Thai Meteorological Department (TMD) and Royal Irrigation Department (RID). The precipitation observation points located in the Chan Phraya River Basin. The spatial resolution of T12 data is in 5 min (1/12 degree resolution) in longitude and latitude. The temporal resolution of T12 data is in daily time scale. While the T12 data provide the precipitation data into the H08 model, Yoshimura et al. provided the other dataset data such as temperature, relative humidity, wind speed, wave radiation, and surface air pressure that used as an input data of the H08 model. The dataset provided by Yoshimura et al. was later expressed as Y08 data [Yoshimura et al., 2008]. Table 2.3.1 shows the summary details of T12 data.

The accuracy of T12 data is discuss in this section. Figure 2.3.1 shows the scatter plot and comparison of the T12 data and observed rainfall (from rain gauge station) in the Chao Phraya River Basin from 1981 to 2011. The coefficient of determination (R^2) was used to discuss the accuracy of T12 data. It was found that R^2 was about 0.69 as shown in Figure 2.3.1 (a). From Figure 2.3.1, the T12 rainfall data trend to underestimate when compared with observed rainfall. Figure 2.3.1 (b) and Figure 2.3.1 (c) show the comparison between T12 rainfall data and observed rainfall (from rain gauge station) in the Chao Phraya River Basin from 1994 to 1995 and 2010 to 2011. From Figure 2.3.1 (b), the T12 rainfall data trend to underestimate in 1994, 2010, and during the peak period (July-September) in 1995. On the other hand, the T12 data trend to overestimate during the peak period in 2011.

The other observed data that used as input data was the geographic data. The geographic data in this study was prepared by previous study [Kotsuki et al., 2010].

Table 2.3.1 Detail of T12 data

Name	T12 (Data provided by Tanaka et al. 2012)
Source	TMD/RID
Range of years	1981-2011
Temporal resolution	Daily
Spatial resolution	5 min (1/12° resolution)

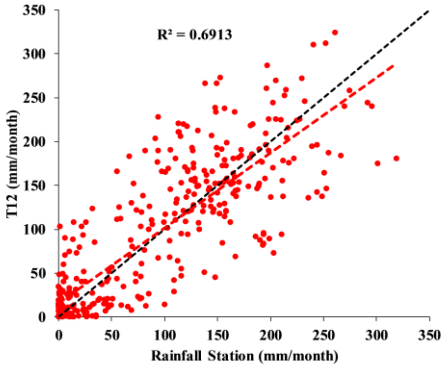

(a)

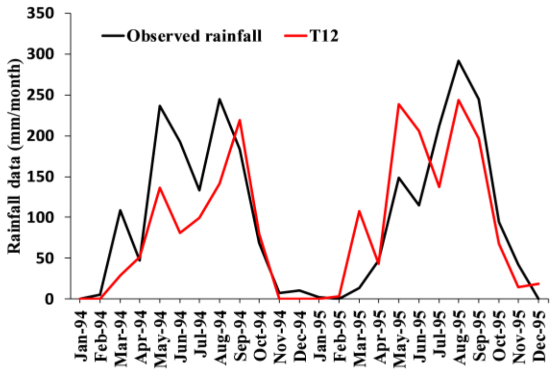

(b)

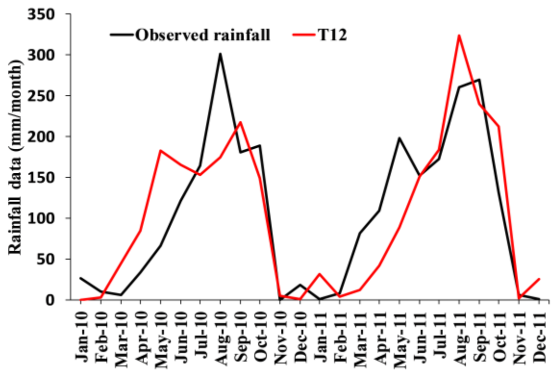

(c)

Figure 2.3.1 Scatter plot of T12 rainfall data and observed rainfall (in mm/month) from rain gauge station in the Chao Phraya River Basin from 1981 to 2011 (a) Comparison of T12 rainfall and observed rainfall

2.3.2 Predictive data

Seasonal precipitation data generated with the European Centre for Medium - Range Weather Forecasts (ECMWF) System 5 [Johnson et al., 2019] were used as input data. The resolution of these precipitation data is 1° in both latitude and longitude. The temporal resolution of seasonal precipitation is daily from 1993 to 2016. ECMWF System 5 predicts precipitation with a forecast range of 6 months and releases ensemble predictions on the first of each month. For each ECMWF System 5 prediction, 25 ensemble members are used. In this study, we selected a starting prediction month of June (the start of the wet season) and conducted seasonal precipitation prediction for July, August, and September. The accuracy of ECMWF System 5 prediction is discussed in Chapter 3. Table 2.3.2 shows the summary of data in this study.

Table 2.3.2 Summary of data in this study

Data Type	Name	Source	Resolution	Data length
Meteorological forcing data	Surface air pressure	Yoshimura et al., 2008	1/12° Every 6 h	1981-2011
	Wind speed			
	Specific humidity			
	Shortwave and Longwave radiation			
	Temperature			
	Rainfall	Tanaka et al., 2012	1/12° Daily	1981-2011
	ECMWF System 5 rainfall	Johnson et al., 2019	1° Daily	June-September 1995, 2011
Geographic data	Geographic map	Kotsuki et al., 2010	1/12°	-
Observed data	Discharge at station C2	Royal Irrigation Department	Daily	1995, 2011
	Outflow and at the Bhumibol and Sirikit reservoir	Electricity Generating Authority of Thailand (EGAT)		
	Dam storage			

Chapter 3

Selecting Reservoir Operation Scheme from Seasonal Streamflow Prediction

Abstract of this chapter

Chapter 3 presents the first method to use the seasonal predictive data to support operation plan in Chao Phraya River Basin. In this chapter, the hydrological model (H08 model) is forced with ECMWF seasonal predictive data to select the operation plan that aim to mitigate flood. The accuracy of the H08 model during 1981 to 2004 and 2010 to 2011 were shown with satisfy results. Then, the bias correction technique is used to improve the accuracy of the ECMWF seasonal predictive data. After that, the three criteria was set to choose an operation scheme out of three alternative operation schemes. Seasonal hydrological predictions were carried out by using ECMWF seasonal rainfall prediction with two different bias correction techniques. The results of using seasonal predictive data to support operation plan at the beginning of the wet season was not sufficient to mitigate flood in 2011. However, if the seasonal predictive data was sufficient, then the most effective operation scheme could decrease the peak discharge around 18 percent by releasing water from reservoirs from the beginning of June until August.

3.1 Model calibration and verification

The accuracy of streamflow prediction is both came from well-organized and accurate of a hydrological model and input data. We separate into two experiments to confirm the accuracy of the H08 model in CPRB. The first experiment to validate the H08 model was done by natural flows, while the second experiment was taken the reservoir operation into account.

In order to simulate the 2011 flood, the important parameter such as bulk transfer coefficient, and shape parameter in the land surface model were followed Mateo et al. [Mateo et al., 2014]. Only the rate of release from two reservoirs are changed. In order to represent the usage of seasonal streamflow prediction for adaptive reservoir operation in this study, dam storage during the 2011 flood need to be well represented. We found that the inflow in 2011 was hugely different compared to another normal year because of the heavy rainfall. The rate of release was calculated based on the mean values of 2010-2011 observed reservoir operation.

The accuracy of the H08 model to simulate the naturalized flow and regulated flow with reservoir operation is verified in this section. The naturalized discharge is the discharge without the effects of reservoir operation that is located in the upstream area. We compared the results of naturalized flow to find the accuracy of hydrological model and input data without the effects reservoir model. Thus, we can discuss the accuracy of hydrological model with the effect of reservoir model and without the effect of reservoir model. The naturalized discharge, which is calculated using observational data, and regulated flow simulation in daily time scale are compared with the naturalized discharge, which is calculated using observational data, at C2 station in Nakhon Sawan province (Figure 3.1.1). The naturalized discharge, which is calculated using observational data, at C2 station is calculated by deducting the effects of reservoir operation upstream of the station as shown in Equation 3.1.1.

$$ND_{C2} = OD_{C2}+[I+P-R-S]_{Bhumibol}+[I+P-R-S]_{Sirikit} \quad (3.1.1)$$

where ND is naturalized discharge, OD is observed discharge, I is observed reservoir inflow, P is observed water pumped into the reservoir, R is observed reservoir release, and S is observed outflow through the spillway.

Table 3.1.1 shows the location of station that was selected to compare the results of river discharge simulation in the Chao Phraya River Basin. The first station is station C2 that is the main representative station of the Chao Phraya River Basin because station C2 is located at the confluence point of four main river (Ping, Wang, Yom and Nan River). Then the other stations were station P1, station N1, station P2A, and station N12A. Station P1 and station N1 were the station at upstream of the Bhumibol and Sirikit reservoir, respectively. These two stations (station P1 and station N1) are considered as the inflow station. On the other hand, station P2A and station N12A are considered as the outflow station because station P2A and N12A are located at downstream of the Bhumibol and Sirikit reservoir (station P2A is located in Ping River, and station N12A is located in Nan River). The longitude and latitude between observed and geographical data [Kotsuki et al., 2010] are different as shown in Table 3.1.1.

Table 3.1.1 Location of the stations used for validation

	Station C2	**Station P1**	**Station N1**	**Station P2A**	**Station N12A**
Observed longitude	100.11	99.008	100.781	99.131	100.541
Observed latitude	15.67	18.786	18.773	16.854	17.736
K10 corrected longitude	100.13	99.028	100.801	99.151	100.561
K10 corrected latitude	15.71	18.826	18.813	16.894	17.776

A good agreement has shown in Figure 3.1.1, we found that the Nash Sutcliffe Efficiency coefficient (NSE) of naturalized observed at station C2 from 1981 to 2004 is about 0.86, where the correlation of determination (R^2) was found about 0.87 as shown in Figure 3.1.1 (b). Although, the simulation of naturalized river discharge trends to be underestimated as shown in Figure 3.1.1 (b). However, the results show a good results and reasonable because T12 rainfall data is also underestimated as shown in Figure 2.3.1 in the previous chapter.

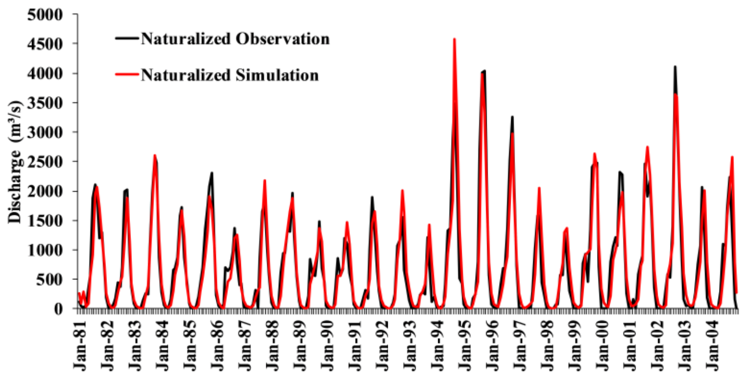

(a)

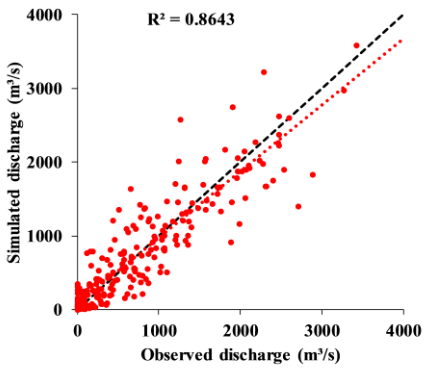

(b)

Figure 3.1.1 Comparison of the naturalized river discharge (a) and scatter plot (b) between observation and simulation at C2 station on monthly scale from 1981 to 2004

Figure 3.1.2 (a) shows the comparison of river discharge between observation and simulation at station C2 from 1981 to 2004. The results show a good result with the NSE about 0.81 and R2 about 0.81 as shown in Figure 3.1.2 (b).

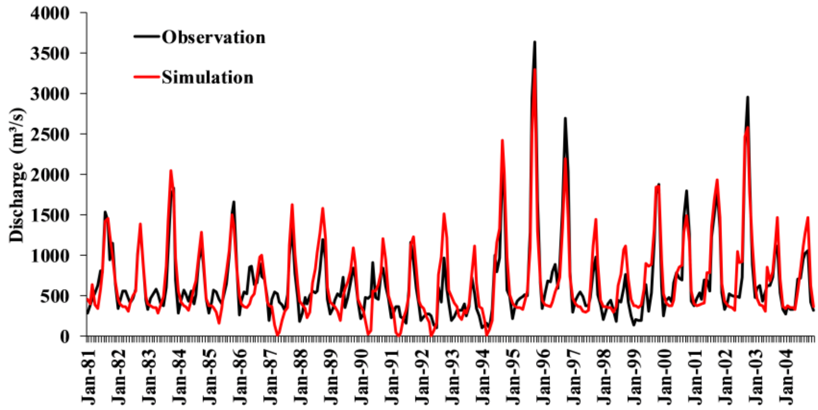

(a)

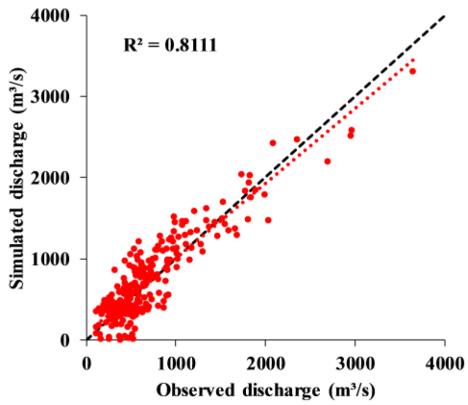

(b)

Figure 3.1.2 Comparison of the monthly river discharge (a) and scatter plot (b) between observation and simulation at station C2 from 1981 to 2004

Figure 3.1.3 shows a good agreement, it is found that the NSE of naturalized observed from 2010 to 2011 at C2 station is about 0.84, where the correlation of determination (R^2) was found about 0.85 (Figure 3.1.3 (b)).

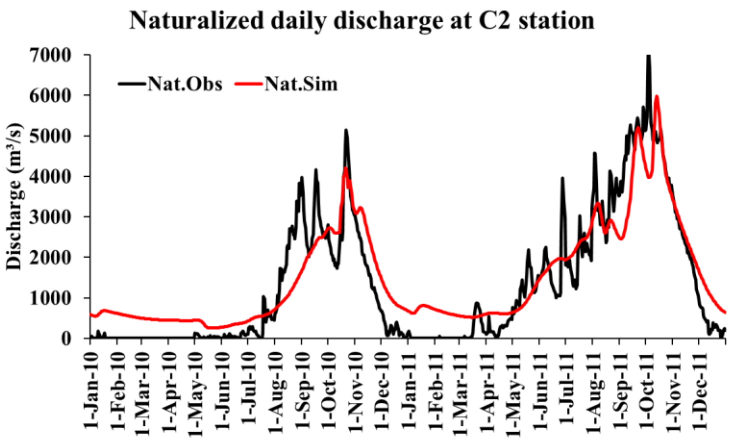

(a)

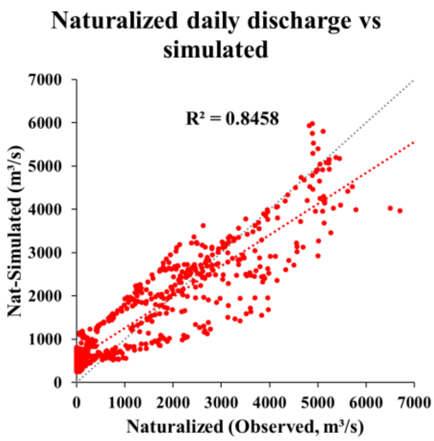

(b)

Figure 3.1.3 Comparison of the daily river discharge (a) and scatter plot (b) between observation and simulation at station C2 from 2010 to 2011

The comparison between observed discharge and simulation with 2011 reservoir operation that calculated following Mateo et al. (2014) method has shown in Figure 3.1.4. We found that the NSE of simulated river discharge at C2 station and R^2 from 2010 to 2011 are about 0.94 (Figure 3.1.4 (b)). These results show that the reservoir operation in 2011 can be represented well and comparable with the results of Mateo et al. (2014).

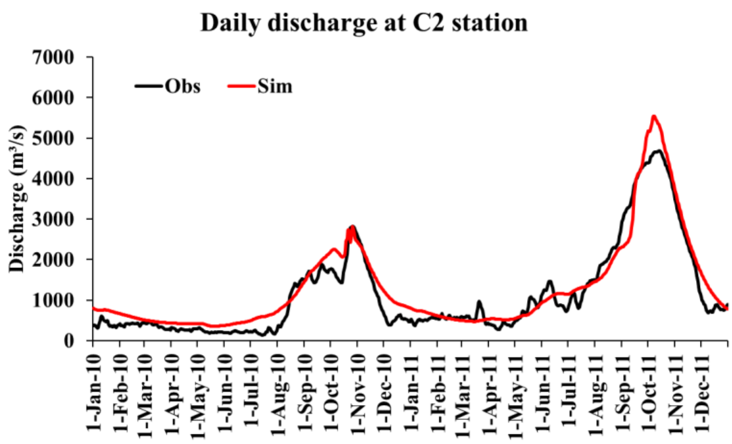

(a)

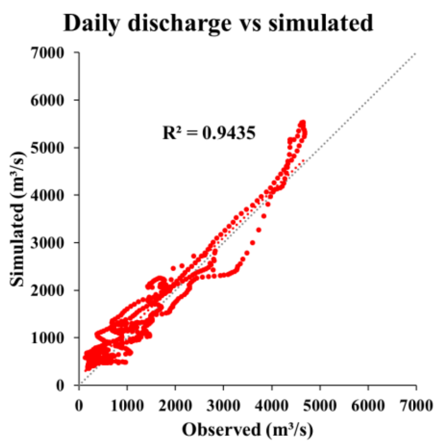

(b)

Figure 3.1.4 Comparison of the daily river discharge (a) and scatter plot (b) between observation and simulation at station C2 from 2010 to 2011

A good result between observation and simulation of river discharge is shown at station C2. Figure 3.1.5 shows the satisfied result between simulation and observation from 1981 to 2004 at station P1, which is the inflow station of the Bhumibol reservoir. Nash Sutcliffe Efficiency coefficient (NSE) of station P1 is about 0.79 and the correlation of determination (R2) is about 0.82 as shown in Figure 3.15b.

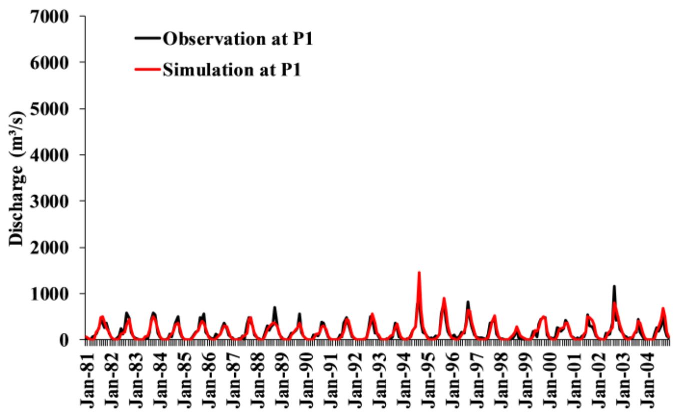

(a)

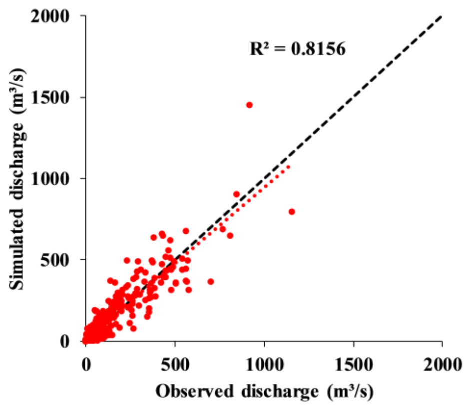

(b)

Figure 3.1.5 Comparison of the monthly river discharge (a) and scatter plot (b) between observation and simulation at station P1 from 1981 to 2004

Although, the results of station C2 and P1 are shown the good results. On the other hand, the results of station N1 is trend to be underestimated with the NSE about 0.48, and R^2 about 0.73 as shown in Figure 3.1.6. However, the accuracy between observation and simulation of river discharge (inflow) at station N1 is matched with the results in the previous study [Mateo 2012].

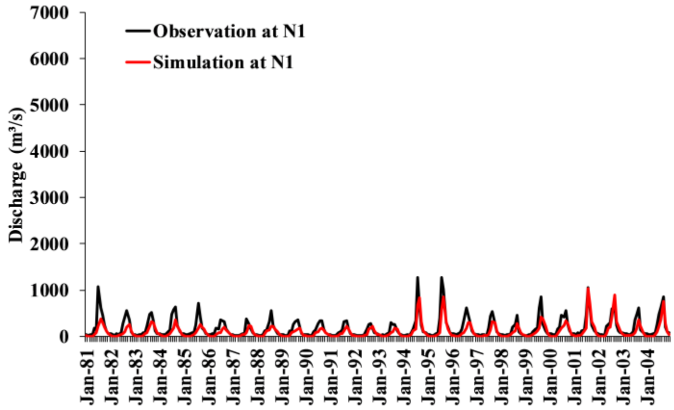

(a)

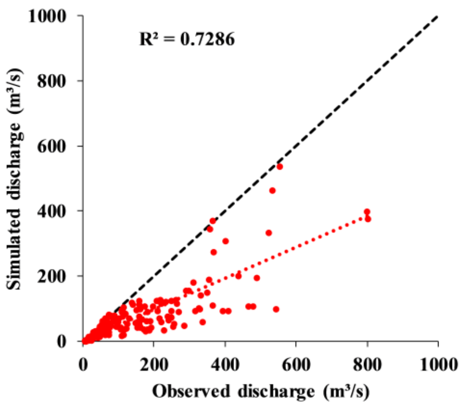

(b)

Figure 3.1.6 Comparison of the monthly river discharge (a) and scatter plot (b) between observation and simulation at station P1 from 1981 to 2004

One of the reason that the accuracy of simulation of river discharge at station N1 is lower when compare with station C2 and station P1 is the calibrated parameters [Mateo 2012]. The calibrated four parameters (bulk transfer coefficient, soil depth, shape parameter, and daily maximum subsurface runoff) were calibrated to apply to all grid cells within the Chao Phraya River Basin, which means that the land cover and soil characteristics in the Chao Phraya River Basin are assumed to be all the same. Another reason, which also mentioned in previous study [Mateo 2012], could be the presence of human activities that were unaccounted for in present study. In addition, an official of the Royal Irrigation Department (RID) said that water is being pumped into Sirikit reservoir (on Nan River) for water supply.

Due to the importance of two reservoirs to CPRB and related to changing reservoir operation, we also verified the dam storage and outflow from both reservoirs, especially in 2011. The simulation of outflow from both reservoirs is shown in Figure 3.1.7. From Figure 3.1.7, the outflow from Bhumibol (Figure 3.1.7 (a)) and Sirikit reservoir (Figure 3.1.7 (b)) are significantly different between observation and simulation. The reason is because we set the outflow for constantly release in the same rate for the dry season and the wet season. We set the same rate of release because the characteristic of CPRB where the dry season and the wet season is visible different. During the dry season, outflow from both reservoir is higher than ouwflow during the wet season. Such rationing phenomena, we have set the outflow with the same release rate as shown in Figure 3.1.7. Furthermore, we have followed the calibration method to set the outflow from both reservoir from previous studies [Hanasaki et al. 2012].

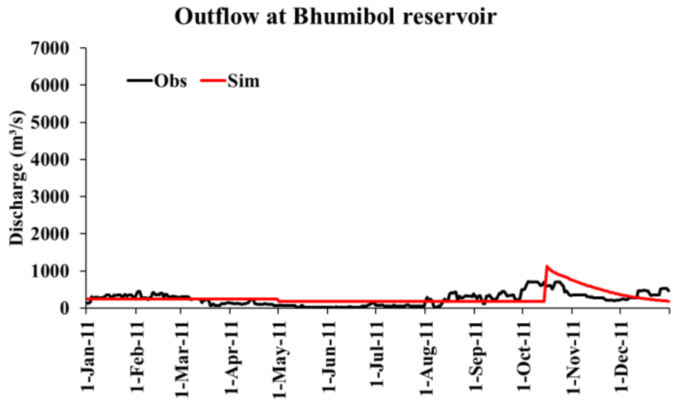

(a)

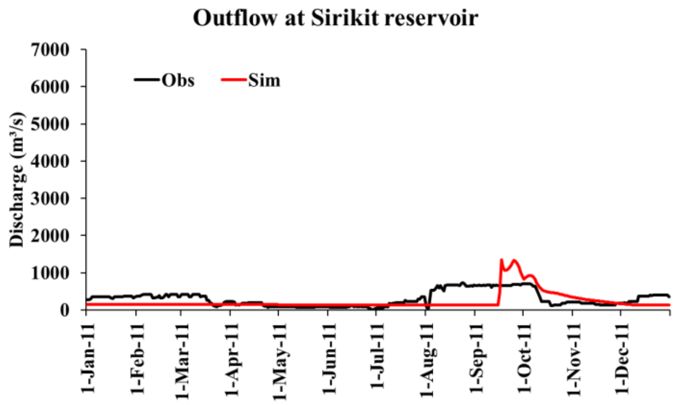

(b)

Figure 3.1.7 Comparison of daily outflow at station P2A (a) and station N12A (b) between observation data (black line) and simulation data (red line)

The outflow simulations are divided into the dry season and the wet season. The outflowd during the dry season usually higher than the wet season. Thus, the outflow from the dry season (January to the end of April) is higher than the outflow in the wet season as shown in the red line in Figure 3.1.7. However, dam storage in both the reservoir starts to reach the maximum storage in September in the Sirikit reservoir and October in the Bhumibol reservoir.

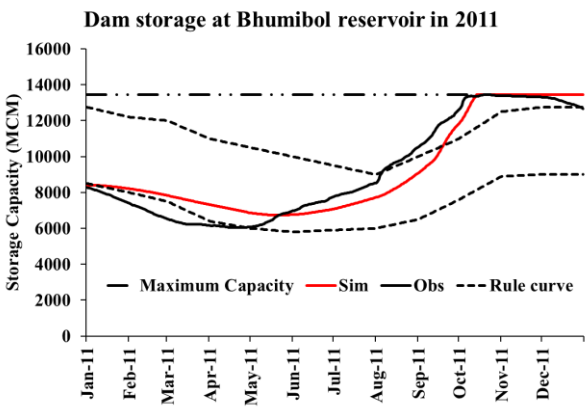

(a)

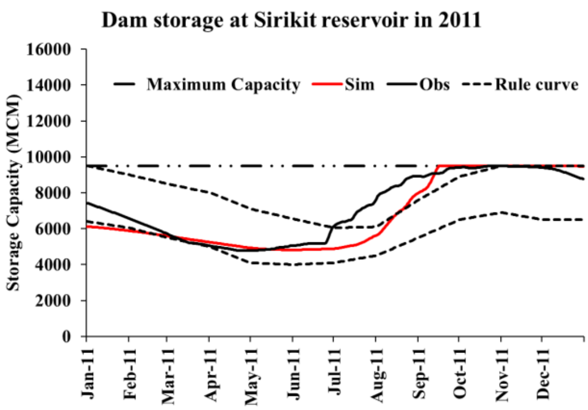

(b)

Figure 3.1.8 Comparison of daily dam storage at Bhumibol (a) and Sirikit reservoir (b) between observation (black line) and simulation (red line)

Then, the outflow in simulation immediately starts to increase the outflow in October in the Bhumibol reservoir and September in Sirikit reservoir as shown in Figure 3.1.8. Thus, there are significant different about volume and peak in outflow as shown in both Bhumibol's outflow (Figure 3.1.7 (a)) and Sirikit reservoir's outflow (Figure 3.1.7 (b)). A good comparison between observed dam storage and the dam storage simulation at Bhumibol and Sirikit reservoir was presented in Figure 3.1.8. The different between dam storage, especially during July and September as shown in Figure 3.1.8, was because the outflow between simulation and observation is different. The reason is because the inflow between observation and simulation, especially in Sirikit reservoir. The simulated inflow tends to lower during July and September as shown in Figure 3.1.9. Also, the different between observed and simulated inflow were mentioned in previous study [Mateo et al. 2014].

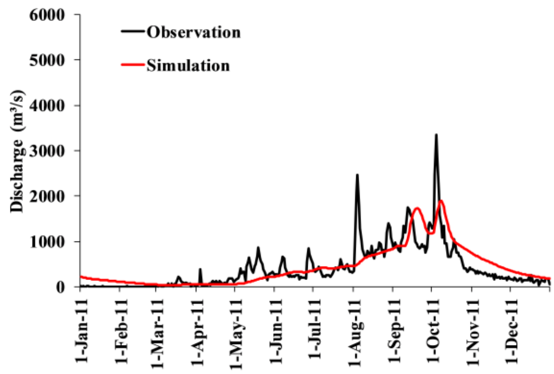

(a)

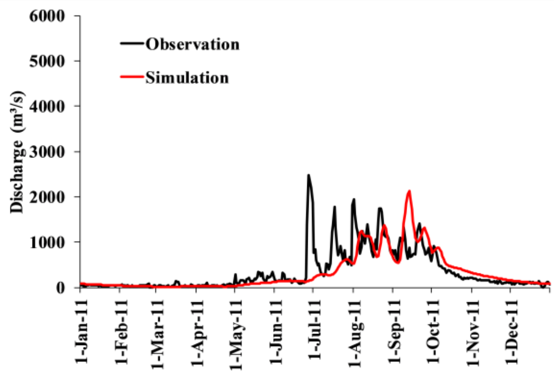

(b)

Figure 3.1.9 Comparison of daily inflow at station P1 (a) and station N1 (b) between observation data (black line) and simulation data (red line)

3.2 Bias correction

The outputs from a climate model are usually produced for a coarse grid-scale, which may lead to biases in the outputs. In this study, the famous bias correction, which is quantile mapping method have been selected to improve the accuracy of the ECMWF system 5 seasonal predictive data.

Quantile mapping enhances the accuracy of seasonal rainfall prediction by correcting mean values in the same month using the reanalyzed precipitation data during 1987 to 2010 period. Equation 3.2.1 represents the quantile mapping equation to bias corrected the rainfall data. In this study, the reanalyzed data (T12 data) from 1987 to 2010 is used as observed data, while the seasonal predictive data is used as simulated data as shown in Equation 3.2.1.

Figure 3.2.1 shows the conceptual of quantile mapping technique, which is used to correct the cumulative distribution function between observed rainfall data and seasonal rainfall prediction data. Equation 3.2.1 to Equation 3.2.3 show the quantile mapping equation [Themeßl et al. 2011].

$$P_t^{cor} = P_t^{raw} + C_t \quad (3.2.1)$$

$$C_t = cdf_{doy}^{obs,cal^{-1}}(P_t) - cdf_{doy}^{mod,cal^{-1}}(P_t) \quad (3.2.2)$$

$$Prop_t = cdf_{doy}^{mod,cal}(P_t^{raw}) \quad (3.2.3)$$

where P is rainfall data, cor is bias-corrected data, raw is raw data or forecast data, obs is observed data, j is a year, doy is a day of the year, t is time in daily scale, cal is calibration period (1993-2016 in this study), C is the difference between observed and model inverse cumulative density distribution (cdf).

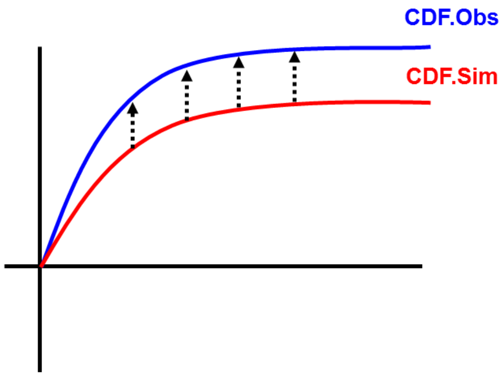

Figure 3.2.1 Conceptual image of quantile mapping technique

3.3 Setting the criteria to select reservoir scheme

In this study, the criteria is set to select a reservoir operation scheme out of three operation schemes, based on streamflow prediction results. Mateo et al. (2014) proposed four alternative operation schemes. However, since the prediction in this study begins in June, only three (PlanU, Rev0.5Jul, and Rev0.25Jul) in their study are determined as the candidates of reservoir operation. The major differences between PlanU, Rev0.5Jul, and Rev0.25Jul are differences in storage that prepares for the up-coming peak period in the wet season. Preparation of enough storage since the beginning of the wet season is the solution to allow reservoirs to have space for storing water caused by heavy rainfall during August, September, and October. Figure 3.3.1 shows a

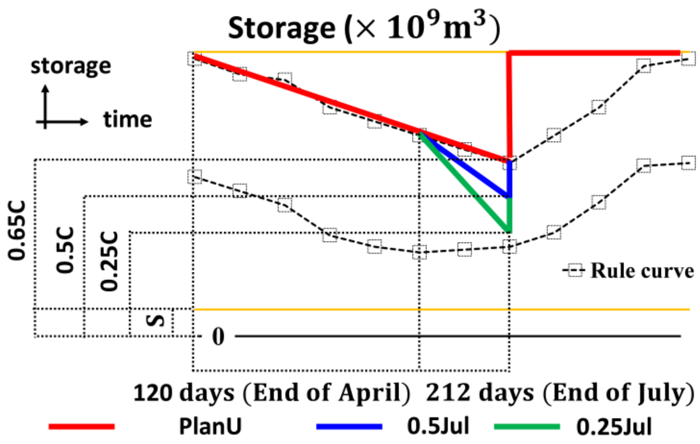

Figure 3.3.1 Algorithms used for reservoir storage constraints for an alternative reservoir scheme

conceptual image of reservoir storage constraints for reservoir operation schemes where 65 percent, 50 percent and 25 percent in total capacity for the highest storage target are PlanU, Rev0.5Jul, and Rev0.25Jul scheme, respectively.

The yellow line represents maximum capacity and dead storage of the reservoir. The black dot-ted line with blank squares represents the rule curve that guides the operations. The blue line represents the upper rule curve. The red line rep-resents the alternative upper rule curve, which use for guiding the operation of the reservoir. C is water storage, while Ko represents the target water storage. Ts represents a time for releasing the water in the the reservoir as shown in Table 3.3.1. The percentage difference in mean streamflow from August to October and that of a flood event is found that 40, 60 and 95 in 2010, 2002 and 1995, respectively. Thus, the current criteria shown in Table 3.3.1 are set, in which the 1995 flood is the second most catastrophic while another bigger and smaller flood happened in 2002 and 1995.

The methodology to select a reservoir operation from streamflow prediction is describe below.

1) Carrying out streamflow prediction with rainfall prediction (25 ensemble members in this study).

2) Calculating the mean natural flow, in this case, a 30-year average natural flow from 1981 to 2010.

3) Calculating the average streamflow from step 2 (for August, September, and October in this study).

4) Compare the results from step 1 and results from step 3. Then, we can decide the reservoir operation scheme by finding the different percentages between each prediction result and the average streamflow in step 3: selecting an operation scheme out of three by following the criteria as shown in Table 3.3.1.

Table 3.3.1 Parameter values used in reservoir operation

Operation scheme	**K_o**	**T_s**	**Criteria**
PlanU	0.65	212 (end of July)	Streamflow prediction ≤ 40 %*
Rev0.5Jul	0.50	212 (end of July)	40 %* ≥ Streamflow prediction ≤ 60 %*
Rev0.25Jul	0.25	212 (end of July)	Streamflow prediction ≥ 60 %*

*Percentage different of natural flow between flood events and average 30 years natural flow from 1981 to 2010 by more than 40, 60 and 95 percentages different in 2010, 2002 and 1995, respectively.

Figure 3.3.2 shows an example of selecting reservoir operation using streamflow prediction data. Case no.1 shows the streamflow prediction in 2011. The average streamflow prediction is about 119.83 millimeter per month, which is higher than the 30-year natural flow about 150 percent. In this case, we will select Rev0.25Jul as the operation scheme for case no.1. On the other hand, in case no.2, we will select Rev0.5Jul as the reservoir operation because the predicted difference in percentage is 56.

It is also crucial to have the criteria for selecting a reservoir operation in view of water re-sources in the next year. The reason is that the difference in reservoir operations will affect the water level in the next year. Figure 3.3.3 shows the image of 2-year river discharge, which used only Rev0.25Jul (green line) as a reservoir operation and the river discharge that also uses the criteria from streamflow prediction to select the reservoir operation (red line). This is a hypothetical case. In the first year, the water is increased due to heavy rainfall and Rev0.25Jul seems the most effective to mitigate flooding, while Rev0.5Jul is selected based on seasonal streamflow prediction. Then, water shortage may arise in the green line case because heavy rainfall on the first year is not huge to allow the reservoir to release enough water during the dry season for the second year. On the other hand, setting the criteria to select a reservoir operation in the red line case allows flood mitigation on the first year as well as gives enough amount of water during the dry season, because reservoir storage has matched with the amount of heavy rainfall in the first year.

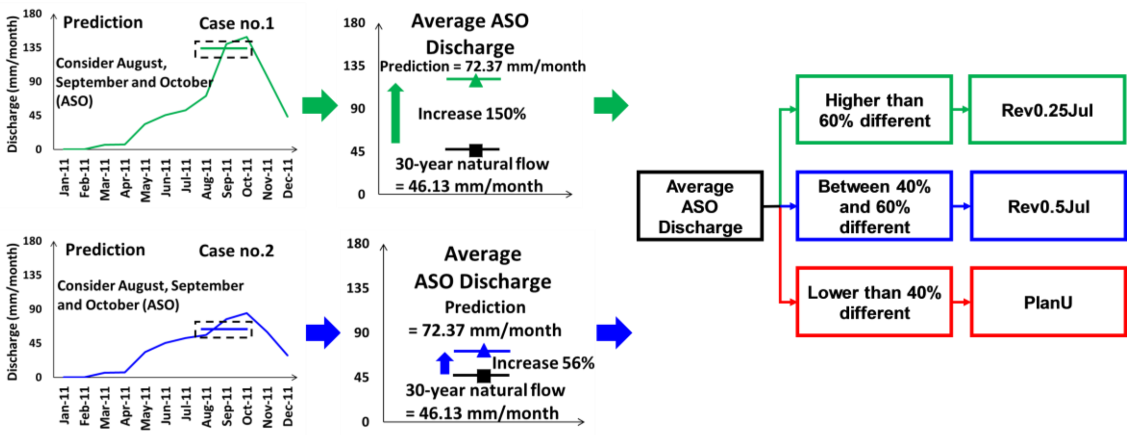

Figure 3.3.2 Example of selecting reservoir operation from streamflow prediction

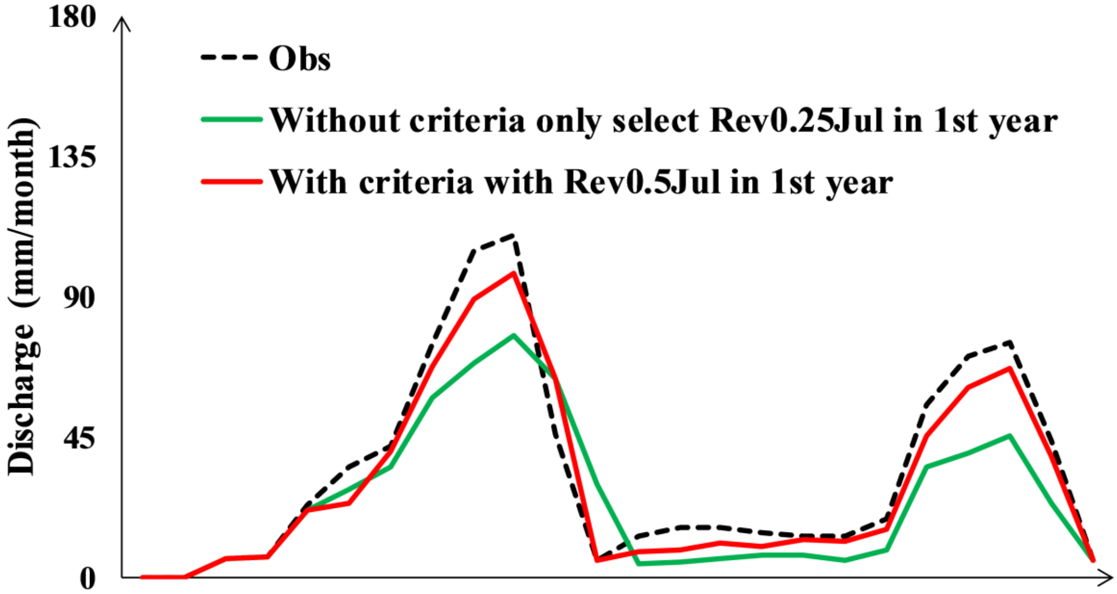

Figure 3.3.3 Example of river discharge with selecting reservoir operation from streamflow prediction (red line) and without setting the criteria to select reservoir operation (green line)

3.4 Results and discussion

3.4.1 Using the bias correction method to improve the accuracy of rainfall prediction

Reanalyzed rainfall data from 1987 to 2010 (23 years) was used as a reference period to correct the accuracy of rainfall prediction in this study. Figure 3.4.1.1 shows the accuracy of bias-corrected rainfall by quantile mapping compared with the raw rainfall prediction data. We compared the results of average rainfall from August to October in CPRB, where peak flows usually occur at this period. Raw data of rainfall prediction shows an overestimation in this period partly because June is the starting prediction month (three to five-month ahead of August to October). Appendix B shows the accuracy of rainfall prediction in monthly time scale. Overall, bias correction techniques can improve rainfall prediction.

Bias correction of rainfall prediction by quantile mapping did not improve the accuracy much in the 2011 flood event, because rainfall prediction of raw data during August to October is already close with observed rainfall data (blue triangle dots). Quantile mapping tends to make less distribution of rainfall prediction because quantile mapping can correct the mean and standard deviation of rainfall prediction.

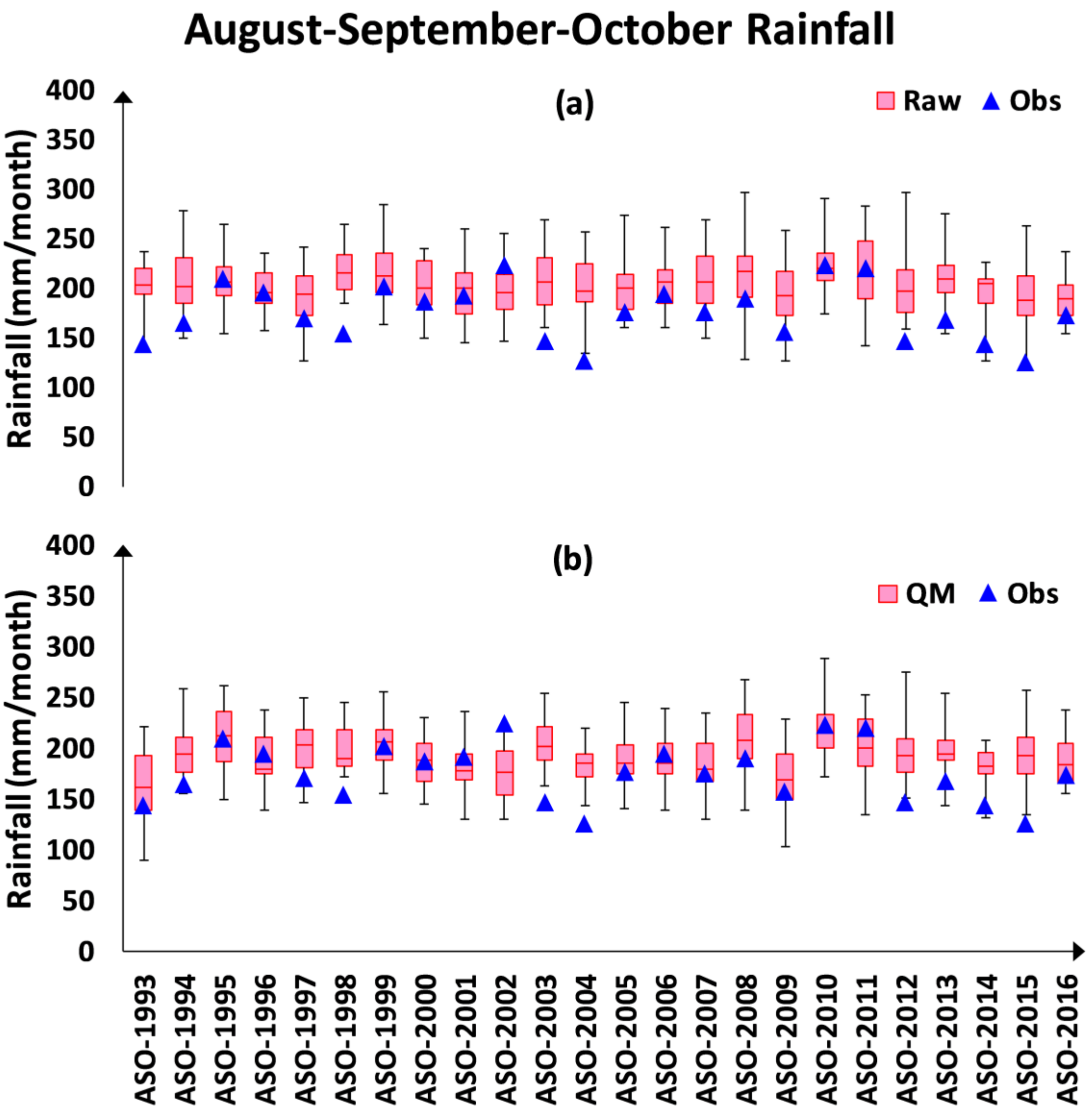

Figure 3.4.1.1 Average seasonal rainfall prediction during August, September, and October from 1993 to 2016 (a) raw (b) bias-corrected by quantile mapping rainfall prediction compares with average observed rainfall. The red box represents the range of standard deviation of prediction data, and blue triangle shows observed rainfall data. Each point represents the average rainfall data from August to October.

3.4.2 Simulation of streamflow prediction in 2011

Since the most sensitive meteorological variable in CPRB is rainfall, seasonal rainfall prediction was used as an input data in this simulation while the other variables were used from the previous study [Yoshimura et al., 2008]. This study focus on the accuracy of streamflow prediction during August, September, and October in 2011. In this study, as noted, we selected June as the initial prediction, which gives enough time for selecting reservoir operation since the beginning of the wet season. Therefore, August, September, and October are with 3, 4 and 5-month prediction lead-time.

A river discharge comparison between streamflow prediction and observed river discharge is shown in Figure 3.4.2.1. Figure 3.4.2.1 shows the deviation results of average discharge during August, September, and October in 2011. Streamflow predictions corrected by quantile mapping are underestimated.

There are two reasons for the underestimation. The first reason is that raw rainfall data from August to October is already close to observed rainfall data. Bias corrected rainfall prediction are underestimated after bias correction with reference rainfall data, where there eventually was an unexperienced rainfall.

The second reason is similar to the first reason but for a different period, which is June to July. Streamflow simulations for August to October require June and July rainfall predictions in this study. In other words, continuously underestimated rainfall prediction since June could cause biases in streamflow predictions.

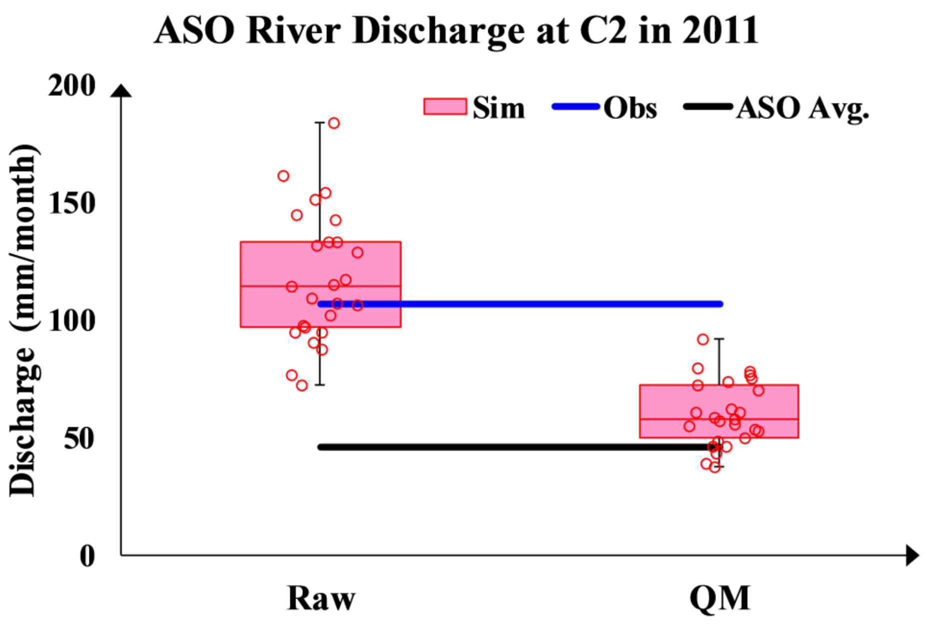

Figure 3.4.2.1 Streamflow prediction in 2011. The red box shows the deviation of prediction results. Blue line shows the observed river discharge in 2011. Black line shows the 30-year average of natural flow during August, September, and October in CPRB. Dot red color represents each 25-predictions results.

3.4.3 Impact of seasonal streamflow prediction on reservoir operation

A set of simulations of H08 with reservoir operation was done to represent the impact of reservoir operation. Figure 3.4.3.1 shows a simulation of dam storage of two reservoirs in 2011. PlanU (Red line) indicates a simulation of H08 with the reservoir model that used PlanU in 2011. The alternative operation schemes are Rev0.5Jul (blue line color) and Rev0.25Jul (green line color).

PlanU shows an underestimation when compared with the observed data in 2011 for both reservoirs because H08 continuously releases the water for the dry season and wet season, while the actual release from both reservoirs is different each month. The concept of Rev0.5Jul and Rev0.25Jul provides enough storage to prepare the upcoming water during the peak period. The storage dramatically drops for Rev0.5Jul and Rev0.25Jul at the end of July, which the target storage is set as 50 and 25 percentages of total storage. After that, the storage is increased for both Rev0.5Jul and Rev0.25Jul by inflow from the upstream area.

Figure 3.4.3.2 shows the impact of reservoir operation on daily river discharge at C2 station. PlanU's river discharge is overestimated from September to October. One of the reasons is the overestimation of input rainfall data. However, the overall results show a good agreement with observed river discharge in 2011 (black dot line). The river discharge by Rev0.5Jul was increased during the beginning of August because reservoirs needed to release more water, which is to prepare enough storage for the peak period. On the other hand, Rev0.25Jul's river discharge is gradually increased from June until August.

The streamflow prediction results from section 3 were used to select a reservoir operation scheme in this section. Table 3.4.3.1 shows the selected operation schemes from streamflow prediction results using the criteria we set. In summary, a set of 25 streamflow predictions using quantile mapping mostly selected PlanU. Only one out of 25 simulations of quantile mapping selected Rev0.25Jul as the reservoir operation.

Nevertheless, the impact of Rev0.5Jul and Rev0.25Jul on discharge and dam storage are shown in Figure 3.4.3.1 and Figure 3.4.3.2. The Rev0.25Jul could mitigate the flood with 18 percent difference when compared to PlanU (red line), while Rev0.5Jul could mitigate around 5 percent during the peak discharge.

Table 3.4.3.1 Selecting operation scheme from streamflow prediction

Simulation	≤ 40 %	40 % - 60 %*	≥ 60 %	Operation scheme
QM	22	2	1	PlanU

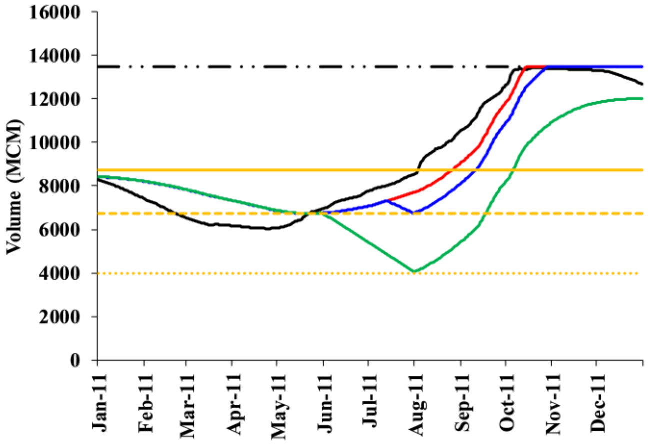

(a)

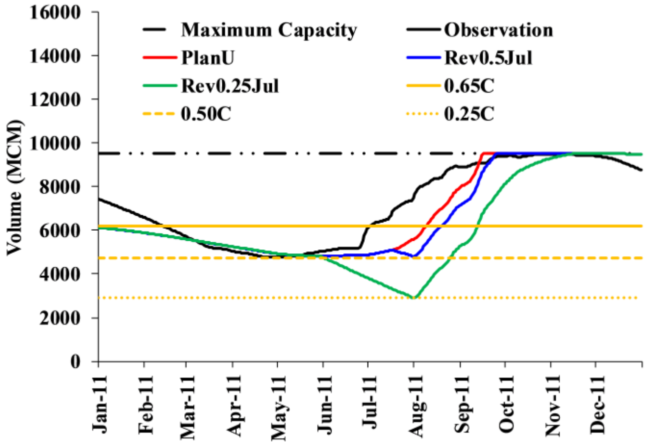

(b)

Figure 3.4.3.1 Dam storage of (a) Bhumibol and (b) Sirikit reservoir in 2011 by PlanU (Red line), Rev0.5Jul (Blue line) and Rev0.25Jul (Green line) scheme.

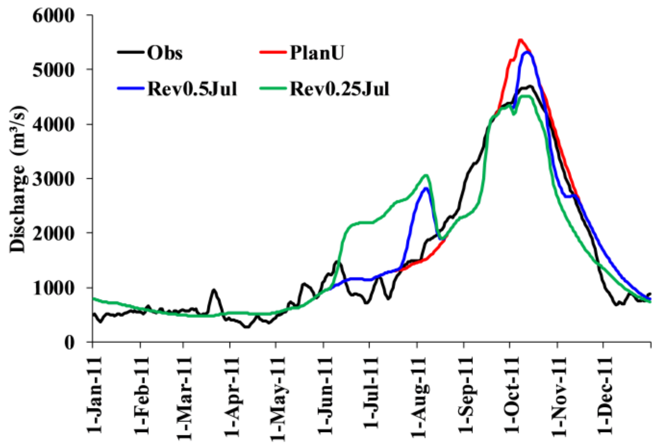

Figure 3.4.3.2 Comparison of daily river discharge at C2 station in 2011 between observed river discharge (Black line), simulation using PlanU (Red line), Rev0.5Jul (Blue line) and Rev0.25Jul (Green line) scheme.

Figure 3.4.3.3 and Figure 3.4.3.4 show the outflow at Bhumibol and Sirikit reservoir. From the results, the outflow rate using Rev0.50Jul and Rev0.25Jul increase during July to August and June to August, respectively.

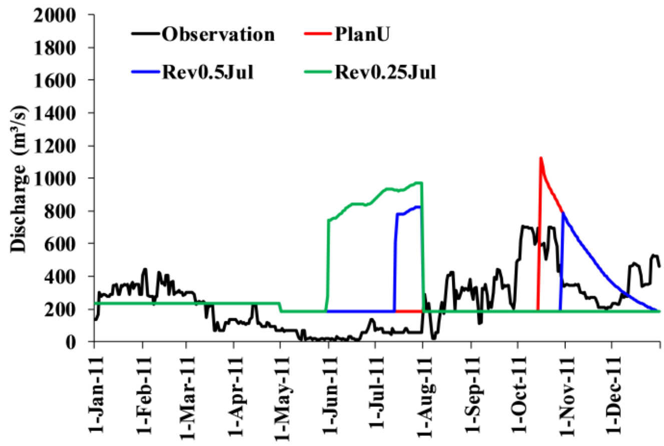

Figure 3.4.3.3 Comparison of daily outflow at Bhumibol reservoir in 2011 between observed river discharge (Black line), simulation using PlanU (Red line), Rev0.5Jul (Blue line) and Rev0.25Jul (Green line) scheme.

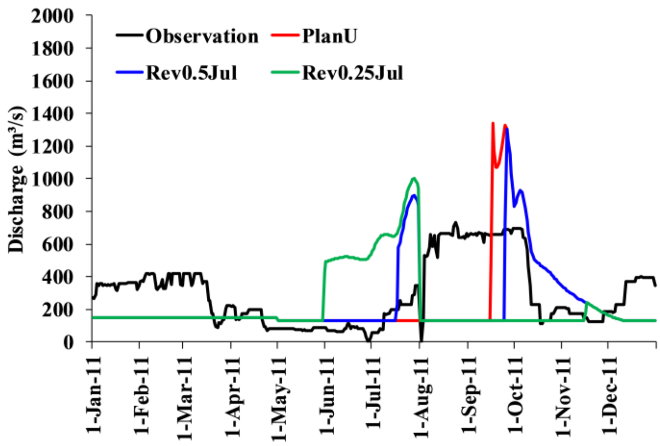

Figure 3.4.3.4 Comparison of daily outflow at Sirikit reservoir in 2011 between observed river discharge (Black line), simulation using PlanU (Red line), Rev0.5Jul (Blue line) and Rev0.25Jul (Green line) scheme.

3.5 Conclusion

The hydrological model (H08 model), which was calibrated from the previous study, can be well represented the hydrological process in the Chao Phraya River Basin, especially at C2 station. Although, there is low accuracy at Nan River due to human activity and the calibrated four parameters were calibrated to apply to all grid cells within the Chao Phraya River Basin, which might be not suitable for Nan river basin.

As for the use seasonal predictive information. This study's chapter set the criteria to select a reservoir operation using seasonal streamflow predictions at the beginning of the wet season. Most of the results of streamflow prediction are lower than 40 percent different from the average natural flow, which leads to select PlanU as the reservoir operation scheme in 2011. One simulation by quantile mapping, out of 25 ensemble members, that selected Rev0.25Jul for an operation that could mitigate flooding during the peak period in October with a lesser peak amount about 18 percent.

However, the advantage of the criteria could be easy to apply. The disadvantage of this method is not the consideration of a drought event that requires further study. In addition, the methodology in chapter 3 was still not the adaptation reservoir operation. In reality, rainfall prediction can be produced every month. Bias correction quantile mapping could improve the accuracy of rainfall prediction. However, due to 2011 raw rainfall prediction was already close with observed data, bias-corrected rainfall prediction was underestimated for the unexperienced 2011 flood.

Chapter 4

Use of Seasonal Streamflow Forecasts for Flood Mitigation with Adaptive Reservoir Operation

Abstract of this chapter

Chapter 4 presents the second method to use the seasonal predictive data to support operation plan in Chao Phraya River Basin. In this chapter, the hydrological model (H08 model) is forced with an ensemble of seasonal precipitation data from European Centre for Medium - Range Weather Forecasts (ECMWF) to select the operation plan. The 6 month ECMWF prediction period was used to support the operation plan for mitigating flooding around each reservoir during the wet season. Decision-making for reservoir operation based on seasonal predictions was conducted on a monthly time scale. In this chapter, two alternative reservoir operation, which are 1) reservoir operation by following the 2011 rule curve and 2) reservoir operation by setting the target storage, are present in this chapter. The results showed that peak river discharge decreased slightly, by around 4%, when seasonal predictive data were used. Moreover, changing the reservoir operation plan and using seasonal predictions decreased the peak river discharge by around 20%.

4.1 Methodology for using predictive data to support reservoir operation

4.1.1 Hydrological model and data

The H08 model [Hanasaki et al., 2008] is also used to simulate the hydrological process in the Chao Phraya River Basin in this chapter. Because this study was focused on the use of seasonal predictive data for water management through reservoir operation, the land surface hydrology, river routing, and reservoir operation models were used. The details of H08 model and the setting of the H08 model is explained in chapter 2 and 3, respectively.

Seasonal precipitation data generated with the European Centre for Medium - Range Weather Forecasts (ECMWF) System 5 [Johnson et al., 2019] were used as input data. The details of ECMWF System 5 is explained in chapter 2. In this chapter, the seasonal ECMWF predictive data was selected a starting prediction month of June (the start of the wet season) and conducted seasonal precipitation prediction for July, August, and September.

Geographic data and meteorological forcing data, such as daily observed temperature, relative humidity, wind speed, wave radiation, and surface air pressure, were obtained from previous research [Yoshimura et al., 2008, Kotsuki et al., 2010].

Prior to using the seasonal predictive data, we used a popular bias correction method, namely, quantile mapping, to increase the accuracy of rainfall prediction. The outputs from the climate model are usually produced at a coarse grid scale, which may lead to errors in capturing forecast uncertainty and introduce biases. Quantile mapping [Themeßl et al. 2011] was used to correct the cumulative distribution function between the observed rainfall data from 1987 to 2010 and the seasonal rainfall forecast data in the CPRB. The bias correction technique was applied to data in a grid-to-grid manner.

4.1.2 Adaptation of reservoir operation based on predictive data

Four parameters are essential to simulating reservoir operation in the reservoir operation sub-model of the H08 model: the rate of release during the dry season, the rate of release during the wet season, target storage, and the target storage date. In a previous study [Mateo et al., 2013], target storage and the target storage date were altered to create an alternative reservoir operation schedule. However, when using predictions for adaptive reservoir operation each month, one can only control the rate of release. Moreover, reservoir operation, particularly during the wet season, is crucial for decision-making to mitigate flooding and storing the appropriate amount of water to support society. Thus, the difference between this study and previous research is that we changed the rates of release from the Bhumibol and Sirikit reservoirs for each month during the wet season based on the monthly predictive data.

Reservoir operation in this study occurred from June to October, because June and October are the first and last months of the wet season, respectively. Two alternative reservoir operations were adaptively applied, as shown in Figure 4.1.2.1. The first

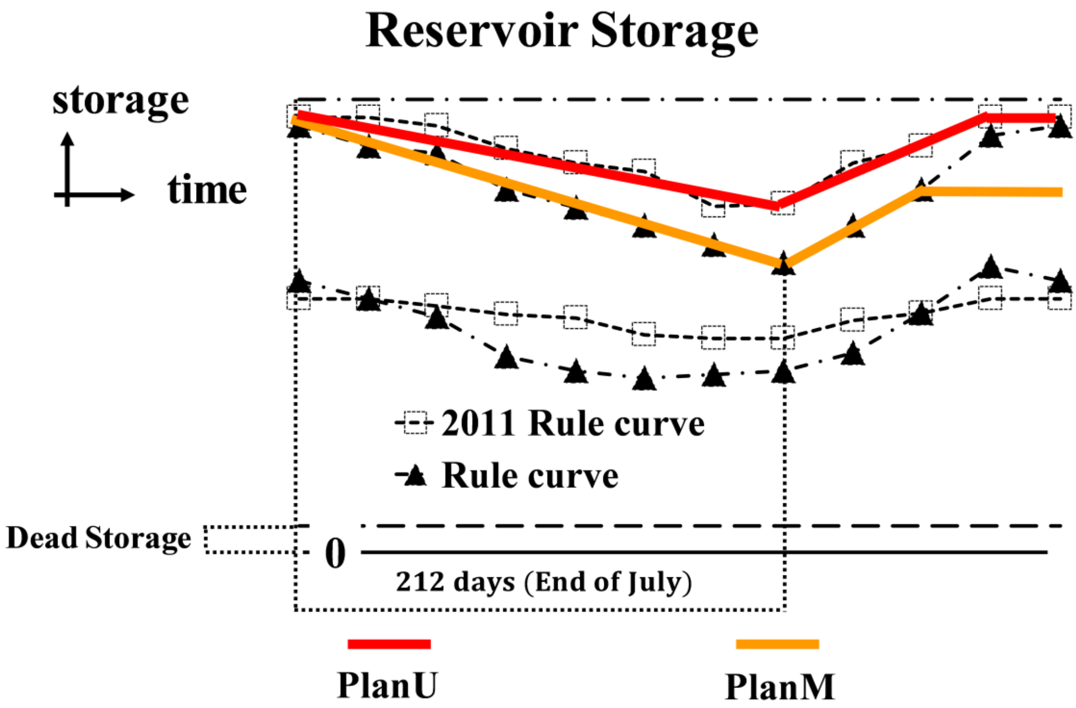

Figure 4.1.2.1. Reservoir operation that used in this chapter; PlanU (red line), and PlanM (yellow line).

alternative operation was simply to follow the rule curve of each reservoir. We refer to this strategy as "PlanU" operation, because reservoir storage is limited by the upper rule curve. The second alternative operation was to follow a new rule curve proposed after the 2011 flood until the end of October. In addition, we set the target storage for each reservoir, which resembled the reservoir operation proposed in a previous study [Mateo et al., 2013]. The second alternative operation is designated "PlanM" operation here. The main difference between the two plans is the amount of reservoir storage.

After the flooding of 2011, the rule curves of the reservoirs were changed (this is usually done once per decade) from the dashed line with squares to the dashed line with triangles shown in Figure 4.1.2.1. If the water manager controls the water level using the rule curve, the maximum reservoir storage available during the wet season to support the dry season is about 15,350 MCM: about 8,750 MCM in the Bhumibol reservoir and about 6,600 MCM in the Sirikit reservoir. In addition, the water demand in the CPRB [Thai water] is about 11,377 MCM per year. Thus, the target storage level to meet water demand can be attained if the Bhumibol and Sirikit reservoirs meet about 78% and 87% of their total storage capacities, respectively. Therefore, the purpose of PlanM is to prevent overflow at both reservoirs by setting the target storage level, thereby mitigating flooding.

In this chapter, the reservoir operation rule was set as followed:

1) No change in reservoir operation if most reservoir storage predictive data (more than 50% of the total ensemble members of prediction) fall between the upper rule curve and lower rule curve.

2) Increase the rate of outflow until most reservoir storage is below the upper rule curve if most predicted reservoir storage is above the upper rule curve.

3) Decrease the rate of outflow until most reservoir storage is above the lower rule curve if most predicted reservoir storage is below the lower rule curve.

4) Stop increasing the rate of outflow if most river discharge predictions are above the river storage capacity at station C2 in that month.

Figure 4.1.2.2 shows an image of operation plan based on seasonal prediction from the above conditions, which is set in this chapter.

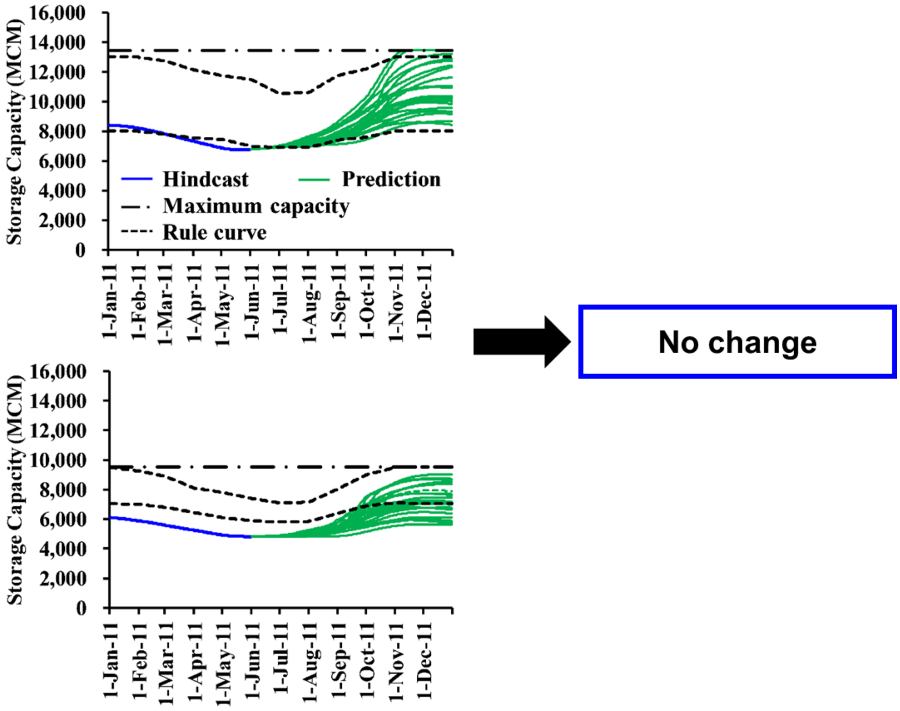
Storage Capacity (MCM)
Hindcast
Prediction
Maximum capacity
Rule curve
No change
1-Jan-11
1-Feb-11
1-Mar-11
1-Apr-11
1-May-11
1-Jun-11
1-Jul-11
1-Aug-11
1-Sep-11
1-Oct-11
1-Nov-11
1-Dec-11

(a)

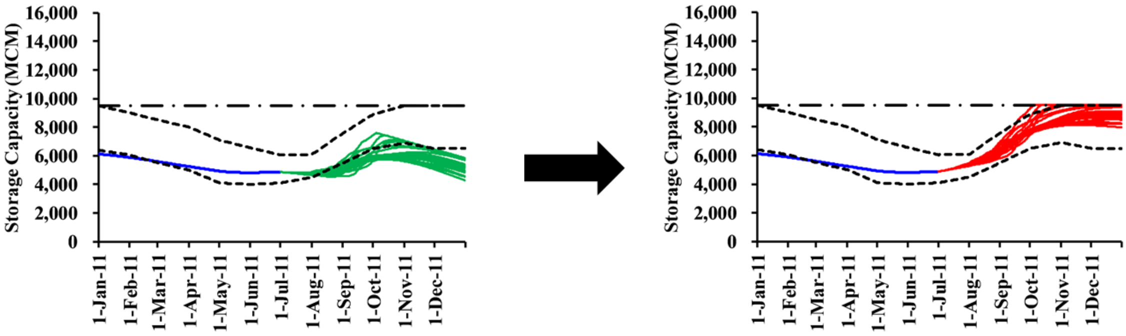
Storage Capacity (MCM)
1-Jan-11
1-Feb-11
1-Mar-11
1-Apr-11
1-May-11
1-Jun-11
1-Jul-11
1-Aug-11
1-Sep-11
1-Oct-11
1-Nov-11
1-Dec-11

(b)

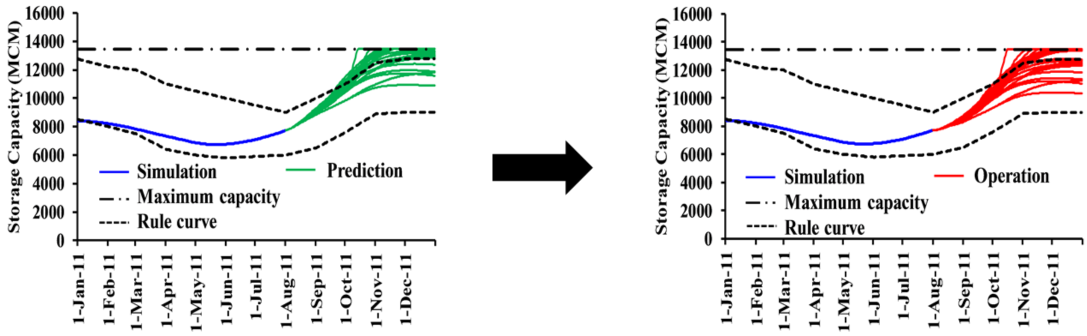

(c)

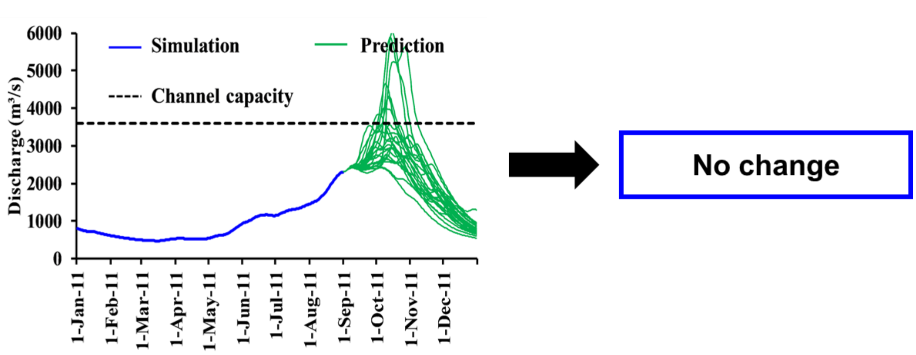

(d)

Figure 4.1.2.2 Image of operation plan setting in this chapter.

Figure 5 shows the flowchart, which represents the methodology of using predictive data to support reservoir operation in this study. The current method use the seasonal predictive data to obtain prediction if river discharge and reservoir storage with a 6-month prediction period. The streamflow prediction and dam storage prediction was produced every month from the beginning of the wet season until the late of the wet season (June to September) with the 6 month lead-time. The Out_{new} is the reservoir release after increase/decrease the release rate, Out is reservoir release before increase/decrease the release rate, and RC is rule curve. The $DisSta_{50}$ is discharge prediction at station in the downstream area (more than 50% of total ensemble members), $DamSto_{50}$ is dam storage prediction (more than 50% of total ensemble members), RivSto is the river storage capacity, and $Adap_{out}$ represents the increasing and decreasing outflow rate.

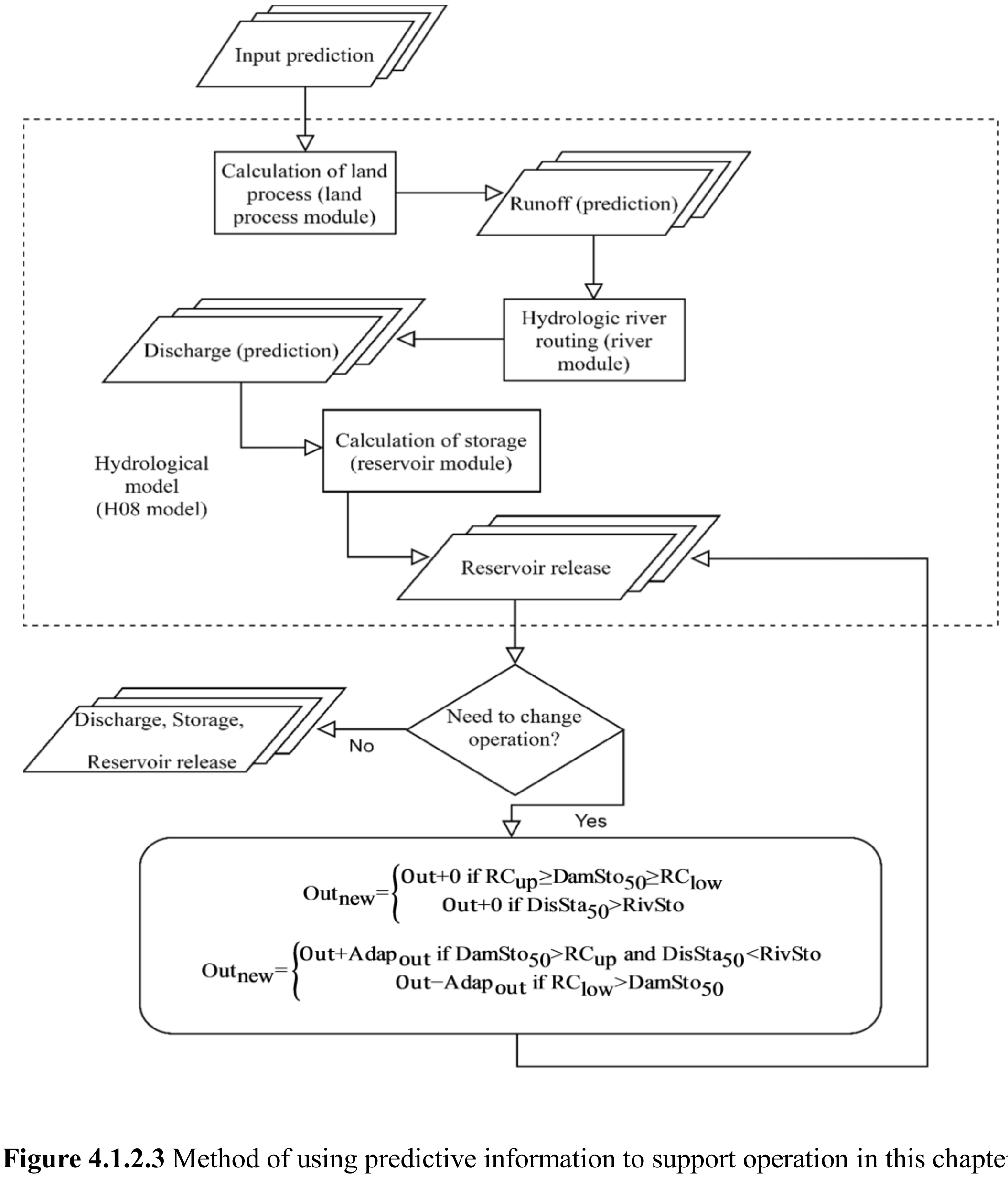

Figure 4.1.2.3 Method of using predictive information to support operation in this chapter.

4.2 Results and discussion

4.2.1 Reliability of the predictive data

Simulations from 25 ensembles for river discharge using the original ECMWF System 5 predictive data and bias-corrected predictive data are shown in Figure 4.2.1.1, with a 0-month lead time from June to October. This section is selected results with a 0-month lead time because the reservoir is operated the reservoir at monthly intervals. The initial conditions for simulating the 0-month lead time predated the prediction month. For example, we used the initial prediction in May for the June prediction. A comparison of daily discharge between the observed data and predictive data using the original ensemble is shown in Figure 4.2.1.1 (a). The ensemble simulation of river discharge using the original ECMWF System 5 predictions (Figure 4.2.1.1 (a)) is generally higher than the observed river discharges. During the peak period in October, simulations using the original ECMWF prediction were higher than the observed data, including the Thai operation simulation. A comparison of predictive data using the bias-corrected ensemble is shown in Figure 4.2.1.1 (b). The ensemble simulation of river discharge using bias-corrected predictive data showed improved accuracy compared with ensemble simulation of river discharge using the original ECMWF prediction.

The ensemble simulation results for river discharge using the bias correction technique were lower than those for Thai operation (red line in Figure 4.2.1.1) but still higher than the observed data. The reason for these differences is that 2011 was an abnormal year, and Thailand had not previously experienced an extreme event like the 2011 flooding. Thus, when we apply a bias correction to historical data, the predicted results are underestimates. Overall, the accuracy of the ensemble river discharge prediction was improved with the quantile mapping bias correction technique. We used the root mean square error (RMSE), relative mean error (RME), coefficient of variation of the RMSE (CV), Nash–Sutcliffe efficiency (NSE), and coefficient of determination (R2) to determine the accuracy. The results for each accuracy index are shown in Figure 4.2.1.2. The 0-month lead time prediction improved after bias correction; in particular, the NSE showed a significant improvement. However, some months, such as August, had lower accuracy after bias correction, because the simulation used original predictive data similar to the observed data, in particular in 2010.

The simulation results using the bias-corrected predictive data were underestimates, in particular for extreme events such as the 2011 flood. The underestimation of simulated discharge after bias correction has been reported in previous studies [Cannon et al., 2015]. This problem is caused by the bias correction itself, which uses previous observations to correct the predictive data. Thus, bias correction does not always improve the accuracy of predictive data, particularly for extreme events.

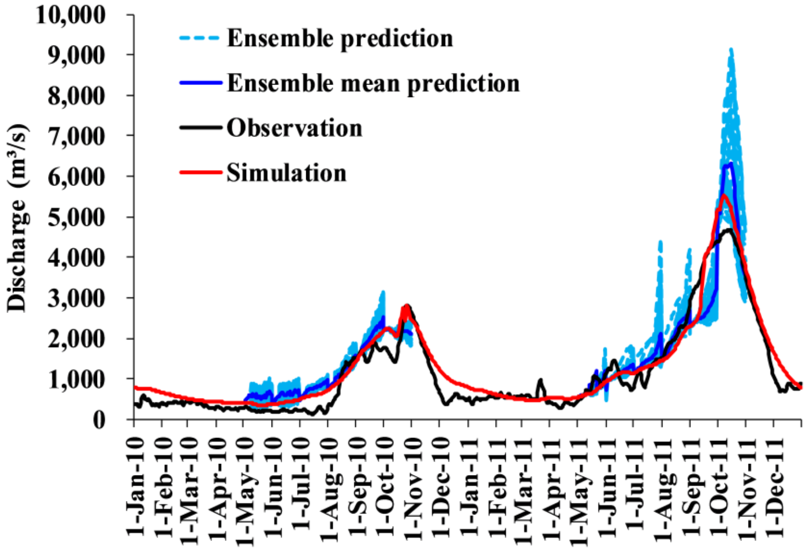

(a)

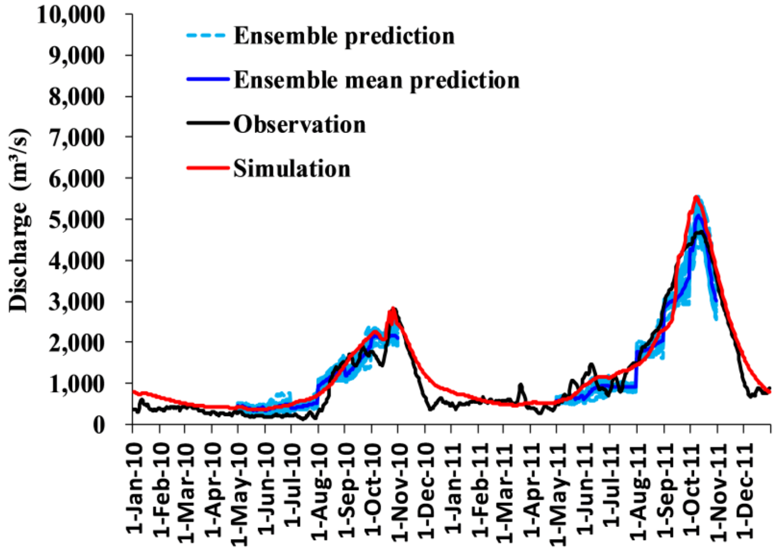

(b)

Figure 4.2.1.1 Comparison of daily discharge at station C2 between observations (black line), simulation results (red line), simulation results using ensemble predicted rainfall data (light blue dotted line), and the median of simulation data using ensemble predicted rainfall data (blue line). Simulation results using (a) the original European Centre for Medium‐Range Weather Forecasts (ECMWF) System 5 ensemble predicted data and (b) bias-corrected ensemble predictions.

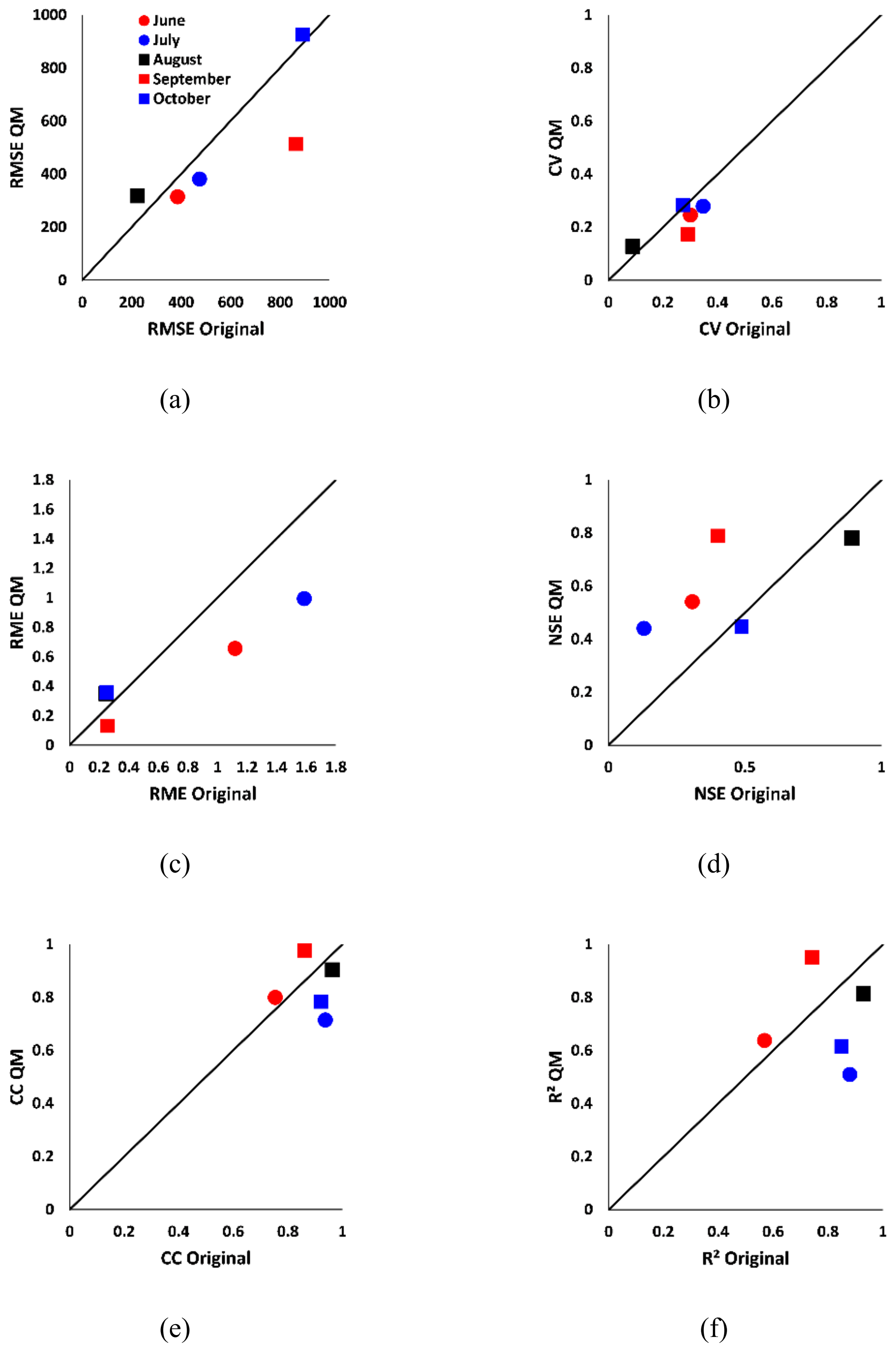

Figure 4.2.1.2 Scatter plot of accuracy indices between simulated daily discharge using the original predicted data (x-axis) and simulated daily discharge using quantile mapping (y-axis). (a) Root mean square error (RMSE); (b) coefficient of variation of the RMSE (CV); (c) relative mean error (RME); (d) Nash–Sutcliffe model efficiency coefficient (NSE); (e) coefficient of determination (R2); (f) correlation coefficient (CC).

4.2.2 Adaptive operation using predictive data

Reservoir storage predictions from June are shown in Figure 4.2.2.1. No change in reservoir operation occurred in June, because most reservoir storage predictions (more than 50% of the total ensemble predictions) fell between the rule curves of both the Bhumibol and Sirikit reservoirs. Although the first prediction month for the Sirikit reservoir fell below the rule curve, most reservoir storage predictions were within that range at the end of December. Prediction of river discharge for July at station C2 is shown in Figure 4.2.2.2 (a). Figure 4.2.2.2 (b) and Figure 4.2.2.2 (c) shows predictions of reservoir storage for July at the Bhumibol and Sirikit reservoir. The tendency for the risk of reservoir storage to be above the maximum capacity is apparent. However, most ensemble predictions remained under the upper rule curve in both reservoirs. Therefore, no changes in the rate of outflow from either reservoir were made in July. Thus, no difference was observed between adaptive operation using predictive data and adaptive operation without predictive data, as shown in Figure 4.2.2.2.

Predictive data without adaptive operation, shown in Figure 4.2.2.3, indicated that most ensemble predictions were higher than the upper rule curve and reached the maximum capacity of both reservoirs (Figure 4.2.2.3 (b) and Figure 4.2.2.3 (c)). Based on this result, we increased the rate of outflow from the two reservoirs until most ensemble predictions for reservoir storage (more than 50% of the total ensemble predictions) fell between the rule curves. The results after we increased the rate of outflow from both reservoirs are shown as a red dashed line. As a result of the increased rate of outflow in August, river discharge increased after adaptive operation using predictive data, as indicated by the pink line in Figure 4.2.2.3 (b) and Figure 4.2.2.3 (c), which shows that most ensemble predictions after adaptive operation fell between the rule curves.

The ensemble predictive data for September, in which we used the increased rate of outflow in August for simulation, are shown in Figure 4.2.2.4 (a), Figure 4.2.2.4 (b), and Figure 4.2.2.4 (c). No adaptive operation was conducted in the Bhumibol and Sirikit reservoirs, because most ensemble predictions for reservoir storage were within the range of the rule curves. The results of ensemble prediction without adaptive operation and with adaptive operation using predictive data are presented in Figure 4.2.2.4 (a), Figure 4.2.2.4 (b), and Figure 4.2.2.4 (c). Because no change in operation occurred in September, there was no difference in September.

The discharge predictions for September tended to decrease from the beginning to the middle of the month. The reason for this could related to the discharge from the upstream area, which was controlled by the two reservoirs. In addition, the amount of rainfall began to decrease in September relative to August. For this reason, the discharge predictions increased rapidly after the middle of the month because dam storage reached its maximum capacity in both reservoirs; that is, the sudden increase in predicted discharge in September was due to concurrent changes in the rates of release from both reservoirs. Because peak discharge is in October, the rate of outflow cannot change in October. Thus, September was the last month in which reservoir operations could be conducted.

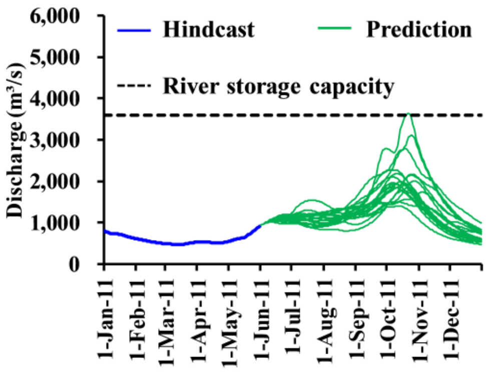

(a)

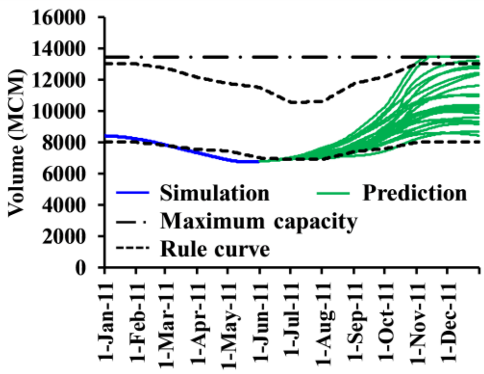

(b)

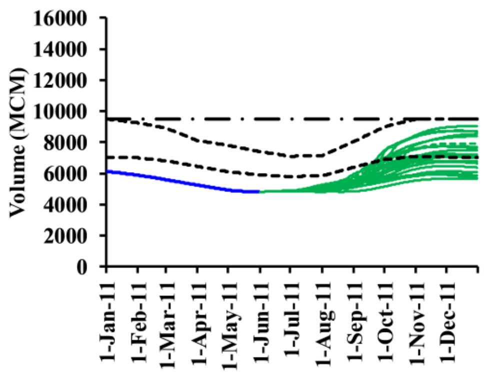

(c)

Figure 4.2.2.1 River discharge at station C2 (a) and reservoir storage predictions (green line) from June until December at the Bhumibol (b) and Sirikit (c) reservoir. Blue line represents simulation using observed meteorological data (hindcast). Black dashed line represents rule curve. Dash-point black line represents maximum storage capacity.

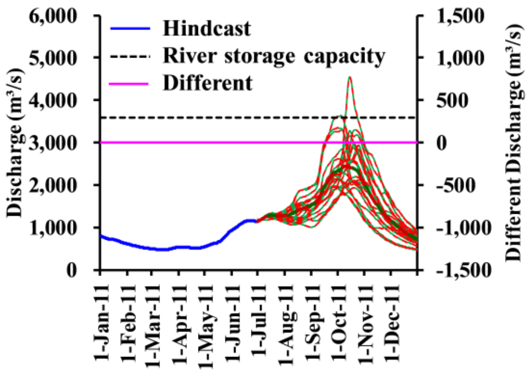

(a)

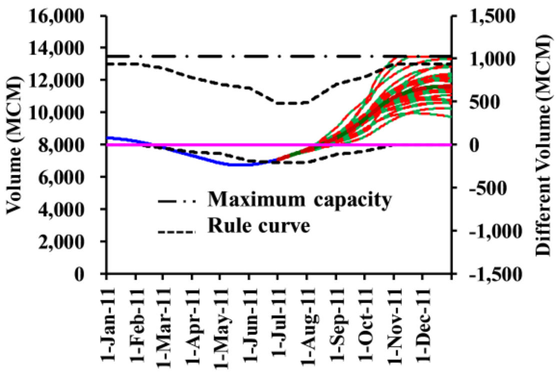

(b)

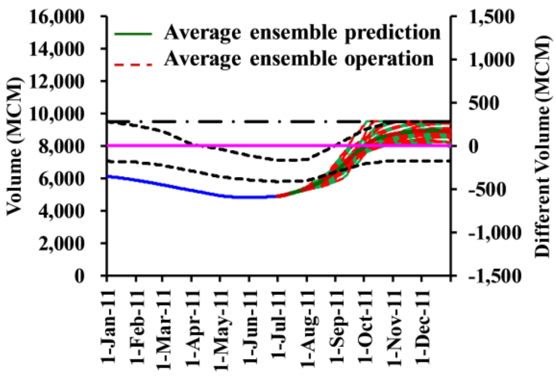

(c)

Figure 4.2.2.2 River discharge predictions at station C2 (a) and storage predictions from July until December at the Bhumibol (b) and Sirikit (c) reservoir, shown with the green line, and river discharge and storage prediction after adaptive operation with predictive data from July until December (red dashed line).

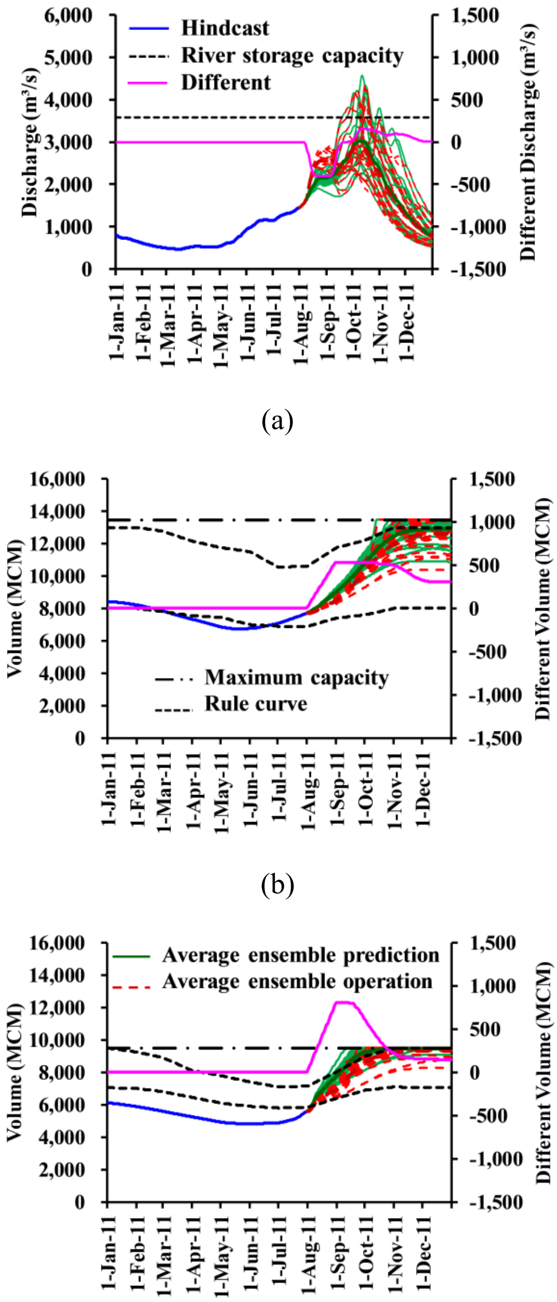

(a)

(b)

(c)

Figure 4.2.2.3 River discharge predictions at C2 station (a) and storage predictions from August until December at the Bhumibol (b) and Sirikit (c) reservoir, shown with the green line, and river discharge and storage predictions after adaptive operation with predictive data from August until December (red dashed line).

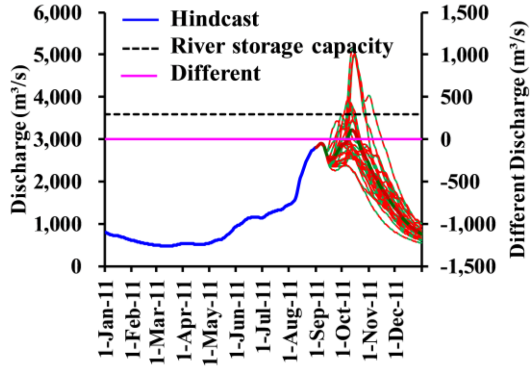

(a)

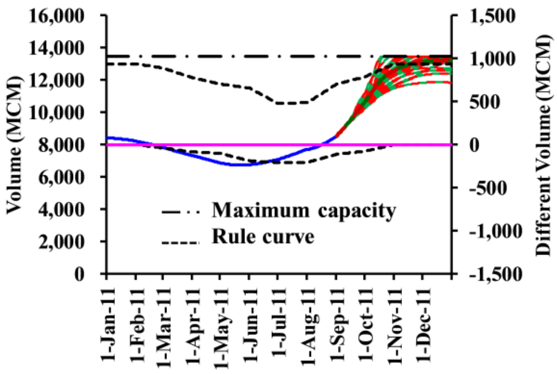

(b)

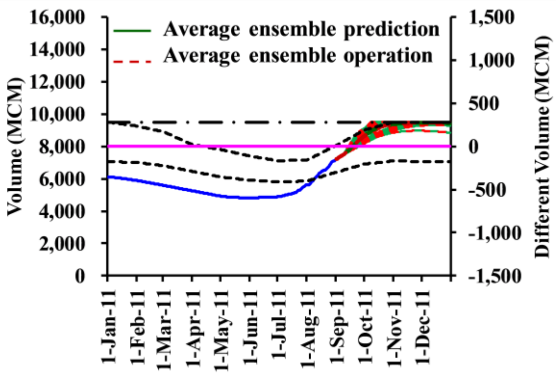

(c)

Figure 4.2.2.4 River discharge predictions at C2 station (a) and storage predictions from September until December at the Bhumibol (b) and Sirikit (c) reservoir, shown with the green line, and river discharge and storage predictions after adaptive operation with predictive data from September until December (red dashed line).

4.2.3 Adaptive operation using predictive data based on PlanM operation

The operating conditions for this simulation were the same as those for the previous simulation, which are explained in Section 4.1.2. The upper rule curve of PlanM is represented with an orange line as shown in Figure 4.1.2.1. Thus, most ensemble predictions for reservoir storage had to fall under the orange line and above the lower rule curve. The prediction period began in June.

The results of adaptive operation with predictive data beginning in July are shown in Figure 4.2.3.1. As shown in Figure 4.2.3.1 (b) and Figure 4.2.3.1 (c), most ensemble predictions for reservoir storage were higher than the target storage (orange dashed line). Therefore, we increased the rate of outflow from both reservoirs in July until the ensemble prediction for reservoir storage was under the target storage level (orange dashed line) and above the lower rule curve shown in Figure 4.2.3.1 (a), Figure 4.2.3.1 (b) and Figure 4.2.3.1 (c). The difference relative to before the adaptive operation is shown with a pink line.

We used the rate of release after adaptive operation using predictive data to obtain predictions for August, as shown in Figure 4.2.3.2 (a), Figure 4.2.3.2 (b) and Figure 4.2.3.2 (c). Most ensemble predictions of reservoir storage were higher than the target storage level (orange dashed line) in both reservoirs. Thus, we increased the rate of outflow in August until most ensemble predictions for reservoir storage (more than 50% of the total ensemble predictions) were under the target storage level (orange dashed line) and above the lower rule curve. The results after adaptive operation using predictive data from PlanM for August are represented by the orange dashed lines in Figure 4.2.3.3 (a), Figure 4.2.3.3 (b) and Figure 4.2.3.3 (c). We increased the rate of outflow from the two reservoirs until the ensemble prediction for reservoir storage was near the lower rule curve and near the river storage capacity at station C2. However, most ensemble predictions remained higher than the target storage of the Bhumibol and Sirikit reservoirs (orange dashed line). Nonetheless, most ensemble predictive data fell between the rule curves for both reservoirs.

The prediction results for September are shown in Figure 4.2.3.3. No adaptive operation was conducted based on predictive data, although most ensemble predictions for reservoir storage were higher than the target storage level (orange dashed line). River discharge in September tended to decrease from the beginning until the middle of the month. The reason for this could be related to the discharge from upstream, which was controlled by the two reservoirs. In addition, the amount of rainfall in September began to decrease relative to August. Thus, the discharge predictions after the middle of the month increased rapidly because the dam storage of both reservoirs reached maximum capacity. No adaptive operation was undertaken in October, because October is the month of peak discharge. Thus, September was the last month of adaptive operation.

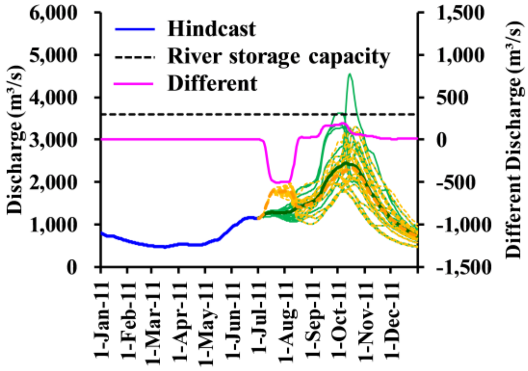

(a)

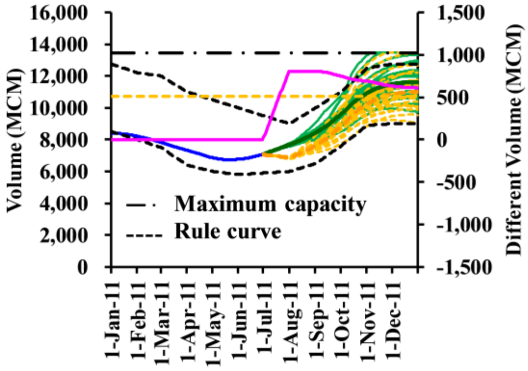

(b)

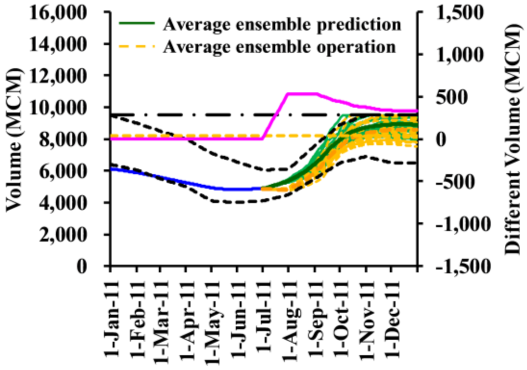

(c)

Figure 4.2.3.1 River discharge predictions at station C2 (a) and storage predictions from July until December at the Bhumibol (b) and Sirikit (c) reservoir, shown with the green line, and river discharge and storage predictions after adaptive operation with predictive data from July until December (orange dashed line).

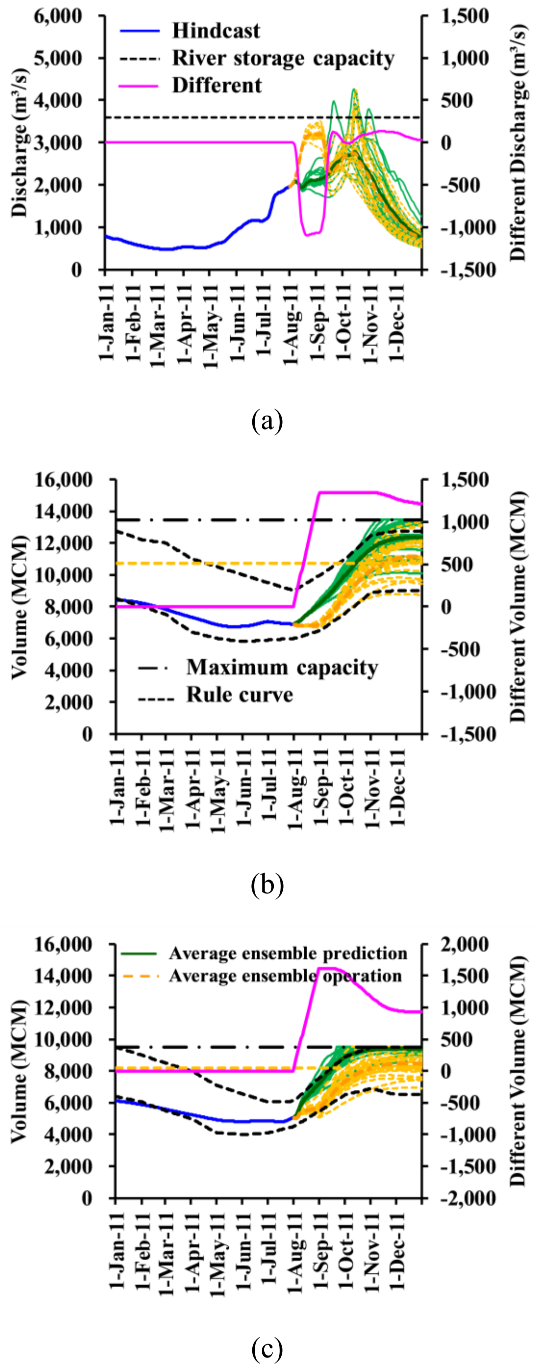

(a)

(b)

(c)

Figure 4.2.3.2 River discharge predictions at station C2 (a) and storage predictions from August until December at the Bhumibol (b) and Sirikit (c) reservoir, shown with the green line, and river discharge and storage prediction after adaptive operation with prediction data from August until December (orange dashed line).

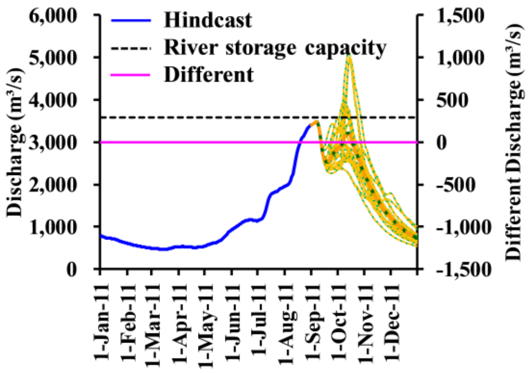

(a)

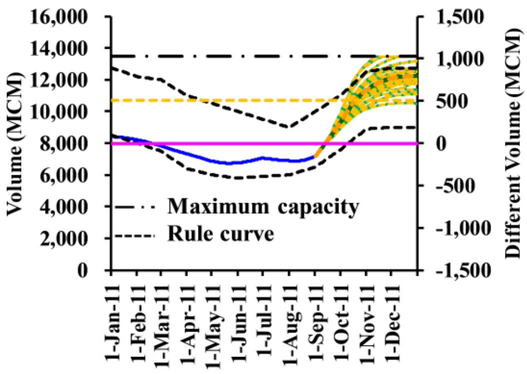

(b)

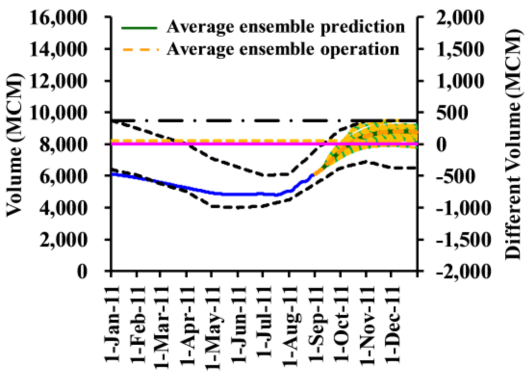

(c)

Figure 4.2.3.3 River discharge prediction at station C2 (a) and storage prediction from September until December at the Bhumibol (b) and Sirikit (c) reservoir, shown with the green line, and river discharge and storage prediction after adaptive operation with predictive data from September until December (orange dashed line).

4.2.4 Sensitivity test on adaptive operation using predictive data

In this section, the sensitivity tests of adaptive operation were carried out. The operation conditions in this section were the same as Section 4.2.2 and Section 4.2.3 except that most of ensemble prediction was changed from 50 percentages into 40 percentages and 60 percentages, respectively.

4.2.4.1 40 percentages

The results of adaptive operation with predictive data beginning in August because most of the ensemble predictions (40 percentages) for reservoir storage had to fall under the upper and lower rule curve in June and July. As shown in Figure 4.2.4.1 (b) and Figure 4.2.4.1 (c), it was found that more than 40 percentages of ensemble predictions were higher than the upper rule curve. Thus, the rate of outflow was increased until 40 percentages of ensemble predictions fall between the upper rule curve and lower rule curve.

Figure 4.2.4.2 shows the results of adaptive operation in September. However, there were no change in both reservoirs although more than 40 percentages of ensemble predictions for reservoir storage were higher than the upper rule curve. The reason that there were no operation changes because if the outflow rate increase then most of discharge predictions were higher at station C2, which reach the reservoir channel capacity.

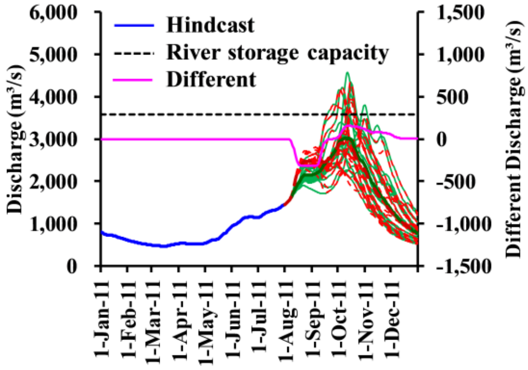

(a)

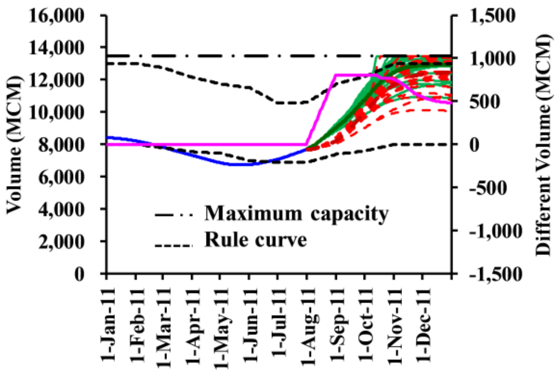

(b)

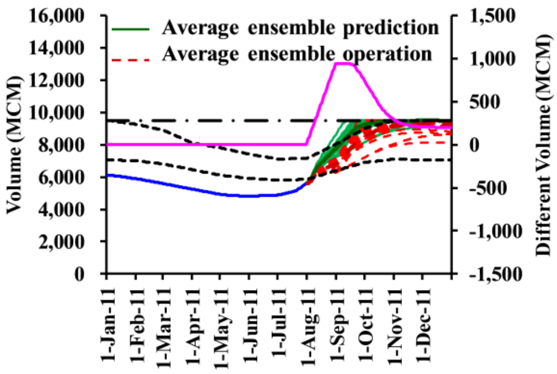

(c)

Figure 4.2.4.1.1 River discharge prediction at station C2 (a) and storage prediction from August until December at the Bhumibol (b) and Sirikit (c) reservoir, shown with the green line, and river discharge and storage prediction after adaptive operation with predictive data from August until December (red dashed line).

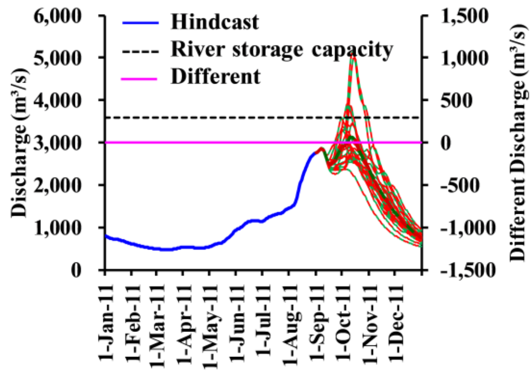

(a)

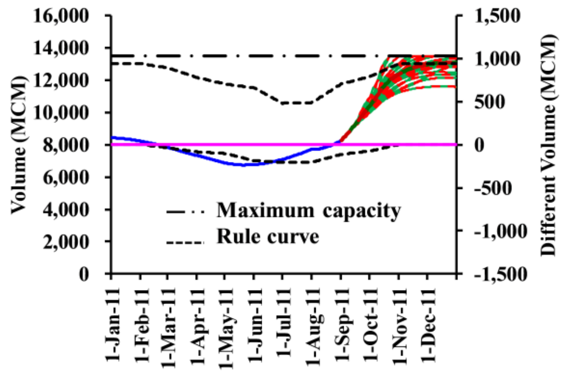

(b)

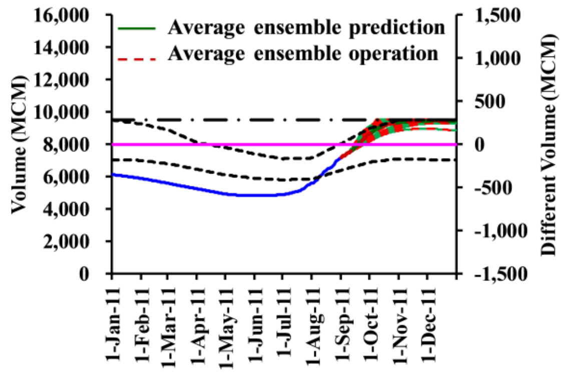

(c)

Figure 4.2.4.1.2 River discharge prediction at station C2 (a) and storage prediction from September until December at the Bhumibol (b) and Sirikit (c) reservoir, shown with the green line, and river discharge and storage prediction after adaptive operation with predictive data from September until December (red dashed line).

4.2.4.2 60 percentages

The results of adaptive operation with predictive data beginning in this section also was in August because most of the ensemble predictions (60 percentages) for reservoir storage had to fall under the upper and lower rule curve in June and July. As shown in Figure 4.2.4.2.1 (b) and Figure 4.2.4.2.1 (c), it was found that most of ensemble predictions (in this case is 60 percentages) were higher than the upper rule curve. Thus, the rate of outflow was increased until 60 percentages of ensemble predictions fall between the upper rule curve and lower rule curve.

There were no change in both reservoirs as shown in Figure 4.2.4.2.2 although more than 40 percentages of ensemble predictions for reservoir storage were higher than the upper rule curve. The reason that there were no operation changes because if the outflow rate increase then most of discharge predictions were higher at station C2, which reach the reservoir channel capacity.

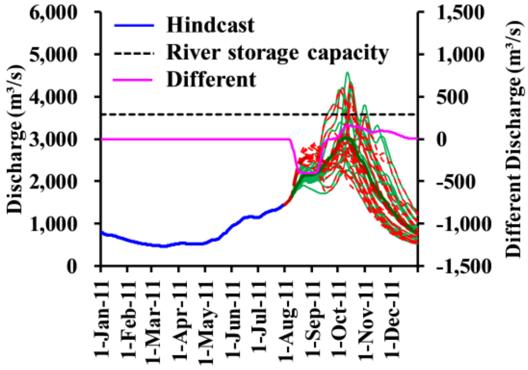

(a)

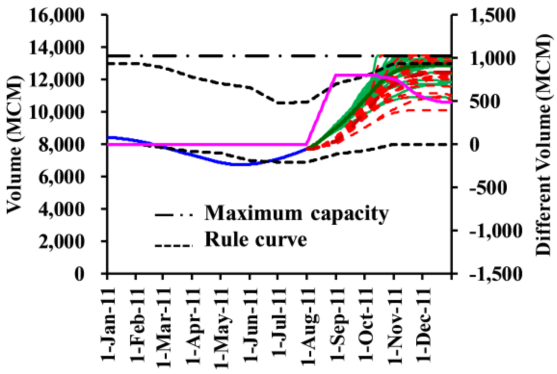

(b)

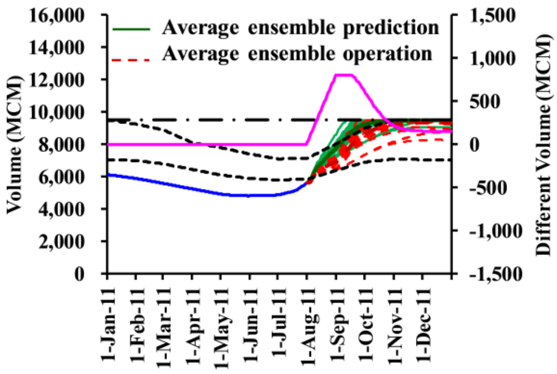

(c)

Figure 4.2.4.2.1 River discharge prediction at station C2 (a) and storage prediction from August until December at the Bhumibol (b) and Sirikit (c) reservoir, shown with the green line, and river discharge and storage prediction after adaptive operation with predictive data from August until December (red dashed line).

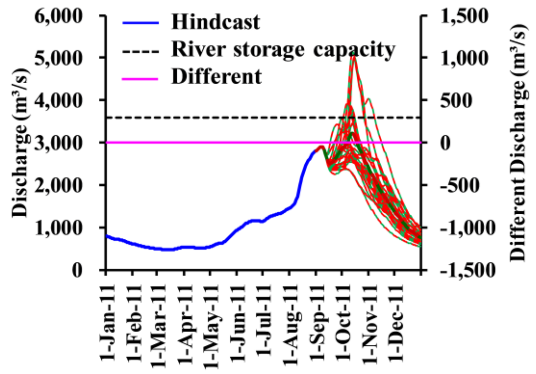

(a)

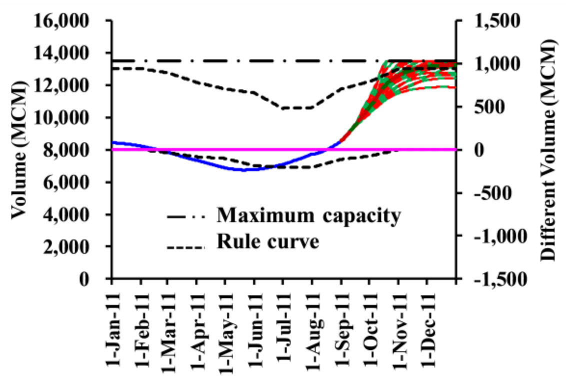

(b)

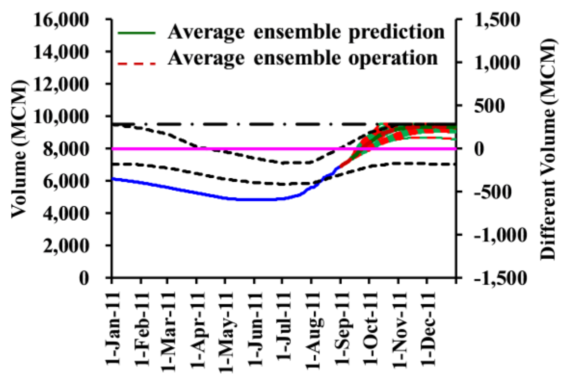

(c)

Figure 4.2.4.2.2 River discharge prediction at station C2 (a) and storage prediction from September until December at the Bhumibol (b) and Sirikit (c) reservoir, shown with the green line, and river discharge and storage prediction after adaptive operation with predictive data from September until December (red dashed line).

4.2.5 Adaptive reservoir operation on flood mitigation

This study updated the previous work of Mateo et al. [Mateo et al., 2013] to develop a method for using seasonal streamflow predictive information to support adaptive reservoir operation. This previous study [Mateo et al., 2013] showed promising results for successful mitigation of the 2011 flood without using predictive information. The authors showed the 2011 flood could have been mitigated by releasing stored water during the early wet season, thus giving reservoirs sufficient storage capacity to retain a greater volume of water during the peak period. However, more benefit could be gained by using seasonal predictive information to support reservoir operations. In reality, reservoirs, particularly in Thailand, cannot always release water during the early wet season because water stored during the wet season is held to support society during the dry season. Thus, the significant difference between models with and without predictive information is that the use of predictive information allows water managers to make more suitable decisions to derive the best benefits for society. In addition, this chapter shows the adaptive reservoir operation on monthly time scale, where the reservoir operation on the chapter 3 was decided at the beginning of the wet season.

Previous studies [Voisin et al., 2006, Alemu et al., 2011, and Anghileri et al., 2016] used ensemble streamflow prediction to design reservoir operations in snow-dominated river basins. These studies used long-term streamflow prediction. The major difference between these previous studies [Voisin et al., 2006, Alemu et al., 2011, and Anghileri et al., 2016] and the current study is the river basin characteristics, because the CPRB, which is located in Thailand, is not affected by snow. In addition, the rule curve is commonly used by Thai water managers to operate reservoirs. Thus, our study used the benefits of the rule curve and seasonal predictive information to support reservoir operation.

An annual comparison of reservoir operation with and without the use of predictive information is presented in Figure 4.2.5.1. The green line represents simulated river discharge in 2011 when predictive data were not used to manage operations. The red and orange lines represent simulated river discharge using predictive data based on 2011 operation and PlanM. When predictive information was used, the peak river discharge was significantly lower because the rate of outflow was increased to prevent overflow from both reservoirs. However, reservoir storage was above the maximum level at the end of October. The increased rate of outflow could also delay the overflow: Because river discharge in the CPRB peaks at the beginning of October, peak river discharge was lower with the use of predictive information than without it. Furthermore, the river discharge based on PlanM tended to be lower than that based on 2011 operation.

Figure 4.2.5.2 compares simulated discharge at station C2 in 2011. Overall, adaptive operation under PlanM reduced peak discharge. Moreover, PlanM operation using seasonal predictions mitigated flooding in 2011.

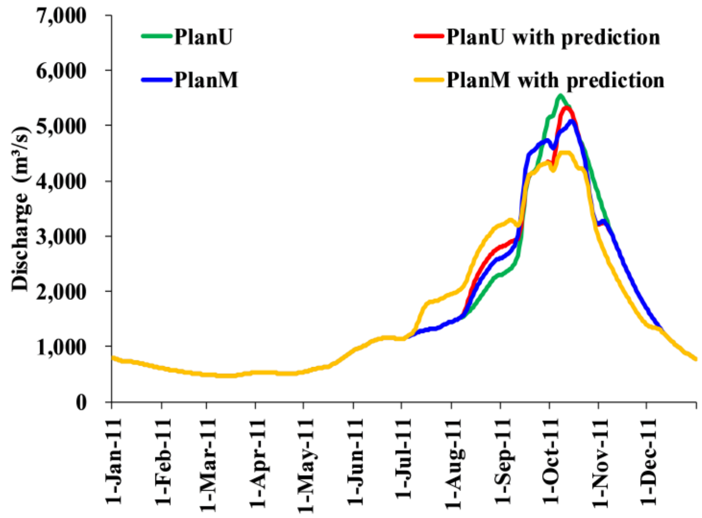

Figure 4.2.5.1 Comparison of river discharge, showing simulated discharge with PlanU operation in 2011 (green line), simulated discharge with PlanM operation in 2011 (blue line), and simulated discharge: (1) after adaptive operation based on 2011 operations using seasonal predictive data (red line) and (2) after adaptive operation based on PlanM using predictive data (orange line).

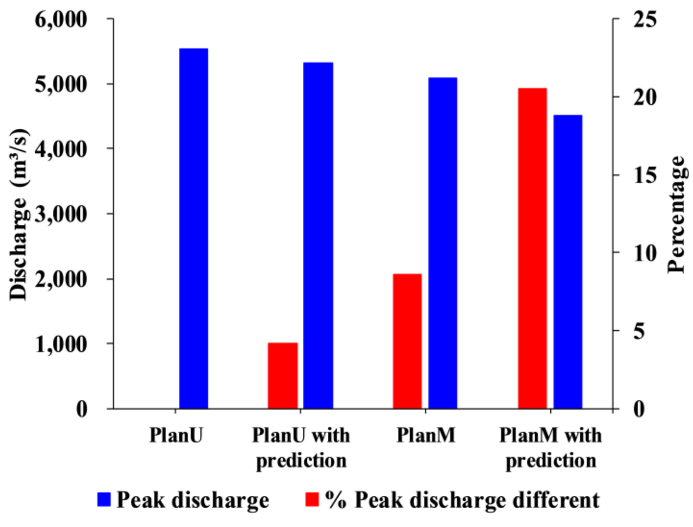

Figure 4.2.5.2 Comparison of peak discharge (blue bar color) and percentage of peak discharge different from simulation (red bar color) between peak simulated discharge using PlanU operation and simulated discharge using PlanM operation in 2011 and simulated discharge: (1) after adaptive operation using predictive data and (2) after adaptive operation using predictive data by PlanM.

Figure 4.2.4.3 shows simulated outflow from the Bhumibol and Sirikit reservoirs in 2011 under PlanU and PlanM operations. The results for outflow using seasonal predictions are indicated by the red and blue lines for PlanU and PlanM, respectively. Because it used seasonal predictions, the rate of outflow under PlanU was elevated only in August, whereas that under PlanM was elevated in both July and August. Because the increased rate of outflow was higher in July and August when seasonal predictive data were used, as shown in Figure 4.2.4.3 for both reservoirs, reservoir storage in July and August was lower under PlanM, which used seasonal predictive data, than under PlanU, as shown in Figure 4.2.4.4. In addition, adaptive operation following PlanM slightly lowered reservoir storage compared to PlanU. However, adaptive operation under PlanM using seasonal predictions lowered reservoir storage, which in turn mitigated flooding during the peak flow period in October, more than adaptive operation under PlanU.

Figure 4.2.5.5 shows the results of river discharge at P12C and N8 station. The results show that the discharge in August at N8 station were above the river channel capacity. While the river discharge at P12C station were under the river channel capacity.

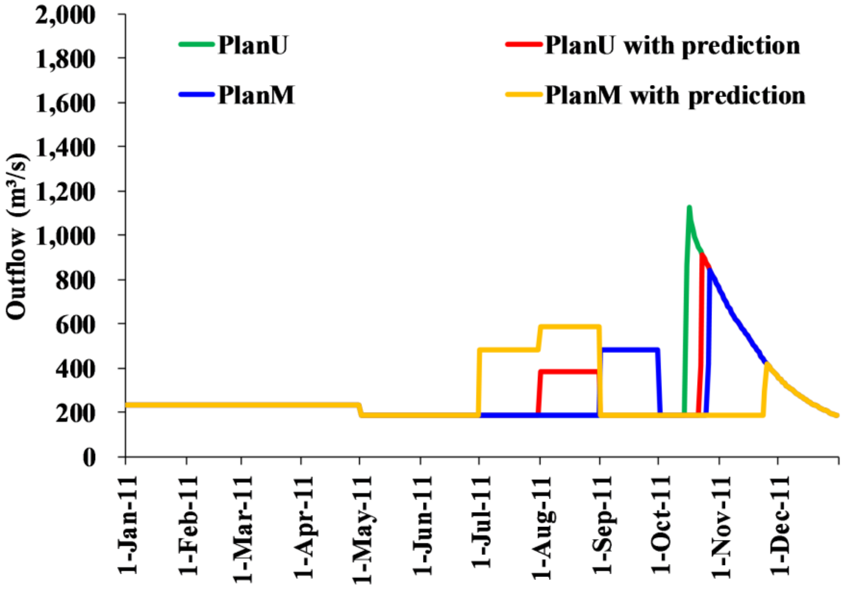

(a)

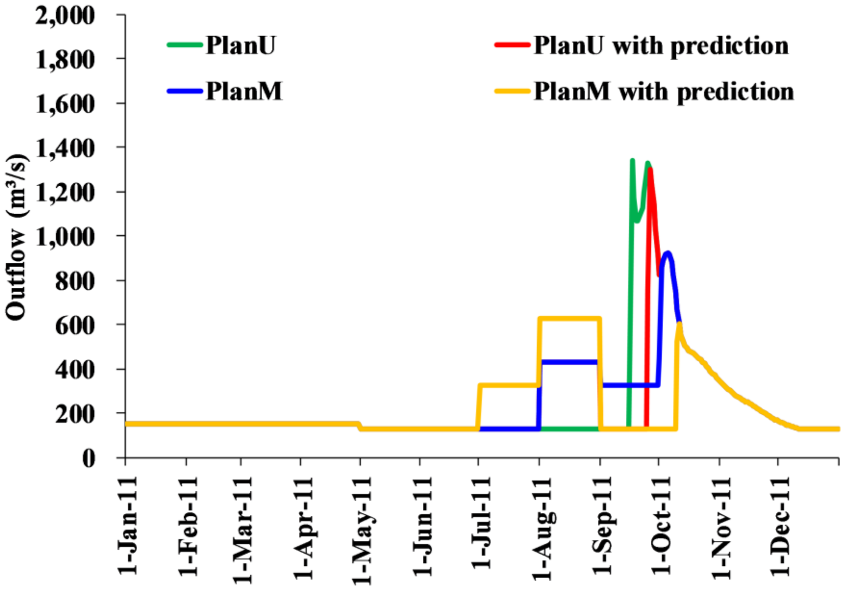

(b)

Figure 4.2.5.3 Comparison of outflow, showing simulated outflow using PlanU operation in 2011 (green line) and simulated discharge using PlanM operation in 2011 (blue line): (1) after adaptive operation using predictive data based on 2011 operations (red line) and (2) after adaptive operation using predictive data based on PlanM (yellow line).

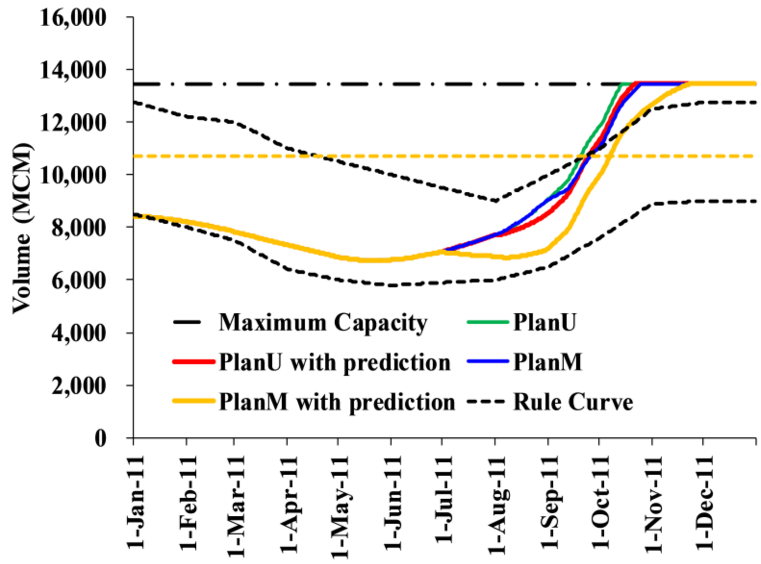

(a)

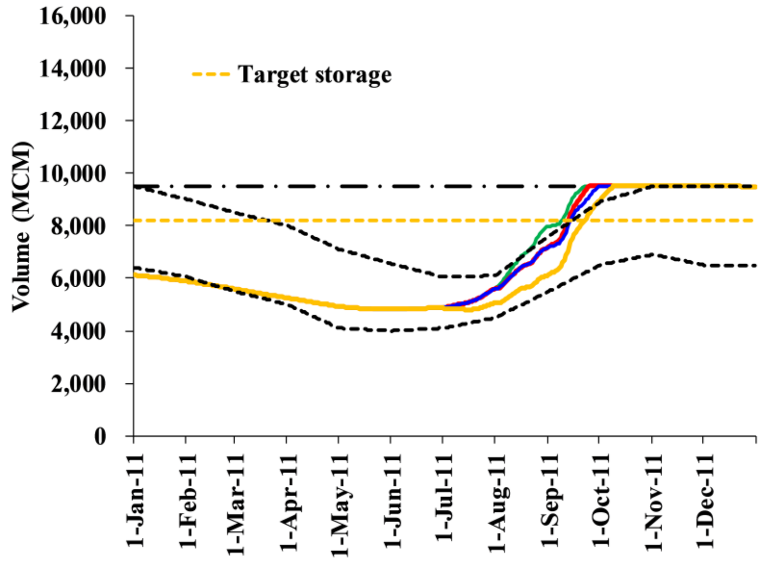

(b)

Figure 4.2.5.4 Comparison of dam storage between simulated storage using PlanU operation in 2011 (green line) and simulated storage using PlanM operation in 2011 (blue line): (1) after adaptive operation using predictive data based on 2011 operations (red line): and (2) after adaptive operation using predictive data based on PlanM (yellow line). The yellow dash line shows the target storage of PlanM in this study.

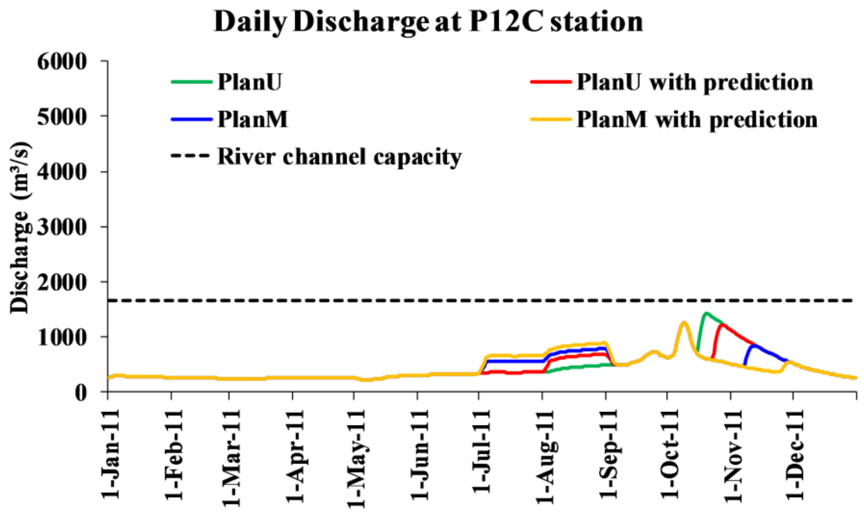

(a)

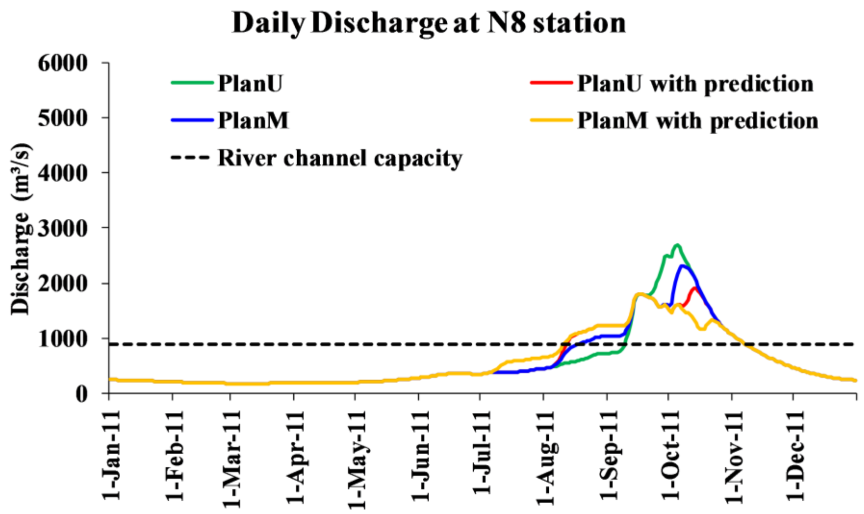

(b)

Figure 4.2.5.5 Comparison of daily discharge at P12C (a) and N8 station (b), showing simulated daily discharge using PlanU operation in 2011 (green line) and simulated discharge using PlanM operation in 2011 (blue line): (1) after adaptive operation using predictive data based on 2011 operations (red line) and (2) after adaptive operation using predictive data based on PlanM (yellow line).

Figure 4.2.5.6 shows the comparison of daily discharge at station C2. The results show the comparison between simulated PlanU with different operation conditions, which are 40 percentages, 50 percentages, and 60 percentages. The results show that operation PlanU with 60 percentages condition (blue line) could be mitigate flood in 2011 when compare with PlanU with 40 percentages condition and PlanU with 50 percentages condition. The reason that PlanU with 60 percentages condition could mitigate flood was due to the rate of outflow from both reservoirs were higher than PlanU with 40 and 50 percentages condition in August as shown in Figure 4.2.5.7. Figure 4.2.5.8 shows the comparison of dam storage at Bhumibol and Sirikit reservoir. Because of the increasing in the rate of outflow in August, so the dam storage was decreased in August from both reservoirs.

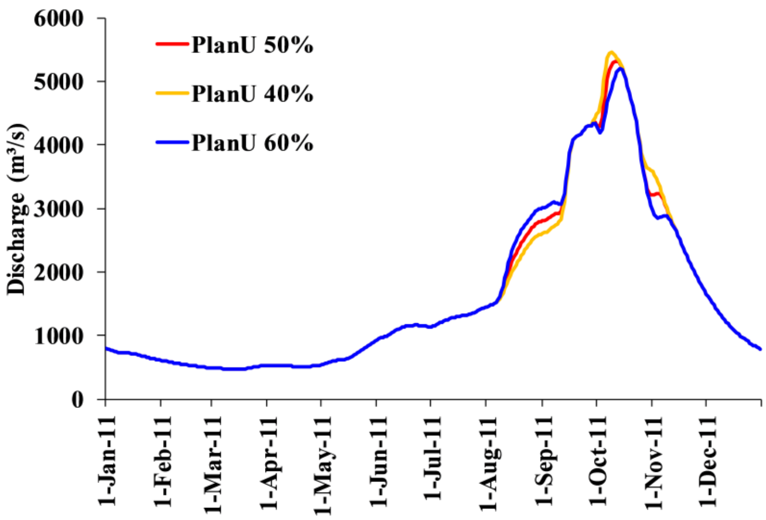

Figure 4.2.5.6 Comparison of river discharge, showing simulated discharge with PlanU operation in 2011 (green line), simulated discharge with PlanU with 40% operation in 2011 (orange line), and simulated discharge with PlanU with 60% operation in 2011 (blue line).

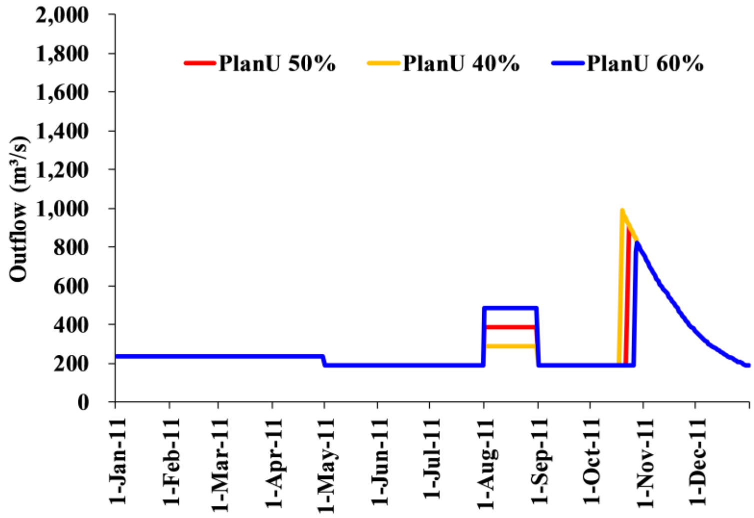

(a)

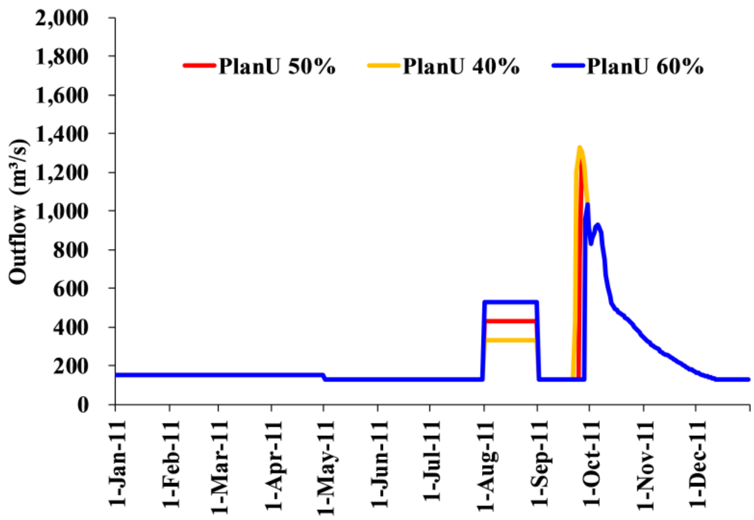

(b)

Figure 4.2.5.7 Comparison of outflow at Bhumibol and Sirikit reservoir, showing simulated outflow with PlanU operation in 2011 (green line), simulated discharge with PlanU with 40% operation in 2011 (orange line), and simulated discharge with PlanU with 60% operation in 2011 (blue line).

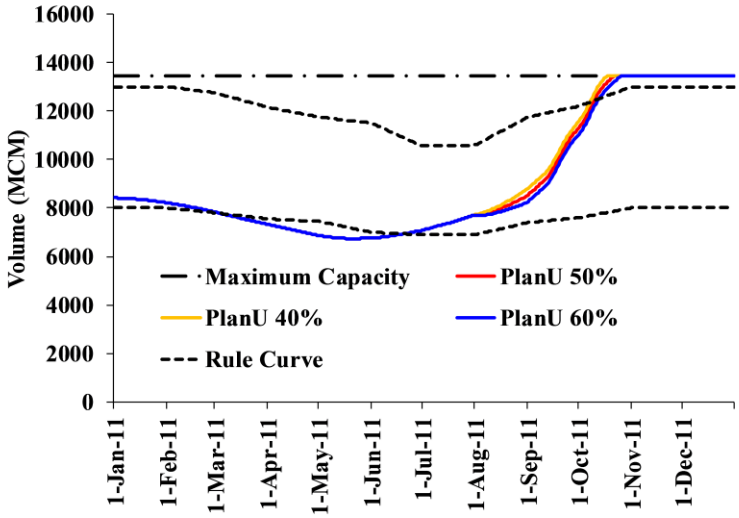

(a)

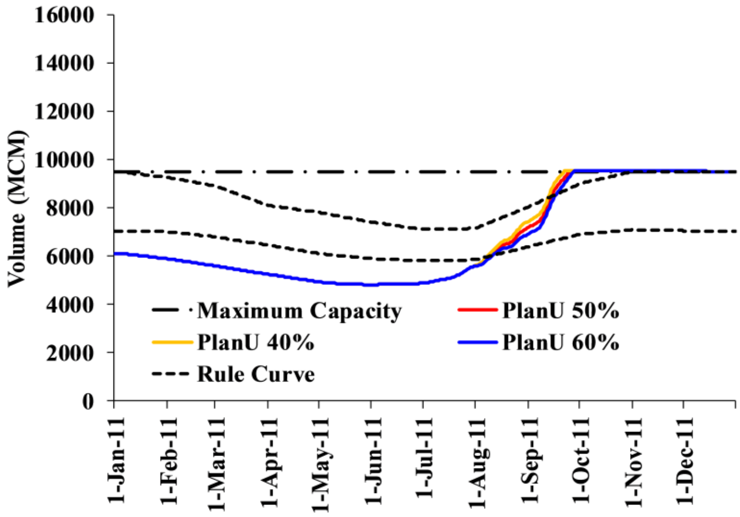

(b)

Figure 4.2.5.8 Comparison of dam storage at Bhumibol and Sirikit reservoir, showing simulated dam storage with PlanU operation in 2011 (green line), simulated dam storage with PlanU with 40% operation in 2011 (orange line), and simulated discharge with PlanU with 60% operation in 2011 (blue line).

4.3 Conclusion

This study updates previous studies, in which various reservoir operations for flood mitigation were proposed, using ECMWF predictive information to support adaptive reservoir operation. This study developed a method for applying seasonal predictions from the ECMWF, demonstrating the use of predictive information for adaptive reservoir operation in the CPRB in Thailand. The methodology for using seasonal rainfall prediction was updated from previous chapter. The H08 model was used, a distributed hydrological model with a reservoir module, to obtain predictions of river discharge and reservoir storage with a 6 month prediction period. In addition, two different operating plans were used to compare river discharge results. The first (PlanU) was simply to follow the 2011 operation schedule, which followed the 2011 rule curve. The second (PlanM) resembled reservoir operations described in a previous study, in which the maximum target storage in 2011 was reduced. The results for river discharge based on seasonal predictions obtained using PlanU showed that seasonal predictive information could be useful for flood mitigation and slightly decreased the peak river discharge, by about 4%, for 2011. In contrast, the results for PlanM showed that peak river discharge was reduced by about 20% relative to the observed 2011 river discharge. The reservoir operation under PlanM, which set target storage levels for each reservoir, tended to make each reservoir release its storage earlier than those under PlanU. That is, a combination of seasonal prediction and PlanM best mitigated flooding.

Furthermore, the results of sensitivity test on selecting 40% and 60% (rather than 50%) to select the reservoir operation were shown in this chapter. The results indicate that with the increasing percentage of the most ensemble predictive members (60%) to support reservoir operation could mitigate flood better than 50% of the most ensemble predictive members. On the other hand, the decreasing percentage of the most prediction (40%) to support reservoir operation could mitigate flood lower than selecting 50% of the most ensemble predictive members.

Chapter 5

Conclusions

The seasonal predictive data from ECMWF was used to support reservoir operation with the purpose of flood mitigation in the Chao Phraya River Basin. The hydrological model (the H08 model) was used in this study to simulate the hydrological process such as river discharge, and dam storage. The H08 model was calibrated from the previous study in order to represent the hydrological process in the Chao Phraya River Basin during flood events such as 1995 and 2011. Although, the previous study [Mateo et al., 2014] showed a fascinated results for successful mitigation of the 2011 flood without using predictive information by releasing stored water during the early wet season. However, reservoirs, particularly in Thailand, cannot always release water during the early wet season because water stored during the wet season is held to support society during the dry season. Therefore, the seasonal predictive data were used to support reservoir operation in this study. This study develops a method for using seasonal predictive information to support adaptive reservoir operation, mainly during the 2011 flood year.

There are two methods for using seasonal predictive information to support reservoir operation in this study. In chapter 3, the reservoir operation was selected from the streamflow prediction at the beginning of the wet season. There are three alternative operations, which are presented in the previous study [Mateo et al., 2014], in chapter 3. The reservoir operation scheme can be decided by finding the different percentages between each prediction results and the average streamflow during August, September, and October (The percentage difference in mean streamflow from August to October and that of a flood event is found that 40, 60 and 95 in 2010, 2002 and 1995, respectively). Most of the results of streamflow prediction lead to select 2011 operation as the reservoir operation scheme, which cannot mitigate flood in 2011. However, one simulation by quantile mapping, out of 25 ensemble members, that selected the alternative operation that could mitigate flooding during the peak period in October with a lesser peak amount of about 18 percentages. The advantage of the method in chapter 3 could be easy to apply. However, the disadvantage of the method in chapter 3 is still not the adaptation reservoir operation. In reality, the seasonal predictive data can be produced every month. Therefore, the method to use the seasonal predictive data to support adaptive operation was updated in chapter 4.

In chapter 4, the method to use the seasonal predictive data for the adaptive operation was updated. The H08 model was used, the hydrological model (H08 model) with a reservoir module, to obtain predictions of river discharge and reservoir storage with a 6 month prediction period. The streamflow prediction and dam storage prediction was produced every month from the beginning of the wet season until the late of the wet season (June to September) with the 6-month lead-time.

There are two alternative operating plans were used to compare the river discharge results. The first (PlanU) was simply to follow the 2011 operation schedule, which followed the 2011 rule curve. On the other hand, the second (PlanM) resembled reservoir operations described in a previous study, in which the maximum target storage in 2011 was reduced. The results for river discharge based on seasonal predictions obtained using

PlanU showed that seasonal predictive information could be useful for flood mitigation and slightly decreased the peak river discharge, by about 4%, for 2011. In contrast, the results for PlanM showed that peak river discharge was reduced by about 20% relative to the observed 2011 river discharge. The reservoir operation under PlanM, which set target storage levels for each reservoir, tended to make each reservoir release its storage earlier than those under PlanU. That is, a combination of seasonal prediction and PlanM best mitigated flooding.

The use of seasonal predictive data for adaptive reservoir operation could mitigate flood in 2011 by two alternative reservoir operations as shown in chapter 4. Although, the seasonal predictive data such as rainfall data was underestimated. Therefore, two additional experiments were investigated in this study as shown in Appendix D. The first experiment is to use the seasonal predictive data for adaptive reservoir operation in 1995. The results show that the use of seasonal predictive data for adaptive reservoir operation could mitigate flood in 1995 with about 3 percentages decreased from the peak. However, there is a reason that the seasonal predictive data can be used to successfully mitigate flood in 1995, which is the dam storage. The simulated dam storage in both reservoirs were near the upper rule curve as shown in Appendix D. Therefore, the overflow incident from both reservoirs can be happened with high rainfall. The second experiment is to use the past rainfall data (1981 to 2010) as predictive data. The purpose of the second experiment is to confirm whether predictive data in 2011 is good or the hydrological process of the Chao Phraya River Basin is slow, which we can input any rainfall data to simulate the 2011 flood event. The result shows that flood mitigation can be also done when using past rainfall as predictive data with about 3 percentages decreased from the peak. Although, the outflow rate was decreased in Sirikit reservoir at the beginning of the wet season due to the ensemble of dam storage using past rainfall data trend to lower than the lower rule curve. While, the outflow rate in August was increased in Sirikit reservoir, which could release stored water before the peak period during September and October. Despite of the result of using past rainfall as predictive data could mitigate flood. However, flood mitigation could be more efficient if the outflow rate was not decreased at the beginning of the wet season in Sirikit reservoir. On the other hand, there is no change in reservoir operation when using the ECMWF seasonal predictive in the beginning of the wet season.

Therefore, the seasonal predictive data, especially the beginning of the wet season, is still required to support reservoir operation in order to give the most benefit to society. If the seasonal predictive data could predict high accurate data since the beginning of the wet season, the water manager can be decided and making a policy more easily (for example; release water for agriculture during the wet season if necessary then stored water during the flood event).

The results of the sensitivity test of choosing 40% and 60% of the most predictive ensemble members (other than 50%) to select the reservoir operation show that the increasing percentage of the most ensemble predictive members (60%) to support reservoir operation could mitigate flood better than 50% of the most ensemble predictive members. On the other hand, the decreasing percentage of the most prediction (40%) to support reservoir operation could mitigate flood lower than selecting 50% of the most ensemble predictive members. However, there still no definite answer whether which

40%, 50% or 60% of the most predictive ensemble members are better for reservoir operation. Due to the risk of whether the operating year is the drought year. Moreover, if the condition of choosing the most ensemble predictive members is more than 60%, then there have a chance that the outflow rate is increasing at the beginning of the wet season due to most of the predictive ensemble members might be lower than the lower rule curve. While, if the condition of selecting the most ensemble predictive members is lower than 40%, then there is a chance that the current method cannot successfully mitigate flood due to the outflow rate is lower when compared with the condition of 50%.

As the next step of this study, the use of seasonal predictive data to support reservoir operation during drought events is suggested to investigate whether the seasonal predictive data could mitigate drought. In addition, the initial month for prediction might be changed because the dry period in Thailand is started from November to May of the next fiscal year. As the hydrological model of this study, the parameters were calibrated from the previous study to well represent the hydrological process in the Chao Phraya River Basin, especially at station C2. However, the accuracy of river discharge at station N1 was still not satisfactory, which was also mentioned in the previous study [Mateo et al., 2014]. Many reasons related to low accuracy in Nan river such as the presence of human activities that were unaccounted for in the present study. In addition, an official of the Royal Irrigation Department (RID) said that water is being pumped into the Sirikit reservoir (on Nan River) for water supply. Another reason is due to the calibrated four parameters (bulk transfer coefficient, soil depth, shape parameter, and daily maximum subsurface runoff) were calibrated to apply to all grid cells within the Chao Phraya River Basin, which means that the land cover and soil characteristics in the Chao Phraya River

Basin are assumed to be all the same. In reality, these four parameters should be different in each basin.

Finally, the high accuracy of seasonal predictive data, especially at the beginning of the wets season, is still necessary for reservoir operation in order to give the most benefit to society. Most of the results show that the release rate was increased during August in both reservoirs. In reality, the river channel capacity was not allowed to increase the rate of release during August in Nan river as shown in Figure D3.2.1 (b) in Appendix D.

Appendix A

Recent studies on streamflow forecast have the ability to forecast up to 6 to 7 month ahead [Greuell et al., 2018]. The hydrological model is forcing with a range of probability in seasonal climate forecast which known as ensemble streamflow prediction (ESP) method. Previous studies have indicated that the accuracy of seasonal hydrological prediction was related to seasonal climate prediction data and watershed initial moisture condition [Crochemore et al., 2016] that lower skills in prediction. Wood et al. found that the largest predictability at seasonal scales are during winter where snowmelt raises soil moisture to generate runoff and streamflow is relatively slow. The smallest predictability found at the end of a climatologically dry period and preceding a wetter one that nearly all forecasts skill derives from the skill of seasonal climate prediction [Wood et al., 2016]. However, none of the previous studies mention the effect of SPB on hydrological forecasts. The SPB defined as the low predictability during the spring (February to May). The cause of SPB has not yet been fully understood, and various hypotheses have been still discussed to explain this phenomenon [Duan et al., 2013]. In addition, during spring (February to May) is the initial prediction time before the wet season (such as Thailand) that could help water management be more effective.

Thus, the objective of Appendix A is to clarify the effect of SPB, which have the evidence in a global scale, to the predictability of river discharge in CPRB and evaluate the accuracy of seasonal streamflow forecasts on each initial prediction day.

A1. Seasonal rainfall prediction

Appendix A

The seasonal rainfall prediction data from a previous study [Imada et al., 2015] were used in this study for two reasons. First reason, this seasonal data easy to access for utilizing. The second reason, they mentioned that their predicting system is less affected by SPB. Another reason is this seasonal rainfall prediction have been focusing on Thailand's meteorology. The available data period range from 1979 to 2011 but this study used 1982 to 2004 to simulate the river discharge from 1982 to 2004. The seasonal rainfall data provided in monthly time scale with four cases about an initial day on the 1st day for prediction, 1) February 2) May 3) August and 4) November. The ability for prediction is six months ahead. As for other seasonal prediction, this seasonal data studied based on ensemble prediction system and provide an anomaly with a reference period between 1961 and 2000. The reason for making a prediction set (or ensemble) instead of producing a single prediction because this prediction set aims to give an indication of the range of possible future states of the atmosphere. The output from this study provided eight ensembles, which difference initial condition, rainfall data. The ensemble with the different initial condition can show the range of possibilities in prediction. In this study, a seasonal rainfall prediction in anomaly was combined with Asian Precipitation Highly Resolved Observational Data Integration Towards the Evaluation of Water Resource (APHRODITE) data [Yatagai et al., 2009] to generate total rainfall prediction data. Seasonal rainfall prediction data was regridded with spline interpolation from 1x1^{o} latitude and longitude grid to a 5x5 minute grid resolution.

Fig. A1 shows the accuracy of raw seasonal prediction data for each initial month. Black lines show the accuracy of K10 data compared with the observed station in CPRB. Each initial month has six months lead-time and eight-ensemble member. Overall, the accuracy of seasonal rainfall prediction is significantly lower especially during February as shown in Fig. A1 (a) and Fig. A1 (d).

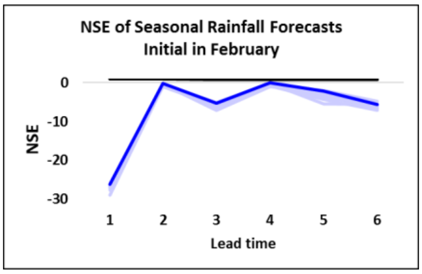

(a)

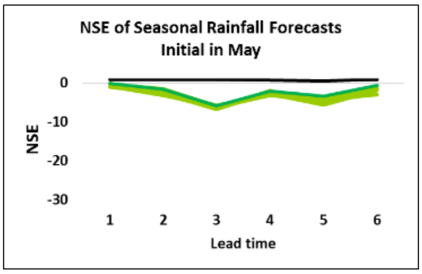

(b)

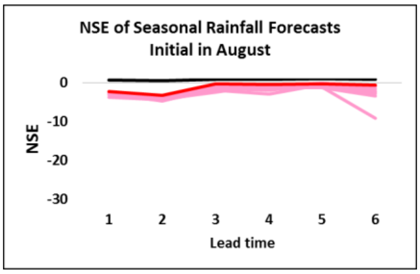

(c)

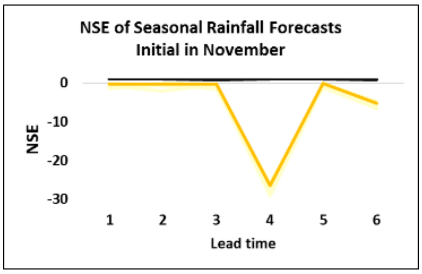

(d)

Figure A1 The accuracy of raw seasonal rainfall prediction for each initial month (a) February (b) May (c) August and (d) November as initial month

A2. Preprocessing (bias correction)

Bias correction by linear scaling used for remove systematic bias for seasonal rainfall prediction using K10 as reference data from 1981 to 2004. Fig. A2 shows the result of preprocessing for each initial month from first lead month until a seventh lead month. Overall predictability was improved after bias corrected seasonal rainfall prediction data especially February and November as an initial month. The smallest predictability on

February (first lead month of the initial month in February and fourth lead month of the initial month in November) were improved the accuracy. The significant predictability is November and February as an initial prediction. The smallest predictability is May which beginning of the wet season in Thailand. The accuracy of mean ensembles member trend to higher accuracy for first-month lead-time and slowly lower accuracy for longer lead-time except for initial month at August. The lower accuracy in August might come from difficulty in peak prediction on the wet season (normally August is the highest rainfall intensity in CPRB).

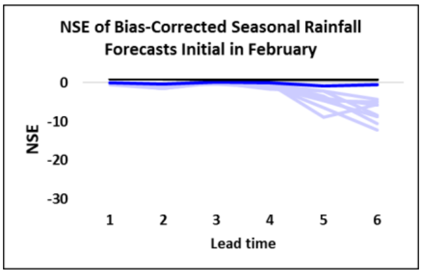

(a)

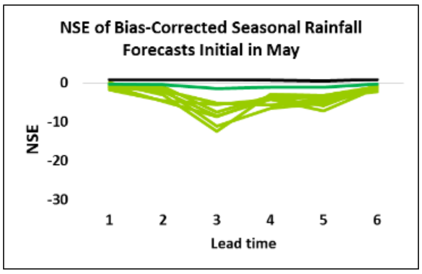

(b)

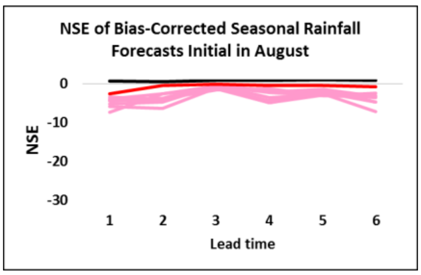

(c)

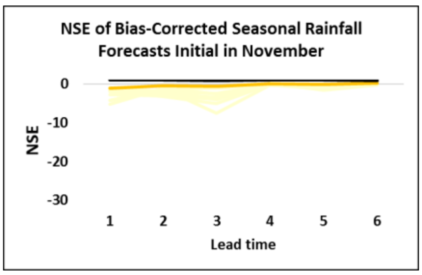

(d)

Figure A2 The accuracy of bias-corrected seasonal rainfall prediction for each initial month (a) February (b) May (c) August and (d) November as initial month

A3 River discharge prediction

After successfully bias correction of seasonal rainfall prediction in preprocessing section. The H08 model was simulated the river discharge by bias-corrected seasonal rainfall. The discharge by bias-corrected seasonal rainfall was compared the results with the gauge station at C2. Figure A3 shows the accuracy of river discharge prediction. The black line shows the accuracy of river discharge simulation using K10 as input data. The results illustrate that the smallest accuracy is in February which both K10 and seasonal rainfall prediction as input data. The reason for low accuracy during February might come from the hydrological model. Soil moisture during January to April found to be low in a hydrological model that makes hydrological model hardly generate the runoff and streamflow in this case. The smallest predictability found in May as an initial month because seasonal rainfall prediction from Fig. 6 found lower in accuracy especially third-month lead-time that lead to lower accuracy in fourth lead-month prediction in Figure A3 (b). However, it is difficult to see how much difference between the accuracy of river discharge simulation using K10 as input data and seasonal rainfall data. Thus, Figure A4 shows the difference NSE. Blue, green, red and yellow color indicates mean different the accuracy of river discharge between K10 and seasonal rainfall prediction as input data to The H08 model. Light color in Figure A4 represents the difference accuracy of river discharge simulation for each ensemble member. The significant differences found in May as an initial month. This large difference generated from the low accuracy of seasonal rainfall prediction during peak period (August to September).

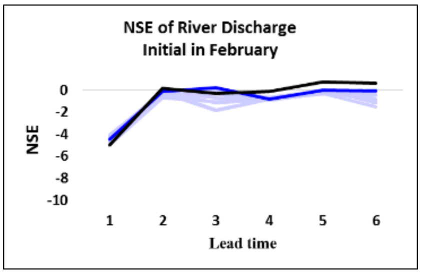

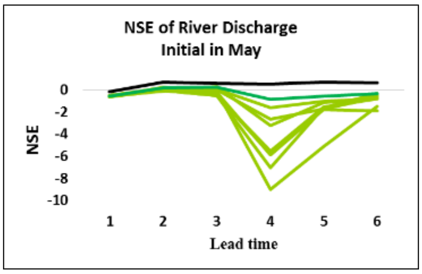

(a) (b)

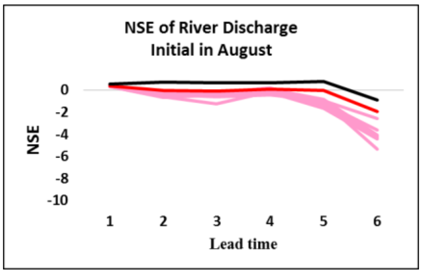

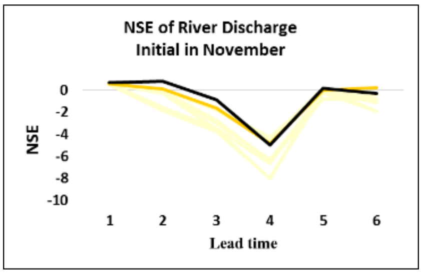

(c) (d)

Figure A3 The accuracy of river discharge prediction for each initial month (a) February (b) May (c) August and (d) November as initial month

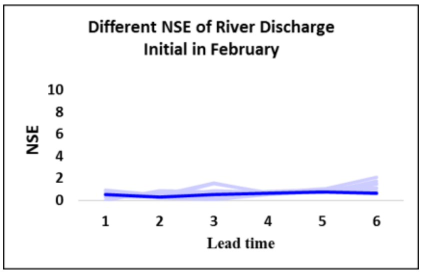

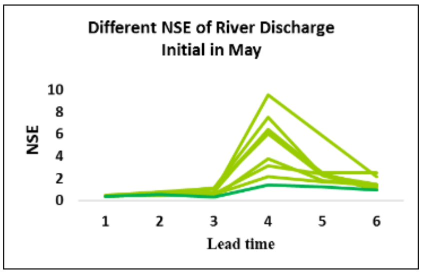

(a) (b)

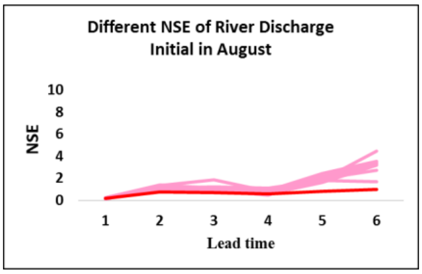

(c)

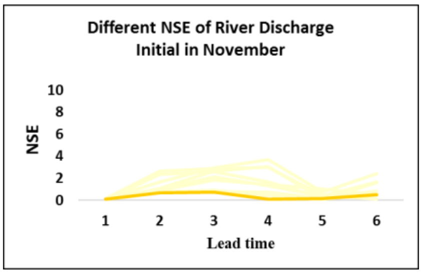

(d)

Figure A4 Difference accuracy of river discharge prediction between K10 and seasonal rainfall prediction as input data to H08 mode for each initial month (a) February (b) May (c) August and (d) November as initial month

A4 Postprocessing

River discharge simulation from the previous section was bias-corrected with observed river discharge in this section. Bias correction by linear scaling removes monthly discharge bias for C2 station. The results of river discharge simulation from postprocessing were shown in Figure A5. Figure A5 is the river discharge simulation from each initial month for prediction with 1 to 3 long lead-time. The accuracy of runoff prediction was indicated by r-coefficient, RMSE and NSE as shown in Figure A5. The horizontal axis in Figure A5 indicates the monthly time step of the results ranges from 1982 to 2004. The vertical axis indicates river discharge in mm/month unit. River discharge prediction for the next 1 to 3 months is more accuracy than river discharge prediction for the next 4 to 6 months. Overall accuracy performance shows an agreement. However, peak river discharge at some period (ex. 1995) was lower than observed river discharge. The overall accuracy of each initial month for prediction shows in Figure A6. Figure A6 shows the accuracy using NSE as accuracy index. Blue, green, red and yellow color shows the accuracy of mean ensemble river discharge from eight ensembles. The results show that the overall accuracy increase after bias-corrected river discharge simulation especially the initial month for prediction at February and November. But the accuracy of May as initial month trends to increase at the 1st to 3rd lead-month before gradually lower the accuracy due to bias correction by linear scaling. The reason that the accuracy of May as an initial month on the 4th lead month drops was due to linear scaling method cannot remove bias for peak river discharge. In another word, linear scaling by remove bias using mean difference cannot remove bias for the peak. The most predictability found in August and November as the initial month that slowly lower accuracy when time pass. The output of each initial month illustrate in hydrograph is shown in Figure A7. Initial month in each graph has a range only six months for each year such as Figure A7 (a) shows the output of river discharge from February to July range from 1982 to 2004, Figure A7 (b) shows the output of river discharge from May to October for each year. The most predictability is November as an initial month; second most predictability is August as an initial month while the less predictability is May as an initial month.

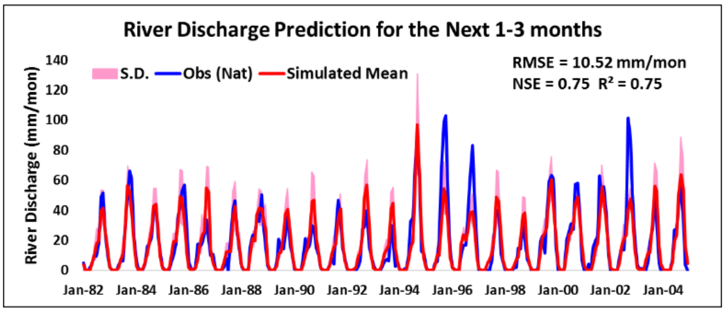

Figure A5 River discharge simulation using bias-corrected rainfall prediction of 1 to 3 months lead time as input data from 1982 to 2004.

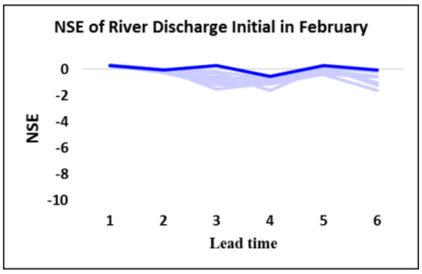

(a)

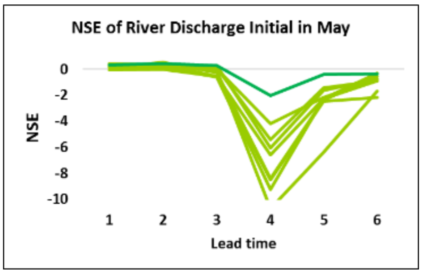

(b)

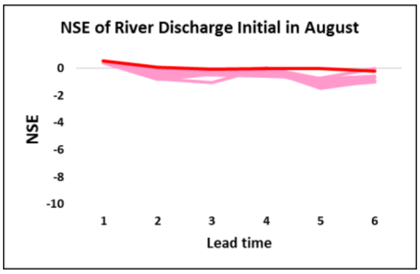

(c)

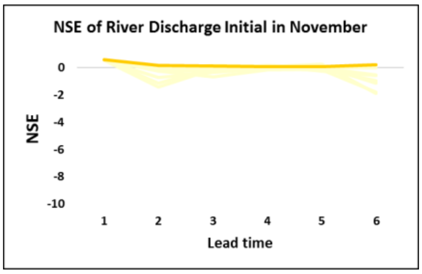

(d)

Figure A6 The accuracy of river discharge simulation using bias-corrected rainfall as input after postprocessing (a) February (b) May (c) August and (d) November as an initial month for prediction.

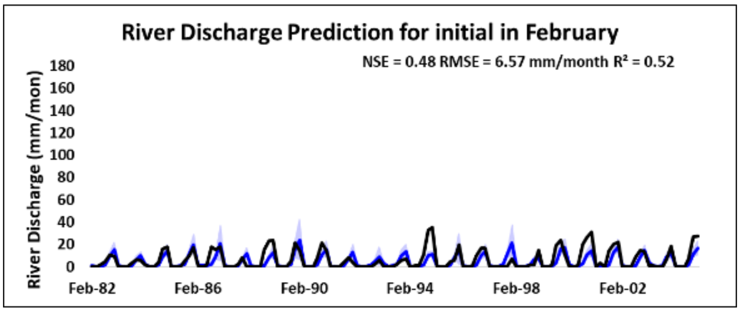

(a)

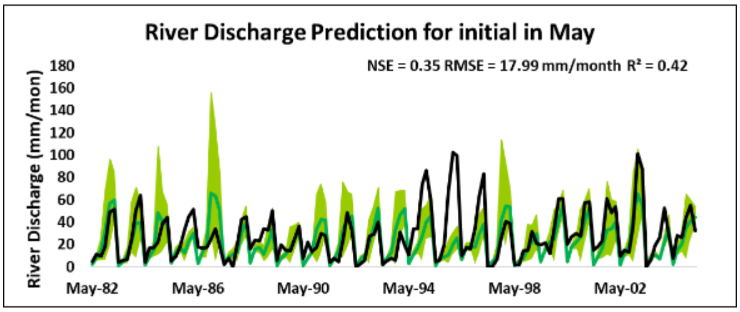

(b)

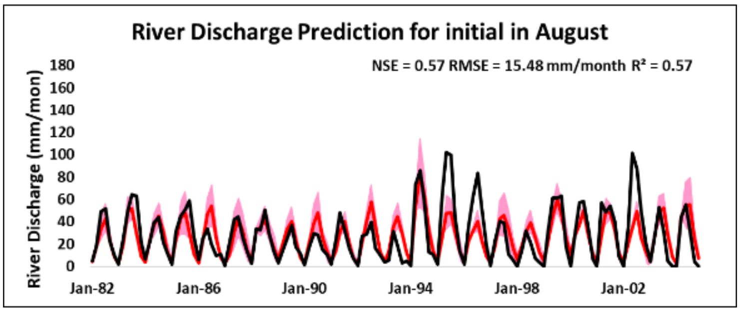

(c)

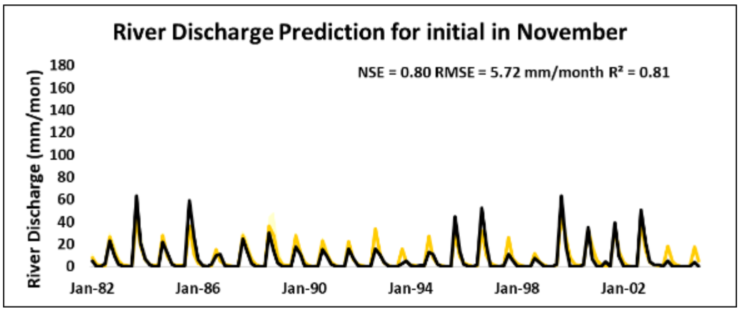

(d)

Figure A7 River discharge simulation for each initial month

Appendix B

Appendix B shows the anomalies graphs of rainfall prediction from ECMWF and observed rainfall data. The anomalies is the difference between average observed rainfall (1981 to 2016) and rainfall prediction.

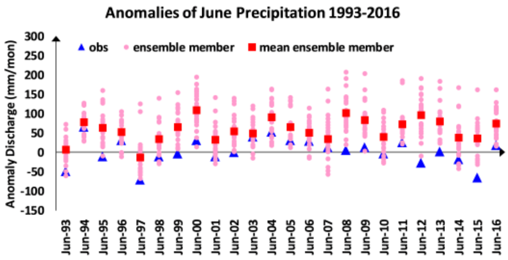

(a)

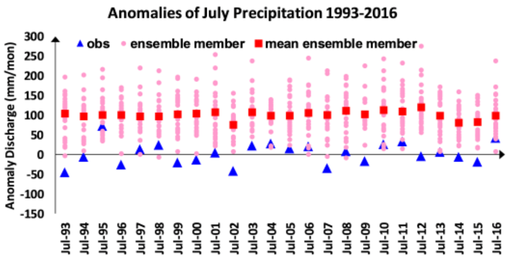

(b)

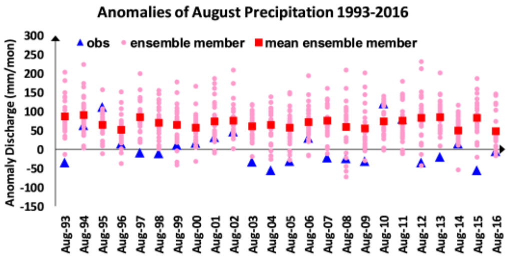

(c)

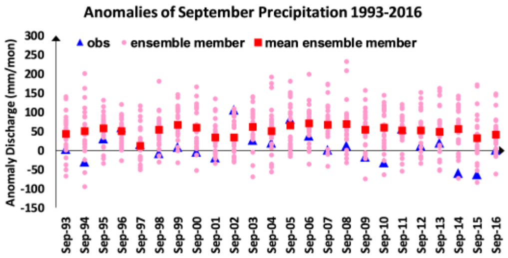

(d)

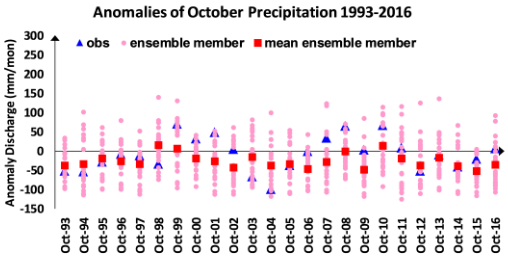

(e)

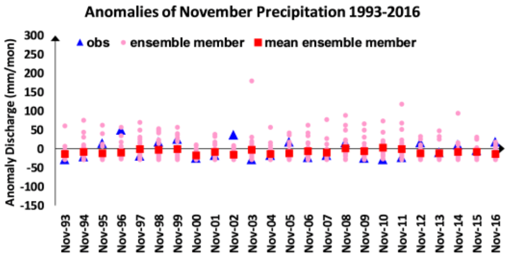

(f)

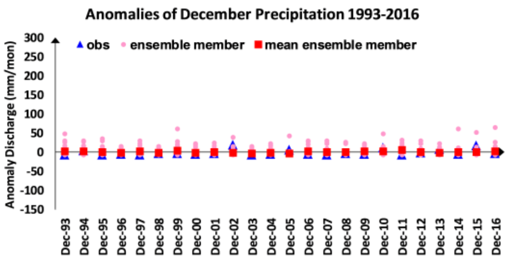

(g)

Figure B1 Anomalies of original ECMWF rainfall prediction from June to December (1993-2016); rainfall prediction on June (a); July(b); August (c); September (d); October (e); November (f); December (g).

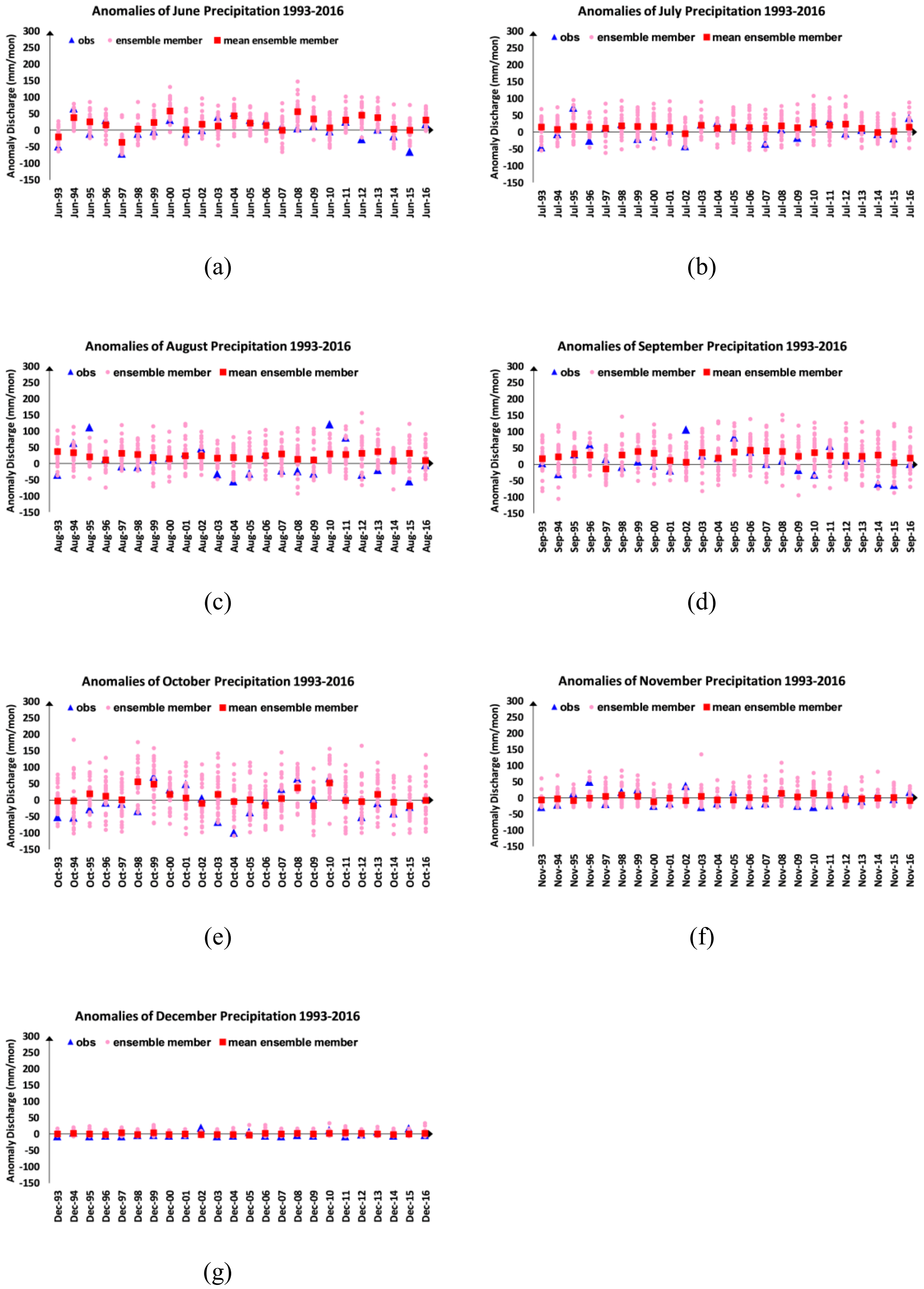

Figure B2 Anomalies of bias-corrected (quantile mapping) ECMWF rainfall prediction from June to December (1993-2016); rainfall prediction on June (a); July(b); August (c); September (d); October (e); November (f); December (g).

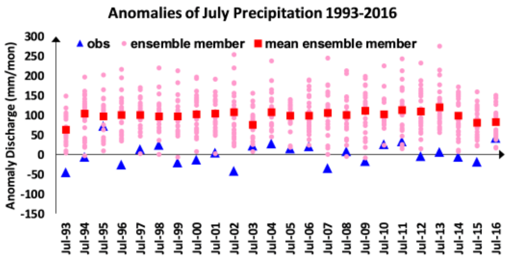

(a)

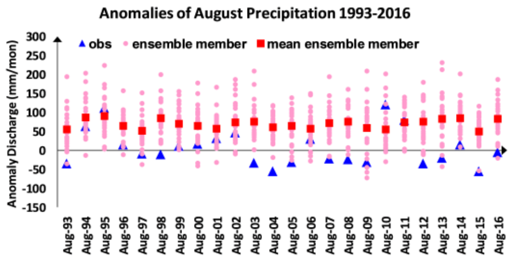

(b)

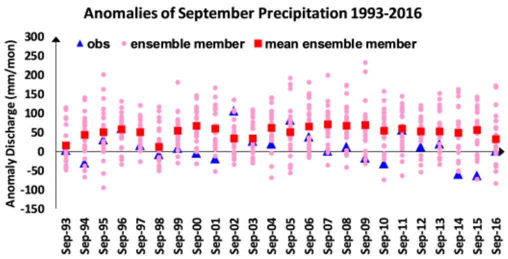

(c)

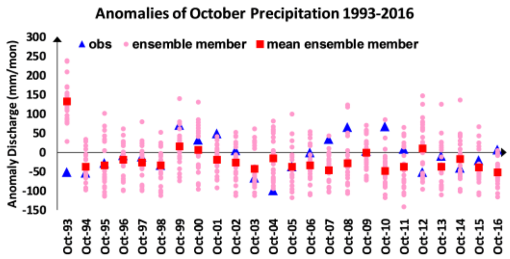

(d)

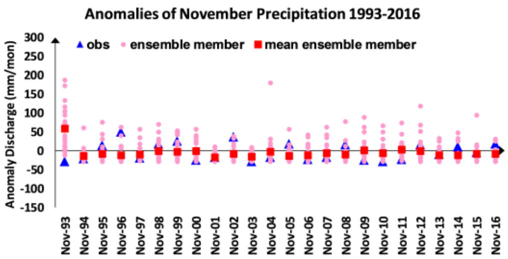

(e)

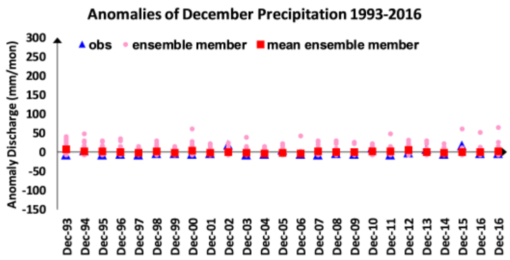

(f)

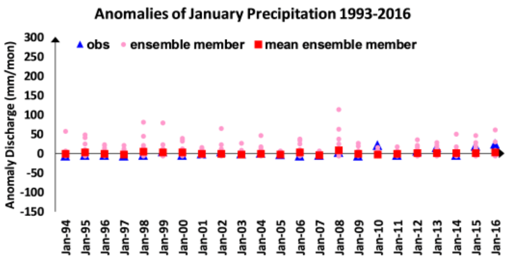

(g)

Figure B3 Anomalies of original ECMWF rainfall prediction from July to January (1993-2016); rainfall prediction on July(a); August (b); September (c); October (d); November (e); December (f); January (g).

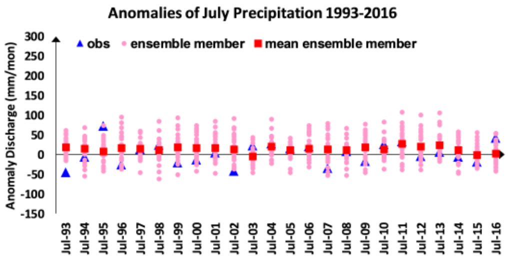

(a)

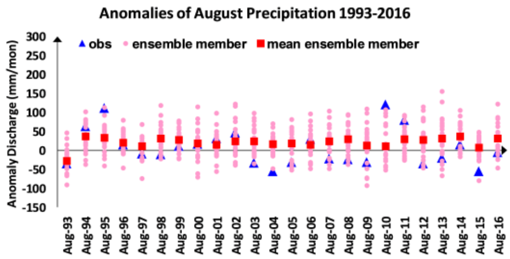

(b)

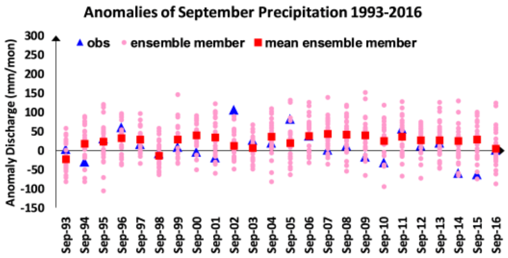

(c)

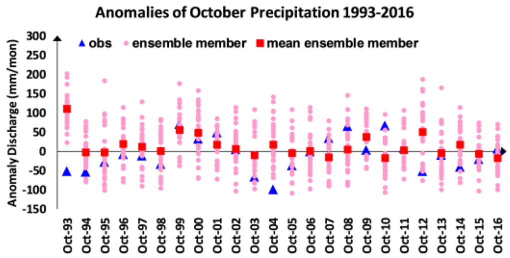

(d)

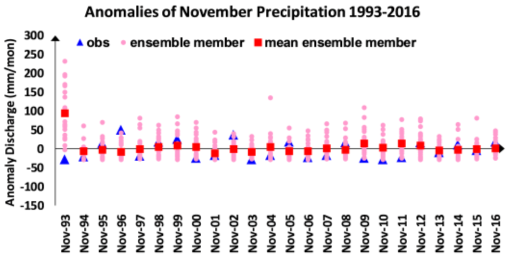

(e)

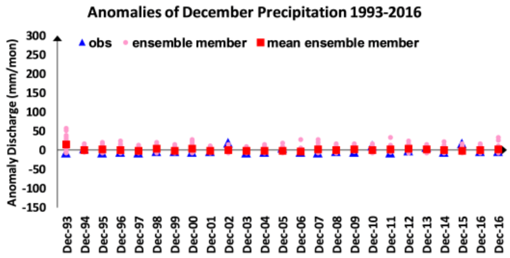

(f)

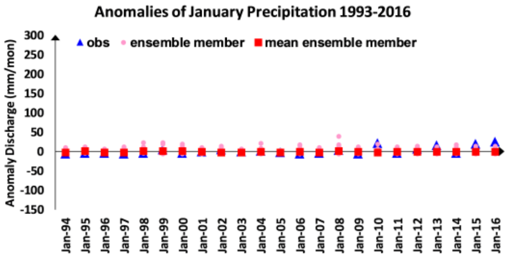

(g)

Figure B4 Anomalies of bias-corrected (quantile mapping) ECMWF rainfall prediction from July to January (1993-2016); rainfall prediction on July(a); August (b); September (c); October (d); November (e); December (f); January (g).

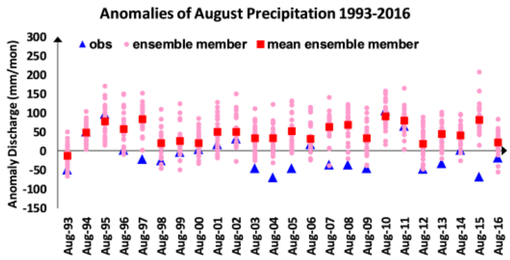

(a)

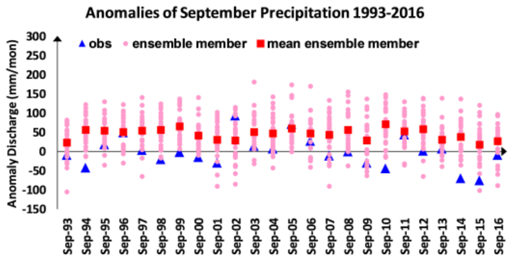

(b)

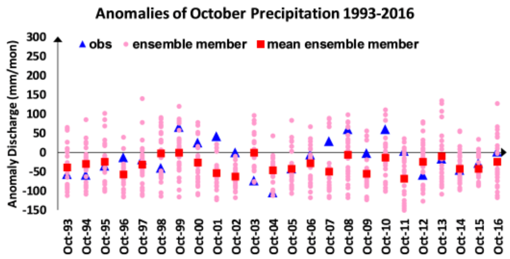

(c)

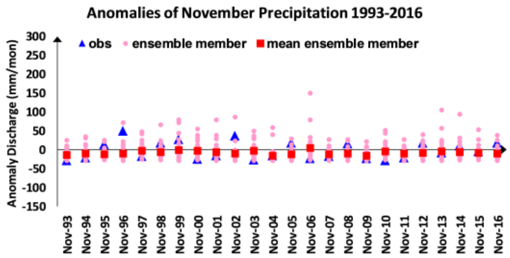

(d)

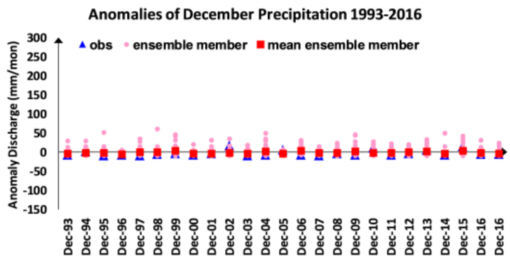

(e)

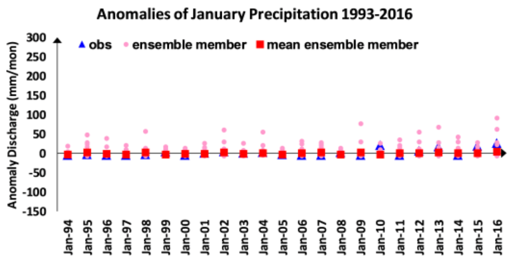

(f)

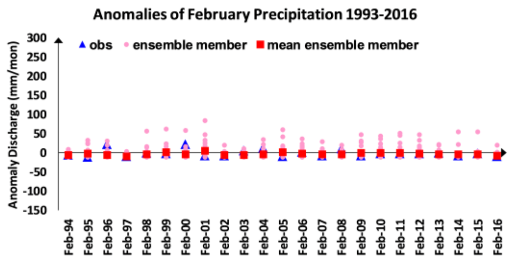

(g)

Figure B5 Anomalies of original ECMWF rainfall prediction from August to February (1993-2016); rainfall prediction on August (a); September (b); October (c); November (d); December (e); January (f); February (g).

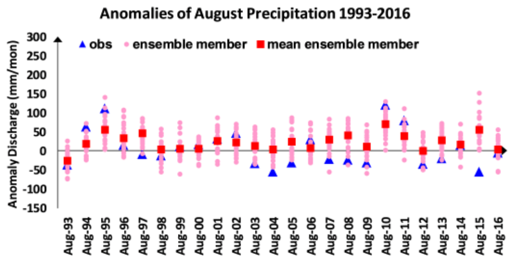

(a)

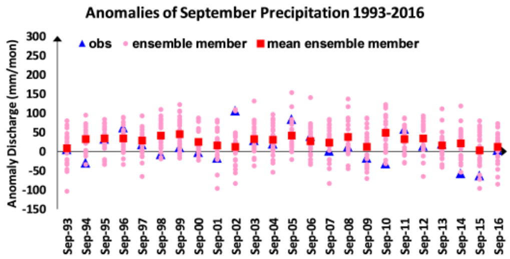

(b)

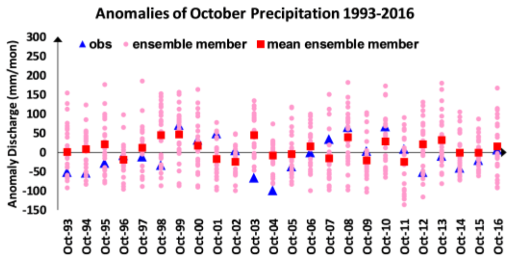

(c)

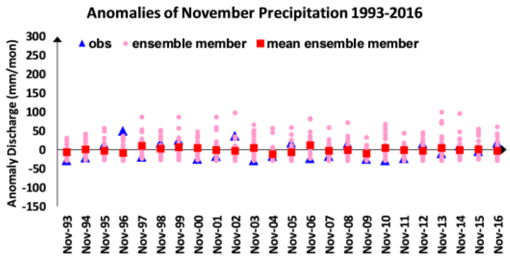

(d)

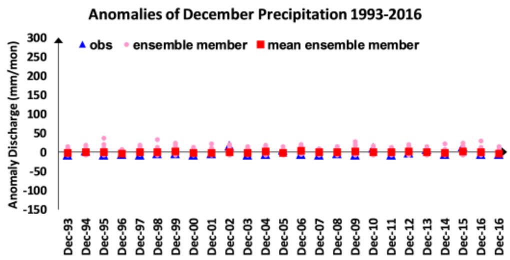

(e)

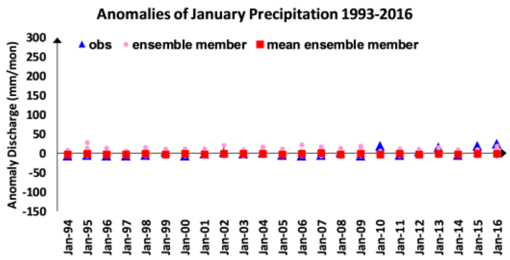

(f)

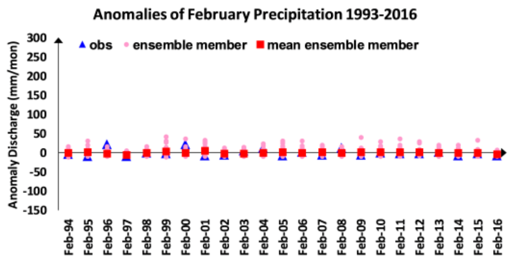

(g)

Figure B6 Anomalies of bias-corrected (quantile mapping) ECMWF rainfall prediction from August to February (1993-2016); rainfall prediction on August (a); September (b); October (c); November (d); December (e); January (f); February (g).

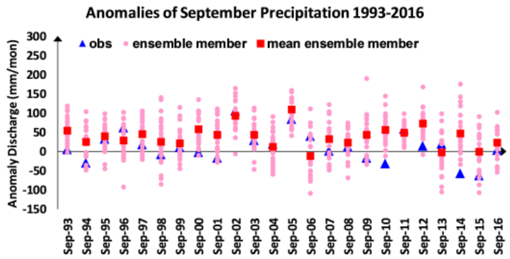

(a)

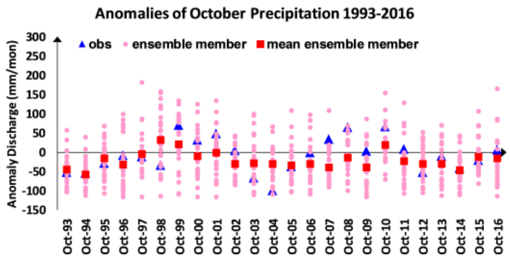

(b)

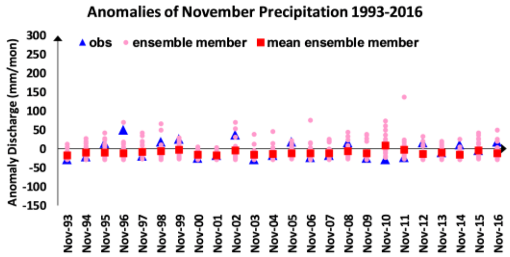

(c)

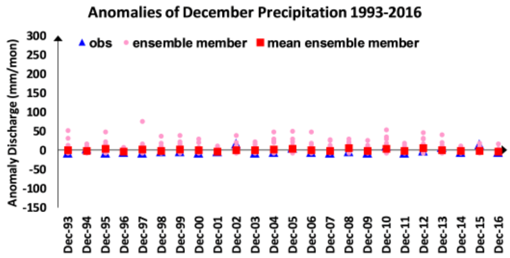

(d)

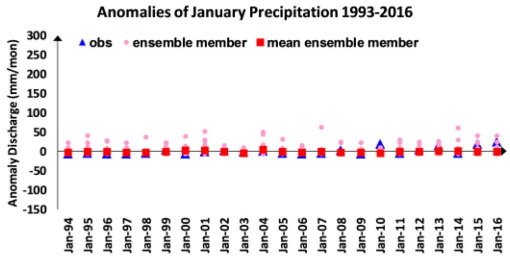

(e)

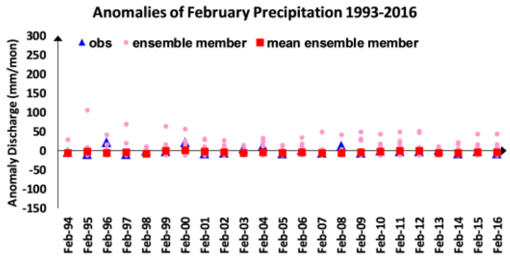

(f)

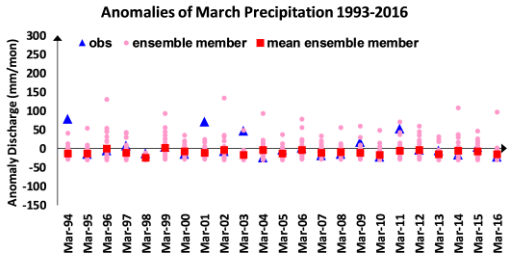

(g)

Figure B7 Anomalies of original ECMWF rainfall prediction from September to March (1993-2016); rainfall prediction on September (a); October (b); November (c); December (d); January (e); February (f); March (g).

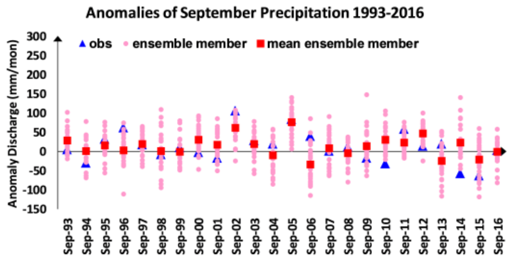

(a)

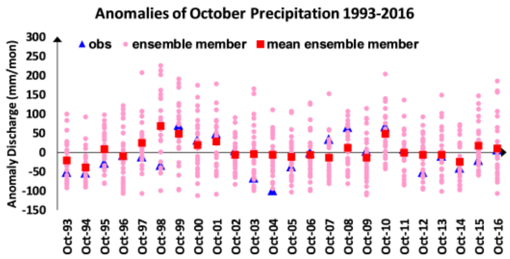

(b)

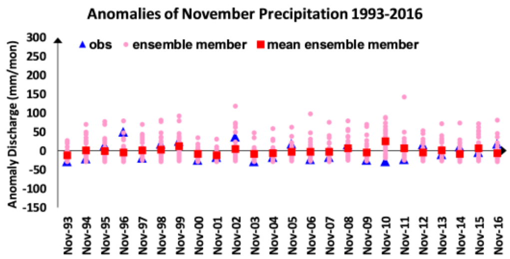

(c)

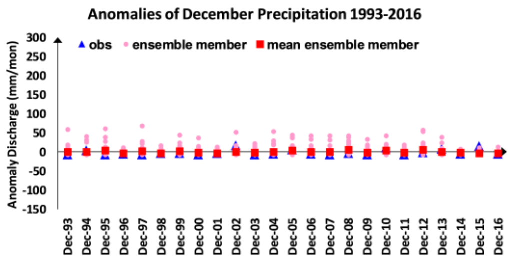

(d)

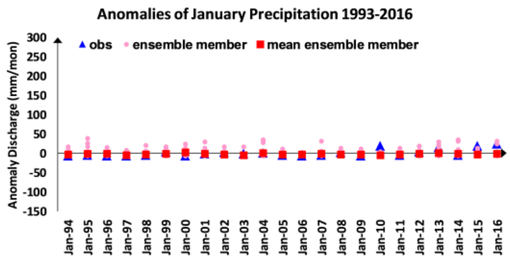

(e)

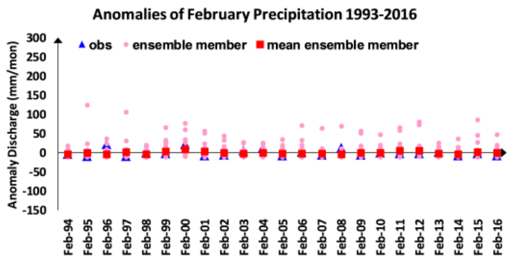

(f)

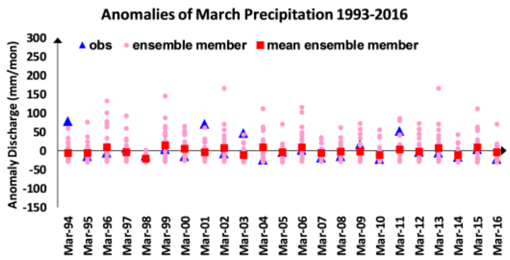

(g)

Figure B8 Anomalies of bias-corrected (quantile mapping) ECMWF rainfall prediction from September to March (1993-2016); rainfall prediction on September (a); October (b); November (c); December (d); January (e); February (f); March (g).

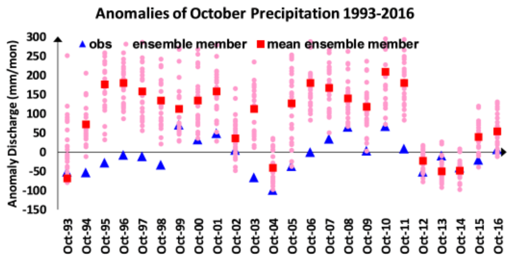

(a)

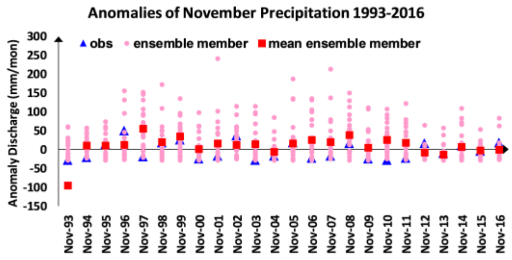

(b)

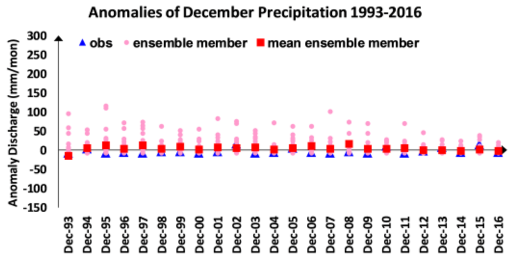

(c)

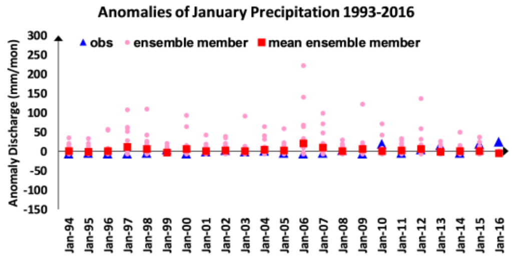

(d)

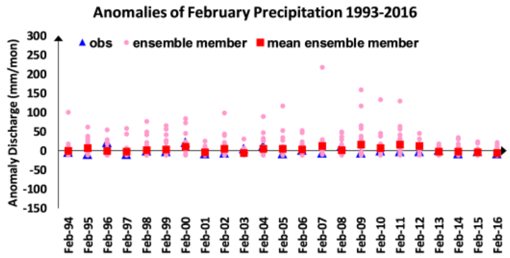

(e)

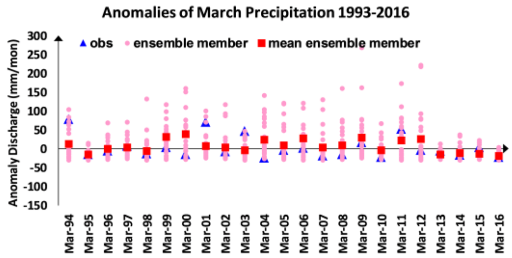

(f)

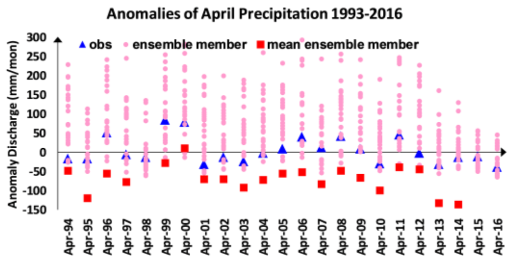

(g)

Figure B9 Anomalies of original ECMWF rainfall prediction from October to April (1993-2016); rainfall prediction on October (a); November (b); December (c); January (d); February (e); March (f); April (g).

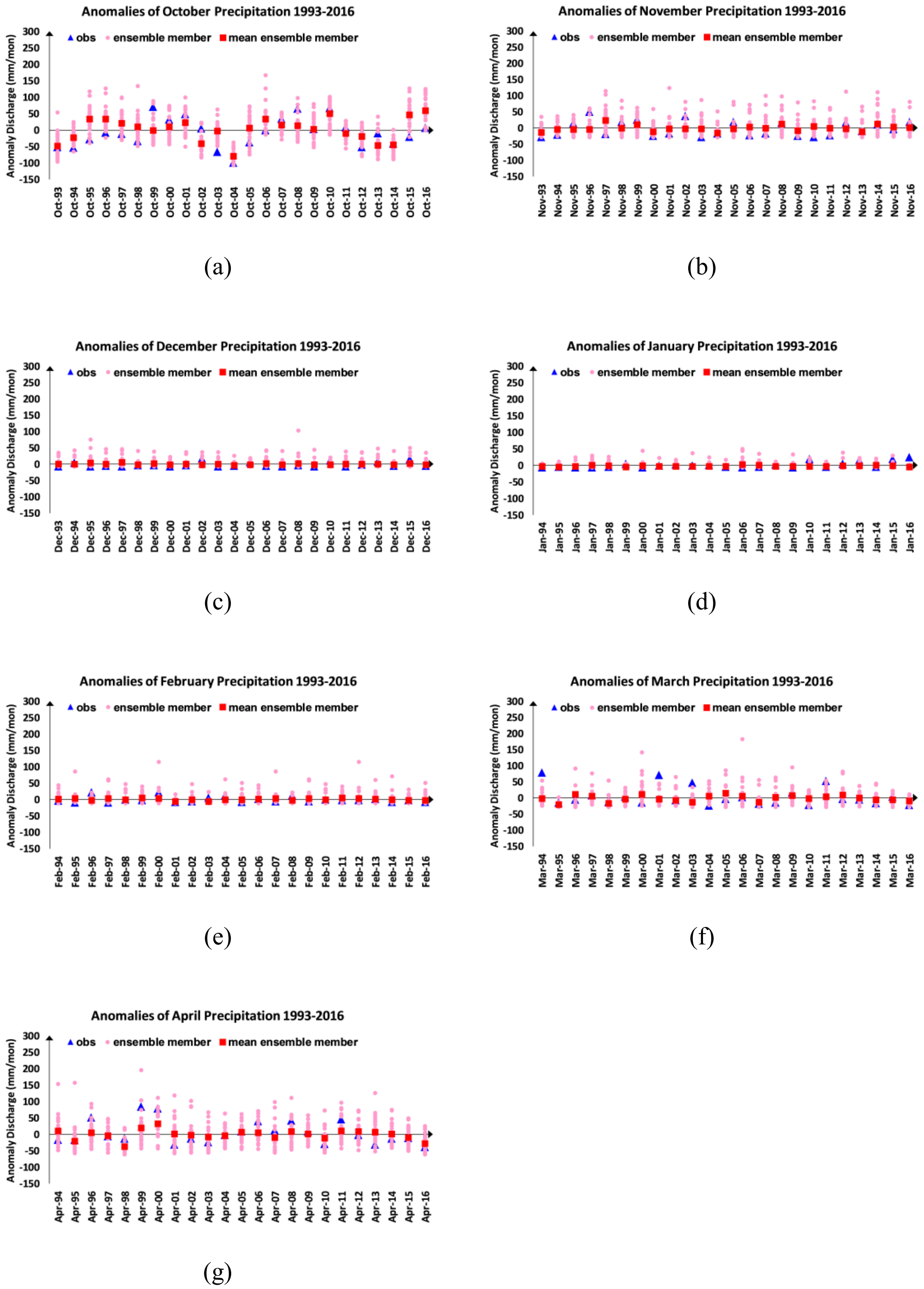

Figure B10 Anomalies of bias-corrected (quantile mapping) ECMWF rainfall prediction from October to April (1993-2016); rainfall prediction on October (a); November (b); December (c); January (d); February (e); March (f); April (g).

Table B1 Pbias and root mean square error (RMSE) of original ECMWF rainfall prediction, bias-corrected by quantile mapping (BCQM) from June to December (1993-2016).

Month	Raw		BCQM	
	Pbias (%)	RMSE (mm/month)	Pbias (%)	RMSE (mm/month)
June	46.63	195.10	14.13	152.72
July	71.88	250.46	9.49	161.74
August	34.07	261.45	8.66	213.61
September	18.59	269.15	7.68	244.65
October	-14.01	99.13	16.90	134.77
November	-18.37	21.50	10.92	29.21
December	31.19	7.48	30.44	7.44

Table B2 Pbias and root mean square error (RMSE) of original ECMWF rainfall prediction, bias-corrected by quantile mapping (BCQM) from July to January (1993-2016).

Month	Raw		BCQM	
	Pbias (%)	RMSE (mm/month)	Pbias (%)	RMSE (mm/month)
July	52.06	229.66	6.14	163.38
August	32.58	261.18	8.43	215.00
September	18.83	262.41	8.70	240.28
October	-15.88	94.81	16.25	130.90
November	-19.34	21.69	6.85	28.58
December	24.69	7.39	25.42	7.43
January	66.64	24.58	5.85	17.63

Table B3 Pbias and root mean square error (RMSE) of original ECMWF rainfall prediction, bias-corrected by quantile mapping (BCQM) from August to February (1993-2016).

Month	Raw		BCQM	
	Pbias (%)	RMSE (mm/month)	Pbias (%)	RMSE (mm/month)
August	31.09	257.54	10.61	218.91
September	20.35	261.05	9.03	236.85
October	-17.45	92.39	13.53	126.40
November	-24.49	19.97	4.13	27.54
December	37.24	7.65	32.73	7.40
January	-21.22	6.16	-25.70	5.81
February	-5.42	36.66	-13.12	34.66

Table B4 Pbias and root mean square error (RMSE) of original ECMWF rainfall prediction, bias-corrected by quantile mapping (BCQM) from September to March (1993-2016).

Month	Raw		BCQM	
	Pbias (%)	RMSE (mm/month)	Pbias (%)	RMSE (mm/month)
September	11.91	251.20	0.75	220.41
October	-11.22	102.33	10.73	123.64
November	-28.13	18.91	7.14	27.41
December	29.01	7.70	20.52	7.20
January	-24.83	5.91	-36.98	4.95
February	-33.34	6.89	2.03	10.56
March	-41.13	19.75	-14.64	28.63

Table B5 Pbias and root mean square error (RMSE) of original ECMWF rainfall prediction, bias-corrected by quantile mapping (BCQM) from October to April (1993-2016).

Month	Raw		BCQM	
	Pbias (%)	RMSE (mm/month)	Pbias (%)	RMSE (mm/month)
October	91.59	220.84	8.20	120.51
November	58.50	41.70	7.84	26.45
December	126.68	12.93	29.15	7.15
January	29.84	10.20	-35.68	5.05
February	38.07	14.28	9.04	11.28
March	9.58	36.75	-15.69	28.28
April	90.57	132.04	-8.35	63.50

Appendix C

Figure C1 shows the results for seasonal rainfall prediction after bias correction from June, July, August, and September until December 2011. The results are on a daily time scale. Figure C2 shows scatter plots of observed rainfall (y-axis) and predicted rainfall (x-axis) and the ensemble range for June until December, with panels showing different prediction lead times. For example, panel (d) in Figure C2 shows a scatter plot of observed and predicted rainfall, with yellow, red, blue, and green representing rainfall predictions for September with 0, 1, 2, and 3 month lead times, respectively.

Based on these results, rainfall predictions tended to be underestimated relative to observed rainfall data. From these results, the adaptive reservoir operation, which increased the outflow rate from reservoirs, only occurred during August when using PlanU to operate in this study. In addition, adaptive reservoir operation could be started prior to August to mitigate flooding in 2011 if the rainfall prediction was more accurate.

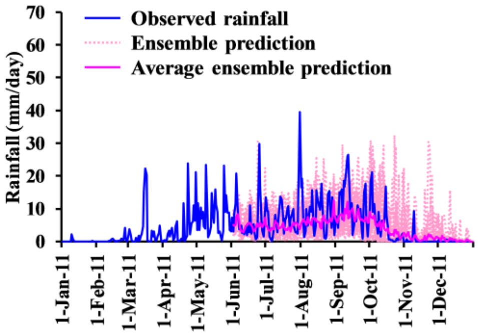

(a)

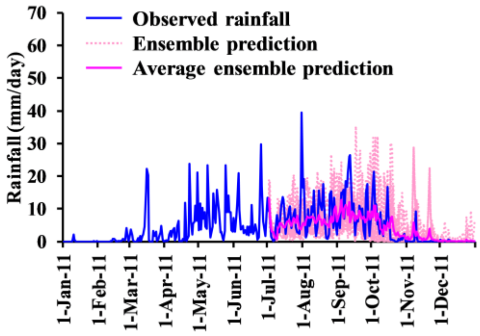

(b)

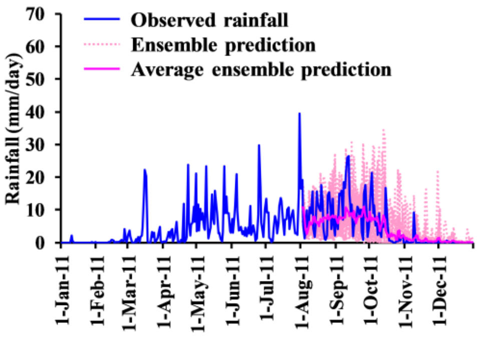

(c)

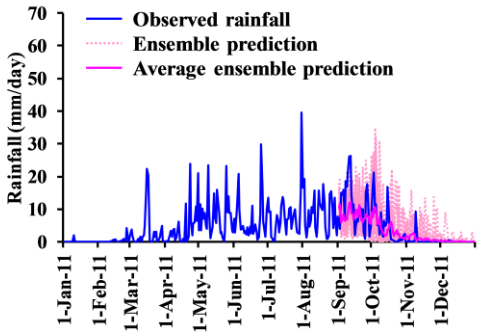

(d)

Figure C1 Comparison of daily rainfall data, showing observed rainfall (blue line), ensemble seasonal rainfall predictions (light pink dashed line), and average ensemble seasonal rainfall prediction (pink line). Rainfall predictions from (a) June until December 2011, (b) July until December 2011, (c) August until December 2011, and (d) September until December 2011.

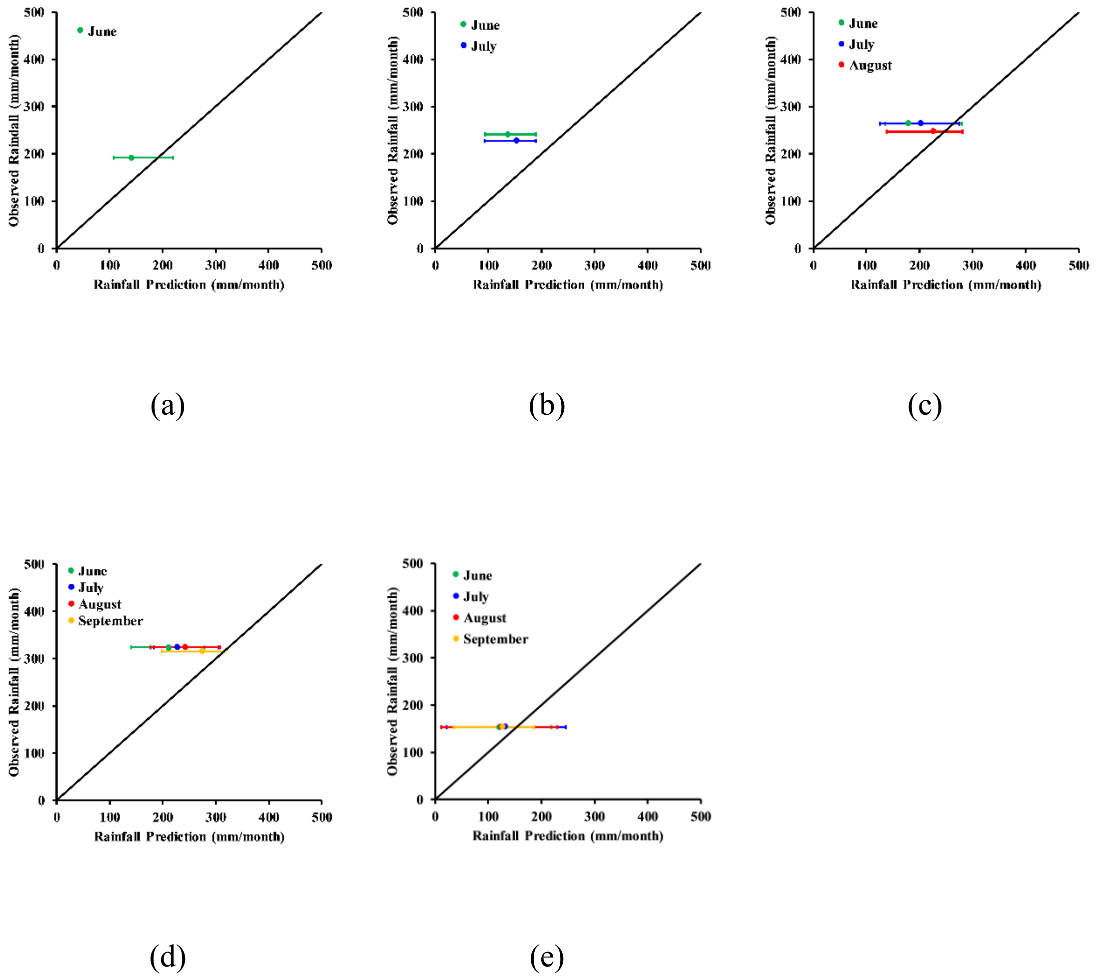

Figure C2 Scatter plot of monthly rainfall data, showing observed rainfall (y-axis) and average rainfall prediction (x-axis) with ensemble seasonal rainfall predictions (colored lines). Rainfall predictions for (a) June 2011, (b) July 2011, (c) August 2011, (d) September 2011, and (e) October 2011.

Appendix D

In this appendix D, the adaptive operation using past rainfall observation from 1981 to 2010 were used to support adaptive operation in 2011 (instead of ECMWF predictive data). The purpose of using 30-year past rainfall for adaptive operation in 2011 was to confirm whether predictive data in 2011 is good or the hydrological process of the Chao Phraya River Basin is slow, which we can input any rainfall data to simulate the 2011 flood event. In addition, the adaptive operation using ECMWF predictive data were used to support adaptive operation in 1995, which is the second most flood year. At the end of Appendix D, the river discharge with various adaptive reservoir operation were compared.

D1 Adaptive operation using past rainfall

The adaptive reservoir operation was begun from June. Figure D1.1 shows the reservoir storage prediction using past rainfall data and reservoir storage prediction after changing the operation in from June to December 2011. From Figure D1 (c), Sirikit reservoir was decreased the outflow rate because most of the prediction ensemble fell below the lower rule curve, which was same as July as shown in Figure D1.2 (c). The outflow rate was increased in August, which shown in Figure D1.3. Most of the reservoir storage ensemble (using past rainfall) fell above the upper rule curve in Sirikit reservoir in August. However, there was no change in reservoir operation in Bhumibol reservoir because most of the reservoir storage ensemble fell between the upper rule curve and lower rule curve as shown in Figure D1.3 (b). No adaptive operation was conducted in the Bhumibol and Sirikit reservoirs in the September, because most ensemble predictions for reservoir storage were within the range of the rule curves. The results of ensemble prediction without adaptive operation and with adaptive operation using predictive data are presented in Figure D1.4 (a), Figure D1.4 (b), and Figure D1.4 (c). Because no change in operation occurred in September, there was no difference in September.

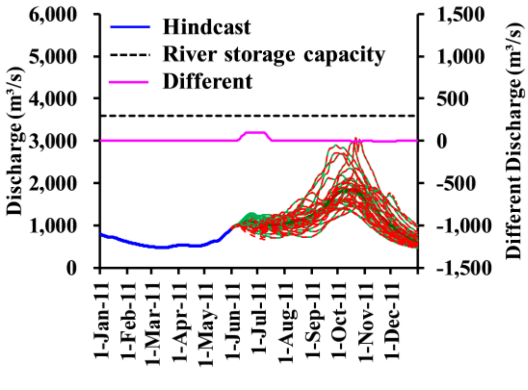

(a)

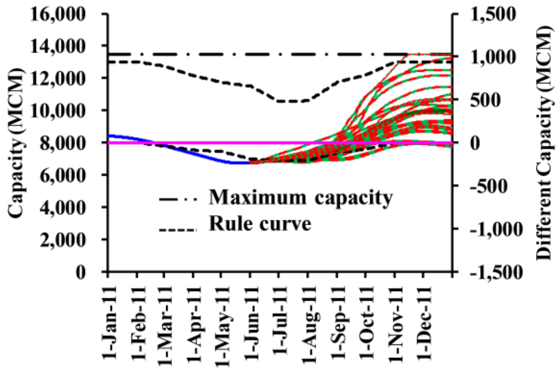

(b)

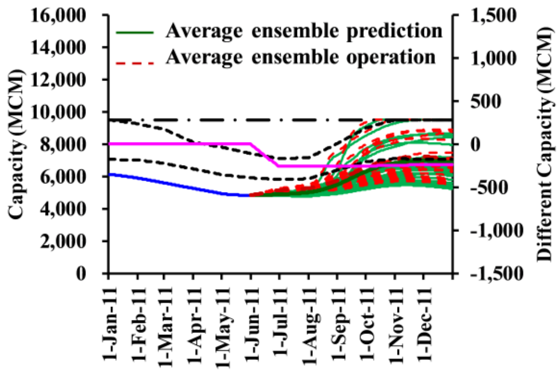

(c)

Figure D1 River discharge predictions at station C2 (a) and storage predictions from June until December at the Bhumibol (b) and Sirikit (c) reservoir, shown with the green line, and river discharge and storage prediction after adaptive operation with predictive data from June until December (red dashed line).

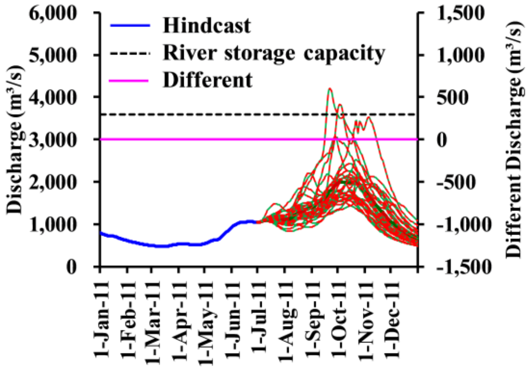

(a)

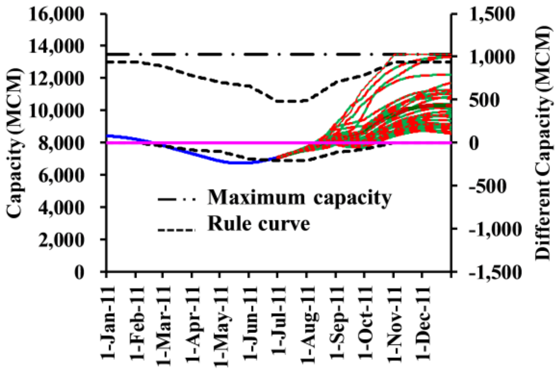

(b)

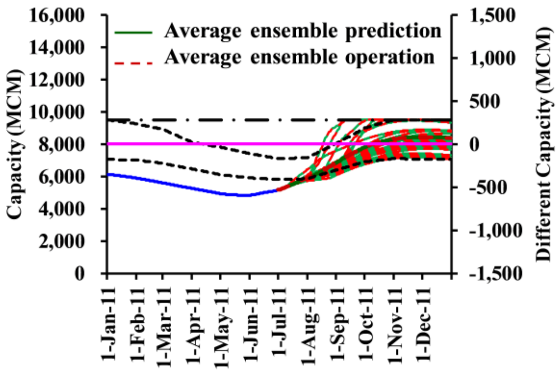

(c)

Figure D2 River discharge predictions at station C2 (a) and storage predictions from July until December at the Bhumibol (b) and Sirikit (c) reservoir, shown with the green line, and river discharge and storage prediction after adaptive operation with predictive data from July until December (red dashed line).

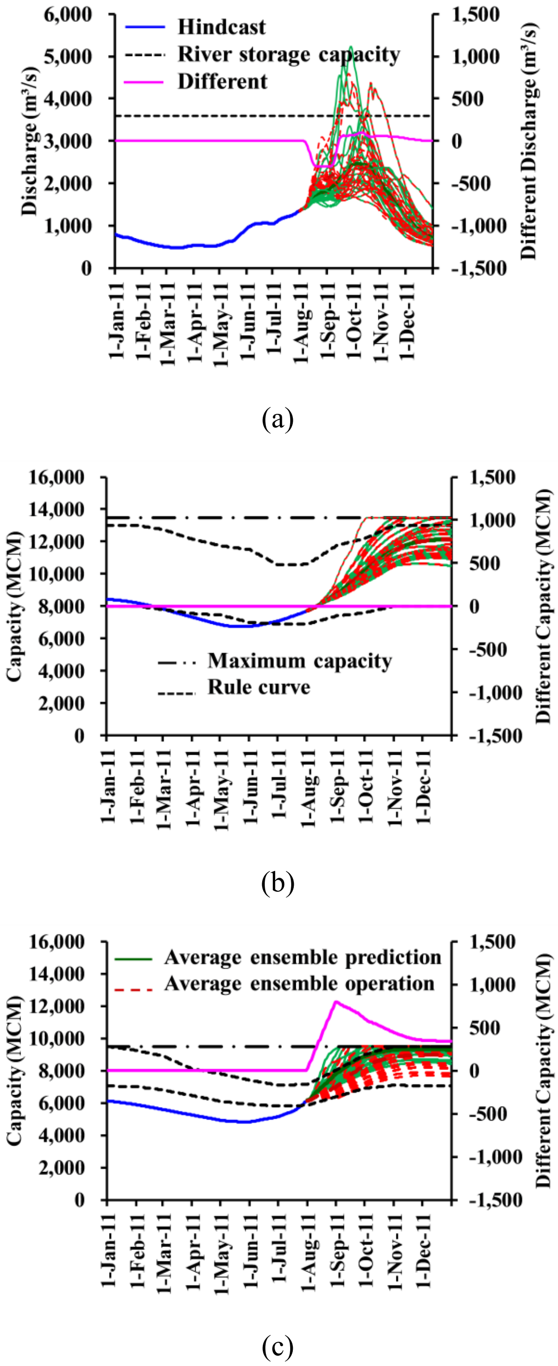

(a)

(b)

(c)

Figure D3 River discharge predictions at C2 station (a) and storage predictions from August until December at the Bhumibol (b) and Sirikit (c) reservoir, shown with the green line, and river discharge and storage predictions after adaptive operation with predictive data from August until December (red dashed line).

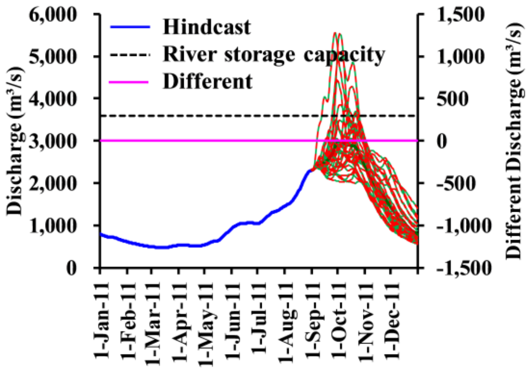

(a)

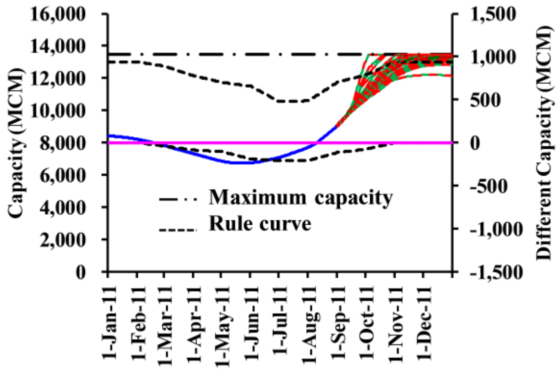

(b)

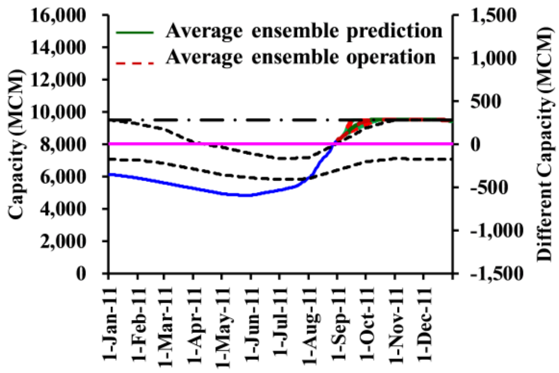

(c)

Figure D4 River discharge predictions at C2 station (a) and storage predictions from September until December at the Bhumibol (b) and Sirikit (c) reservoir, shown with the green line, and river discharge and storage predictions after adaptive operation with predictive data from September until December (red dashed line).

D2 Adaptive operation using predictive data in 1995

Reservoir storage predictions from June are shown in Figure D5. There was no change in reservoir operation occurred in June, because most reservoir storage predictions (more than 50% of the total ensemble predictions) fell between the rule curves of both the Bhumibol and Sirikit reservoirs. The tendency for the risk of reservoir storage to be above the maximum capacity is apparent. However, most ensemble predictions remained under the upper rule curve in both reservoirs. Therefore, no changes in the rate of outflow from either reservoir were made in June. Thus, no difference was observed between adaptive operation using predictive data and adaptive operation without predictive data, as shown in Figure D5.

Figure D6 shows the reservoir storage prediction using past rainfall data and reservoir storage prediction after changing the operation in from July to December 1995. The reservoir operation in 1995 was begun in July at Bhumibol reservoir. Most of the predictive storage fell above the upper rule curve as shown in Figure D6 (b). There was no operation change in Sirikit reservoir in July since most of the predictive data were fell between the upper and lower rule curve as shown in Figure D6 (c). However, the outflow rate was increased from both reservoirs in August and September. Figure D7 and Figure D8 show the reservoir storage prediction using past rainfall data and reservoir storage prediction after changing the operation in from August to December 1995 and September to December 1995, respectively. Unlike the 2011 case, the outflow rate can be increased in September because the river discharge at C2 station was still not reach the river storage capacity as shown in Figure D8 (a).

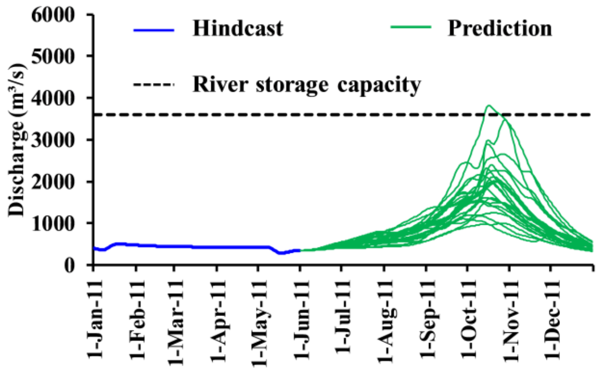

(a)

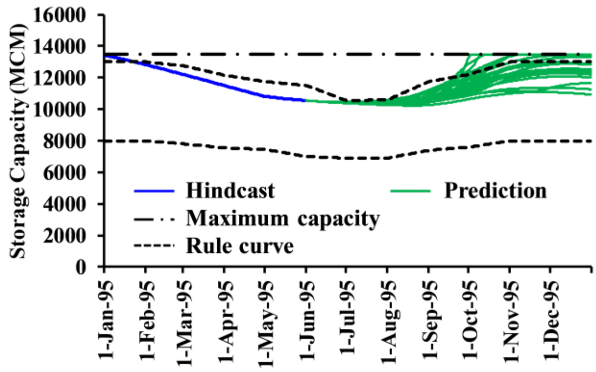

(b)

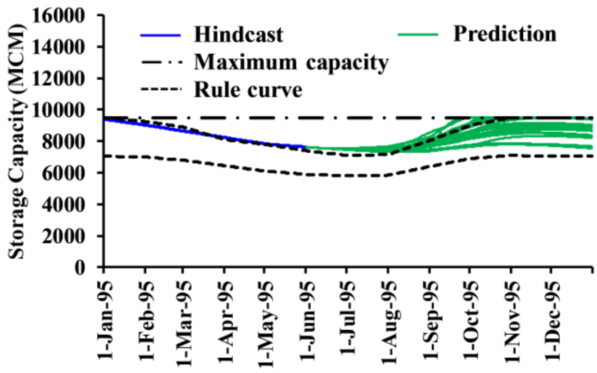

(c)

Figure D5 River discharge at station C2 (a) and reservoir storage predictions (green line) from June until December at the Bhumibol (b) and Sirikit (c) reservoir. Blue line represents simulation using observed meteorological data (hindcast). Black dashed line represents rule curve. Dash-point black line represents maximum storage capacity.

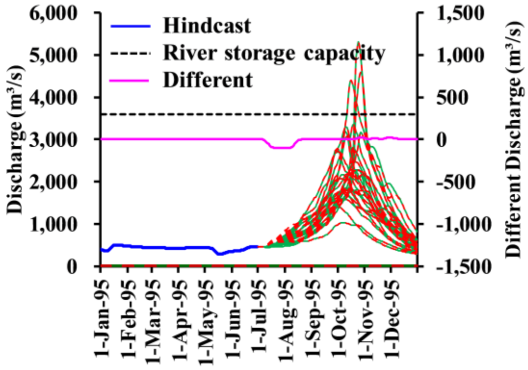

(a)

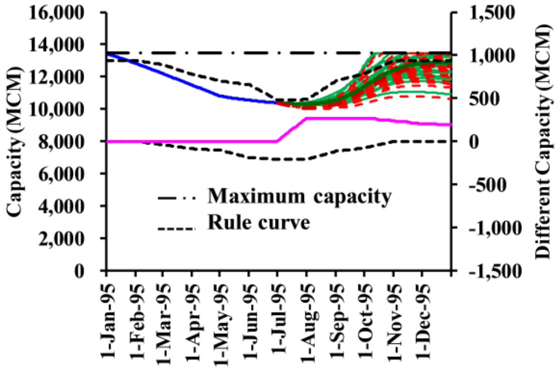

(b)

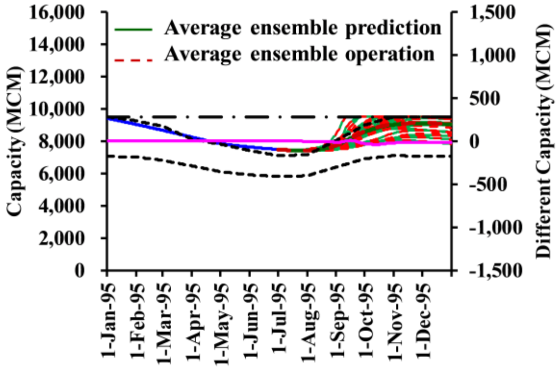

(c)

Figure D6 River discharge predictions at station C2 (a) and storage predictions from July until December at the Bhumibol (b) and Sirikit (c) reservoir, shown with the green line, and river discharge and storage prediction after adaptive operation with predictive data from July until December (red dashed line).

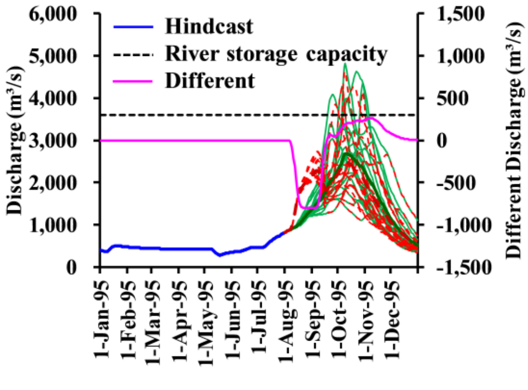

(a)

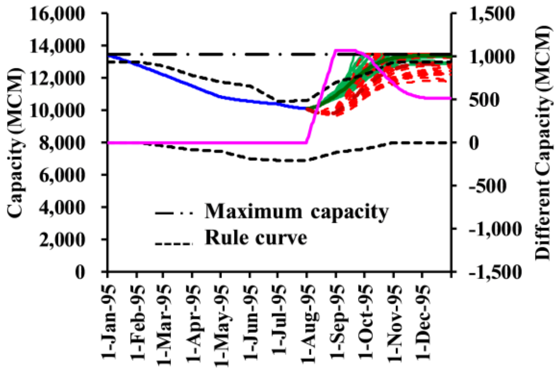

(b)

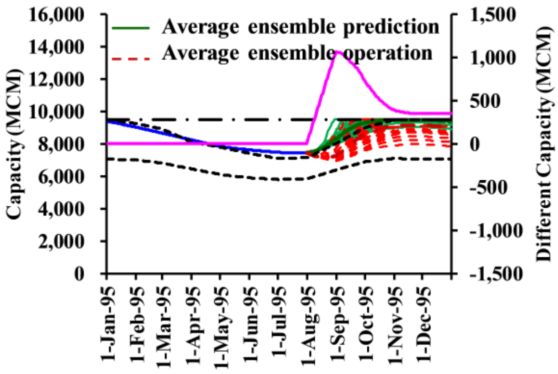

(c)

Figure D7 River discharge predictions at C2 station (a) and storage predictions from August until December at the Bhumibol (b) and Sirikit (c) reservoir, shown with the green line, and river discharge and storage predictions after adaptive operation with predictive data from August until December (red dashed line).

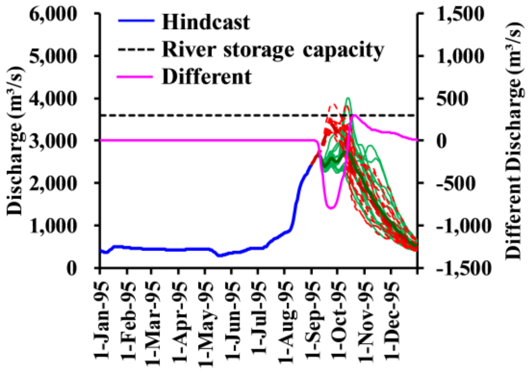

(a)

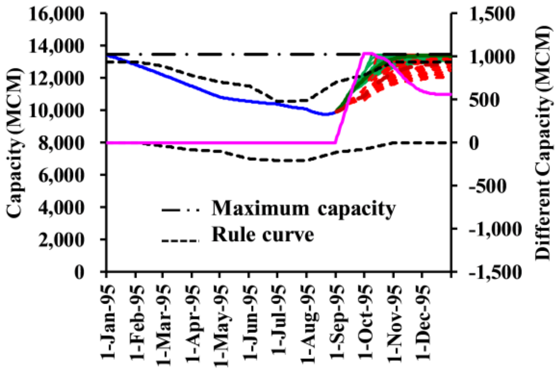

(b)

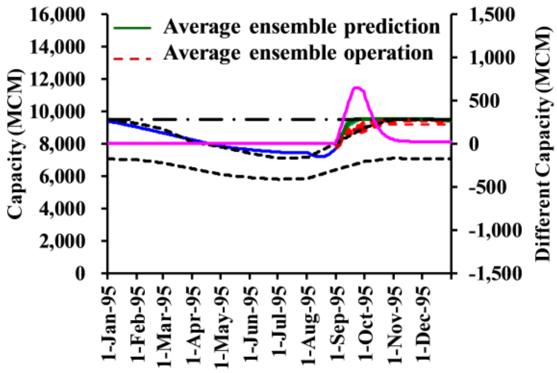

(c)

Figure D8 River discharge predictions at C2 station (a) and storage predictions from September until December at the Bhumibol (b) and Sirikit (c) reservoir, shown with the green line, and river discharge and storage predictions after adaptive operation with predictive data from September until December (red dashed line).

D3 Comparison of adaptive reservoir operation

D3.1 1995

The annual comparison of reservoir operation with and without the use of predictive data in 1995 is represented in Figure D3.1.1. Figure D3.1.2 shows the simulated outflow rate at Bhumibol and Sirikit reservoirs. Figure D3.1.3 compares simulated reservoir storage at Bhumibol and Sirikit reservoir in 1995. At last, the comparison of peak discharge at C2 in 1995 are compared in Figure D3.1.4.

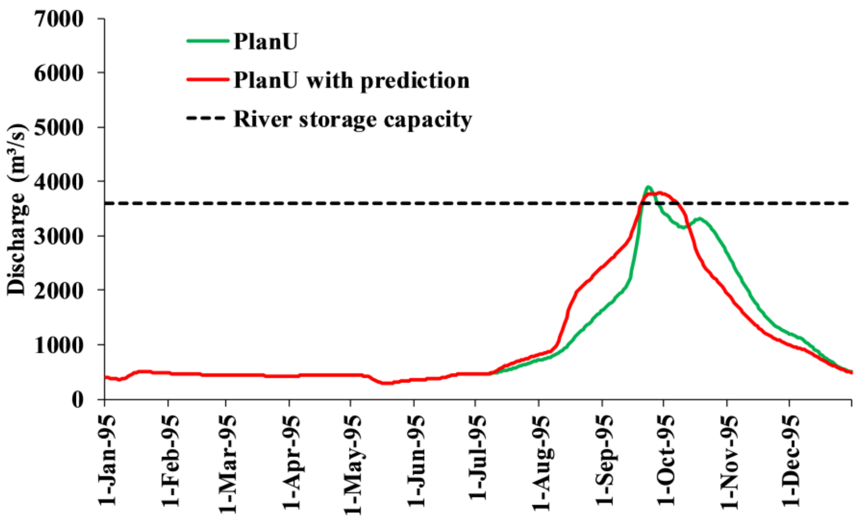

Figure D9 Comparison of river discharge, showing simulated discharge with PlanU operation in 1995 (green line), and simulated discharge after adaptive operation based on rule curve using seasonal predictive data (red line).

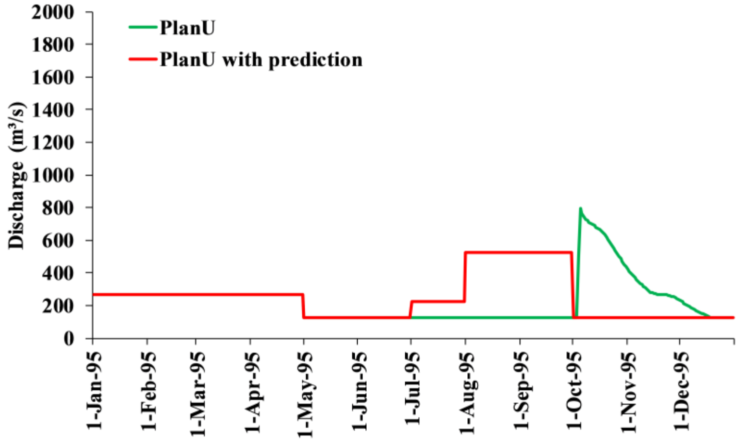

(a)

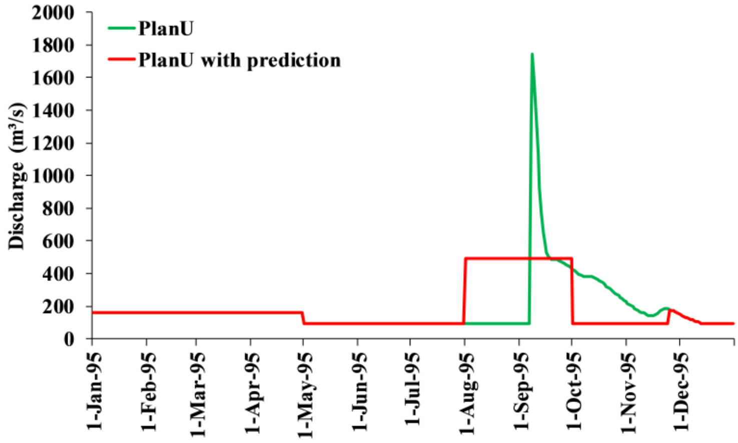

(b)

Figure D10 Comparison of outflow, showing simulated outflow using PlanU operation in 2011 (green line) and simulated discharge using PlanM operation in 2011 (blue line): (1) after adaptive operation using predictive data based on 2011 operations (red line) and (2) after adaptive operation using predictive data based on PlanM (yellow line).

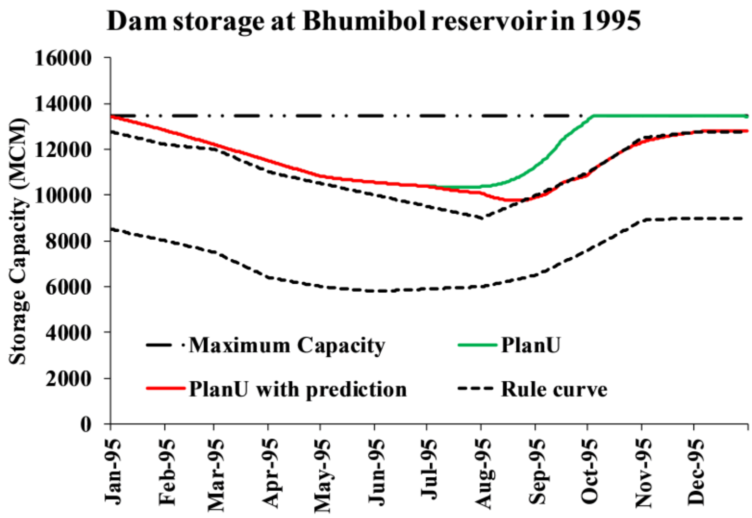

(a)

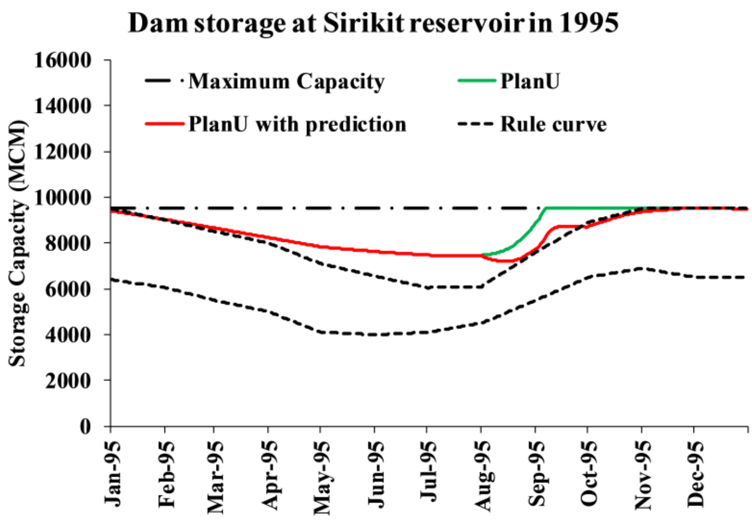

(b)

Figure D11 Comparison of outflow between simulated discharge using PlanU operation in 1995 (green line) and simulated discharge after adaptive operation using predictive data based on 1995 operations (red line).

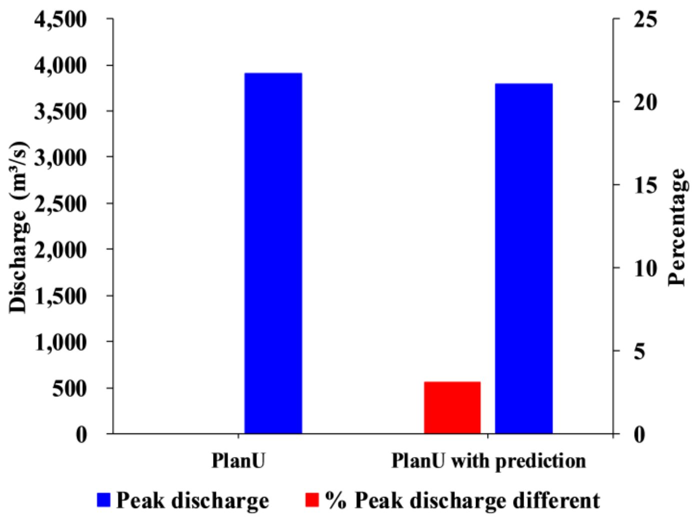

Figure D12 Comparison of peak discharge (blue bar color) and percentage of peak discharge different from simulation (red bar color) between peak simulated discharge using PlanU and simulated discharge after adaptive operation using predictive data.

D3.2 2011

In this Appendix D3.2, all of the adaptive operation in this study are compared. The annual comparison of reservoir operation with and without the use of predictive data in 2011 at station C2 is represented in Figure D3.2.1. In addition, the annual of reservoir operation with the use of past rainfall data is also presented in Figure D3.2.1. Figure D3.2.2 shows the simulated outflow rate at Bhumibol and Sirikit reservoirs. Figure D3.2.3 compares simulated reservoir storage at Bhumibol and Sirikit reservoir in 2011. The annual comparison of river discharge with adaptive reservoir operation at station P12C and N8 are presented in Figure D3.2.4 (a) and Figure D3.2.4 (b).

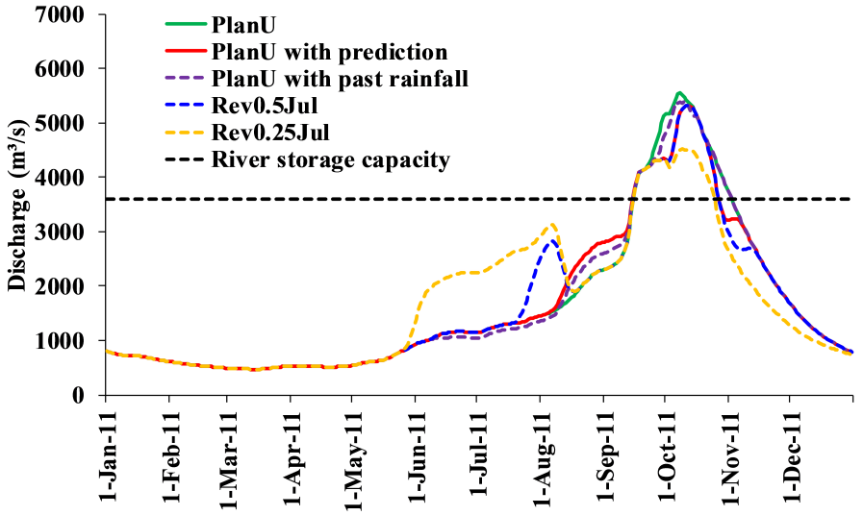

Figure D13 Comparison of river discharge, showing simulated discharge with PlanU operation in 2011 (green line), after adaptive operation based on 2011 operations using seasonal predictive data (red line) and past rainfall data (purple dash line), with Rev0.5Jul (blue dash line), and with Rev0.25Jul (yellow dash line).

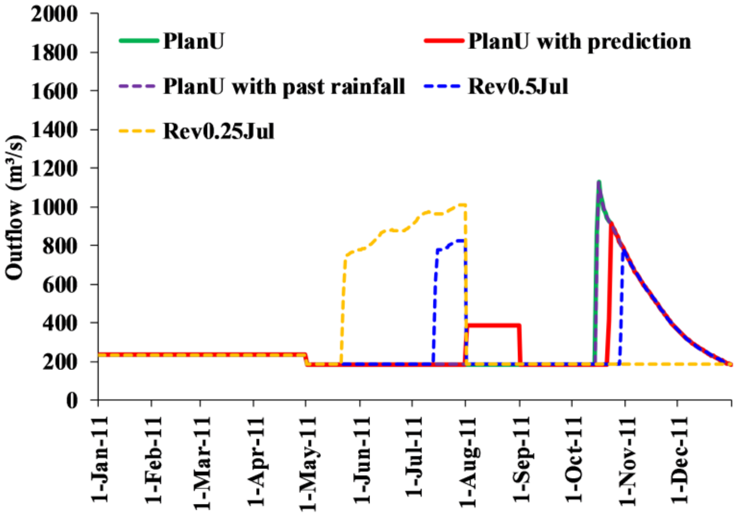

(a)

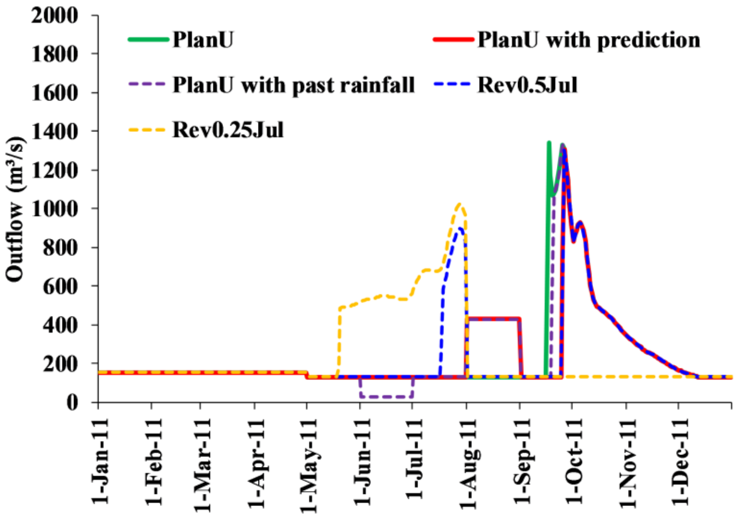

(b)

Figure D14 Comparison of outflow, showing simulated outflow using PlanU operation in 2011 (green line), after adaptive operation based on 2011 operations using seasonal predictive data (red line), and past rainfall data (purple dash line), with Rev0.5Jul (blue dash line), and with Rev0.25Jul (yellow dash line).

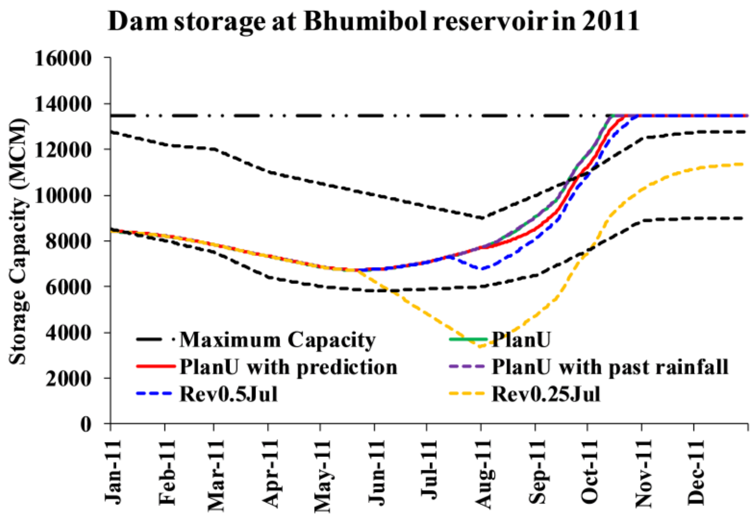

(a)

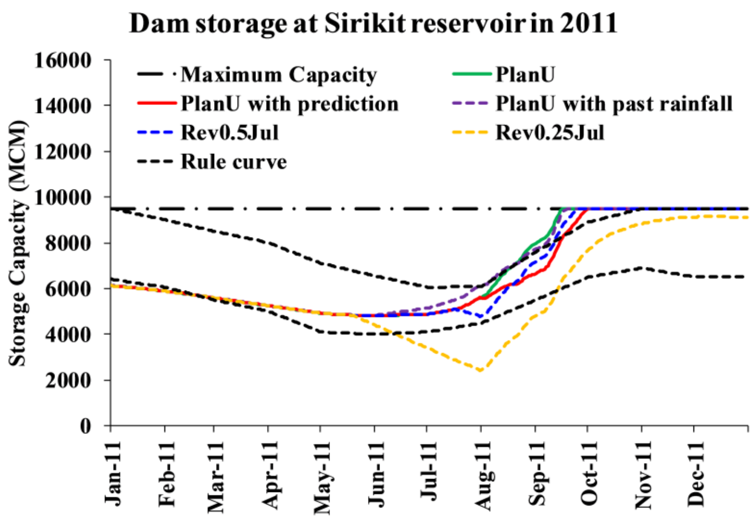

(b)

Figure D15 Comparison of dam storage between simulated discharge using PlanU operation in 2011 (green line) and simulated discharge after adaptive operation using predictive data based on 2011 operations (red line), and past rainfall data (purple dash line), with Rev0.5Jul (blue dash line), and with Rev0.25Jul (yellow dash line).

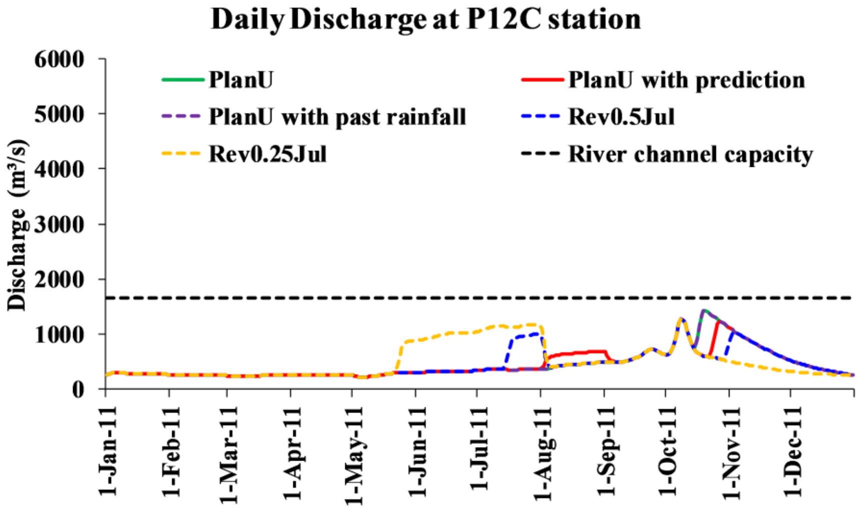

(a)

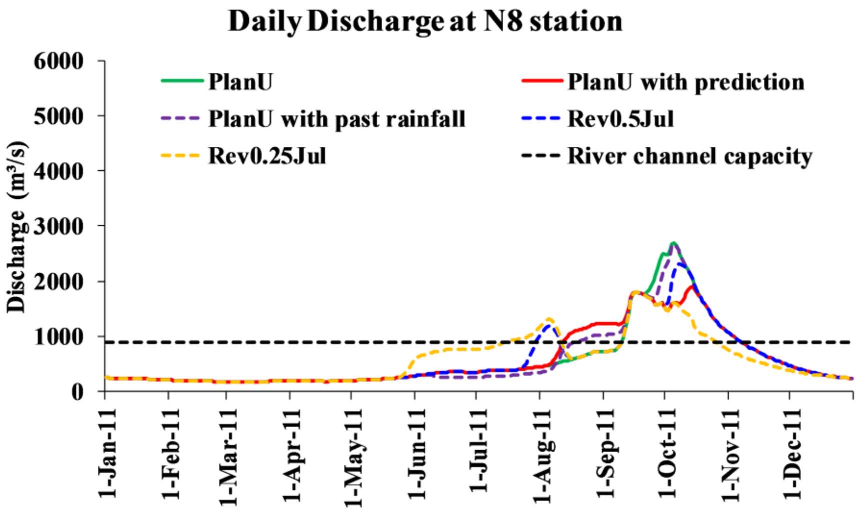

(b)

Figure D16 Comparison of river discharge, showing simulated discharge at station P12C (a) and N8 (b) with PlanU operation in 2011 (green line), after adaptive operation based on 2011 operations using seasonal predictive data (red line) and past rainfall data (purple dash line), with Rev0.5Jul (blue dash line), and with Rev0.25Jul (yellow dash line).

Reference

Alemu, E. T.; Palmer, R. N.; Polebitski, A.; Meaker, B. Decision Support System for Optimizing Reservoir Operations Using Ensemble Streamflow Predictions. Journal of Water Resources Planning and Management, 2011, 137(1), 72-82.

Anghileri, D.; Voisin, N.; Castelletti, A.; Pianosi, F.; Nijssen, B.; Lettenmaier, D. P. Value of long-term streamflow forecasts to reservoir operations for water supply in snow-dominated river catchments. Water Resources Research, 2016, 52(6), 4209-4225.

Berhane, G.; Gebreyohannes, T., Martens, K., & Walraevens, K. Overview of micro-dam reservoirs (MDR) in Tigray (northern Ethiopia): Challenges and benefits. Journal of African Earth Sciences, 2016, 123, 210–222.

Cannon, A. J.; Sobie, S. R.; Murdock, T. Q. Bias Correction of GCM Precipitation by Quantile Mapping: How Well Do Methods Preserve Changes in Quantiles and Extremes? Journal of Climate, 2015, 28(17), 6938–6959.

Crochemore, L.; Ramos, M.-H.; Pappenberger, F. Bias correcting precipitation forecasts to improve the skill of seasonal streamflow forecasts. Hydrology and Earth System Sciences, 2016, 20(9), 3601–3618.

Ehsani, N.; Vörösmarty, C. J.; Fekete, B. M.; Stakhiv, E. Z. Reservoir operations under climate change: Storage capacity options to mitigate risk. Journal of Hydrology, 2017, 555, 435–446.

Ehteram, M.; Mousavi, S.-F.; Karami, H.; Farzin, S.; Emami, M.; Othman, F. B.; Zahra, A.; Ozgur, K.; El-Shafie, A. Fast convergence optimization model for single and multi-purposes reservoirs using hybrid algorithm. Advanced Engineering Informatics, 2017, 32, 287–298.

Emergency Events Database (EMDAT). Available online: https://ourworldindata.org/grapher/natural-disasters-by-type (accessed on 11

November 2020).

Fadul, E.; Masih, I.; Fraiture, C. D. Adaptation strategies to cope with low, high and untimely floods: Lessons from the Gash spate irrigation system, Sudan. Agricultural Water Management, 2019, 217, 212–225.

Fang, G. H.; Yang, J.; Chen, Y. N.; Zammit, C. Comparing bias correction methods in downscaling meteorological variables for a hydrologic impact study in an arid area in China. Hydrology and Earth System Sciences, 2015, 19(6), 2547–2559.

Field, C.B.; Barros, V.; Stocker, T.F.; Qin, D.; Dokken, D.J.; Ebi, K.L.; Mastrandrea, M.D.; Mach, K.J.; Plattner, G.-K.; Allen, S.K.; Tignor, M.; Midgley, P.M. IPCC. Managing the Risks of Extreme Events and Disasters to Advance Climate Change Adaptation. A Special Report of Working Groups I and II of the Intergovernmental Panel on Climate Change. Cambridge University Press, Cambridge, United Kingdom and New York, NY, USA, 2012, 582 pp.

Gale, E. L.; Saunders, M. A. The 2011 Thailand flood: climate causes and return periods. Weather, 68(9), 2013, 233–237.

Hanasaki, N., Mateo, C., Saito., Y. : H08 Manual User's Edition Supplement 1: Regional Application -Case Study of the Chao Phraya River, 43 pp, National Institute for Envi-ronmental Studies, Tsukuba, Japan., 2012.

Hanasaki, N.; Kanae, S.; Oki, T.; Masuda, K.; Motoya, K.; Shirakawa, N.; Shen, Y.; Tanaka, K. An integrated model for the assessment of global water resources – Part 1: Model description and input meteorological forcing. Hydrology and Earth System Sciences, 2008, 12(4), 1007–1025.

Harrigan, S.; Prudhomme, C.; Parry, S.; Smith, K.; Tanguy, M. Benchmarking Ensemble Streamflow Prediction Skill in the UK. Hydrology and Earth System Sciences, 2018, 22(3), 2023–39.

Johnson, S. J.; Stockdale, T. N.; Ferranti, L.; Balmaseda, M. A.; Molteni, F.; Magnusson, L.; Tietsche, S.; Decremer, D.; Weisheimer, A.; Balsamo, G.; Keeley, S. P. E.; Mogensen, K.; Zuo, H.; Monge-Sanz, B. M. SEAS5: the new ECMWF seasonal forecast system. Geoscientific Model Development, 2019, 12(3), 1087–1117.

Kangrang, A.; Prasanchum, H.; Hormwichian, R. Development of Future Rule Curves for Multipurpose Reservoir Operation Using Conditional Genetic and Tabu Search Algorithms. Advances in Civil Engineering, 2018, 1–10.

Komori, D.; Nakamura, S.; Kiguchi, M.; Nishijima, A.; Yamazaki, D.; Suzuki, S.; Kawasaki, A.; Oki, K.; Oki, T. Characteristics of the 2011 Chao Phraya River flood in Central Thailand. Hydrological Research Letters, 2012, 6, 41–46.

Kotsuki, S.; Tanaka, K.; Kojiri, T.; Hamaguchi, T. The water budget analysis with land surface model in Chao Phraya River basin, 23rd annual conference, JSHWR, 2010, pp. 44-45

Li, Y.; Jiang, Y.; Lei, X.; Tian, F.; Duan, H.; Lu, H. Comparison of Precipitation and Streamflow Correcting for Ensemble Streamflow Forecasts. Water, 2018, 10(2), 177.

Ligaray, M., Kim, H., Sthiannopkao, S., Lee, S., Cho KH., Kim, JH.: Assessment on Hydrologic Response by Climate Change in the Chao Phraya River Basin, Thailand. Water. Vol. 7, No.12, pp. 6892-6909, 2015.

Liu, H.; Deng, B.; Liu, Y.; Jiang, C.; Wu, Z.; Long, Y. Preliminary Numerical Analysis of the Efficiency of a Central Lake Reservoir in Enhancing the Flood and Drought Resistance of Dongting Lake. Water, 2018, 10(2), 225.

Long, Y.; Wang, H.; Jiang, C.; Ling, S. Seasonal Inflow Forecasts Using Gridded Precipitation and Soil Moisture Information: Implications for Reservoir Operation. Water Resources Management, 2019, 33(11), 3743–3757.

Lucatero, D.; Madsen, H.; Refsgaard, J. C.; Kidmose, J.; Jensen, K. H. Seasonal streamflow forecasts in the Ahlergaarde catchment, Denmark: the effect of preprocessing and post-processing on skill and statistical consistency. Hydrology and Earth System Sciences, 2018, 22(7), 3601–3617.

Manabe, S. Climate And The Ocean Circulation1. Monthly Weather Review, 1969, 97(11), 739–774.

Marcinkowski, P., and Grygoruk, M.: Long-Term Down-stream Effects of a Dam on a Lowland River Flow Regime: Case Study of the Upper Narew, Water, Vol. 9, No.10, pp. 783. doi:10.3390/w9100783, 2017.

Mateo, C. M., Hydrological modelling with reservoir operation in the Chao Phraya River Basin for flood mitigation. Master's thesis documentation, 2012.

Mateo, C. M.; Hanasaki, N.; Komori, D.; Tanaka, K.; Kiguchi, M.; Champathong, A.; Sukhapunnaphan, T.; Yamazaki, D.; Oki, T. Assessing the impacts of reservoir operation to floodplain inundation by combining hydrological, reservoir management, and hydrodynamic models. Water Resources Research, 2014, 50(9), 7245–7266.

Mercer, J.; Kelman, I.; Taranis, L.; Suchet-Pearson, S. Framework for integrating indigenous and scientific knowledge for disaster risk reduction. Disasters, 2009, 34(1), 214–239.

Office of Natural Water Resources Committee (ONWRC) of Thailand Working Group, Chao Phraya River Basin, Thailand, in: World Water Development Report – 2003 , Bangkok, Thailand, 2003, part V, chap. 16, pp. 387– 400.

Oki, T.; Sud, Y. C. Design of Total Runoff Integrating Pathways (TRIP)—A Global River Channel Network. Earth Interactions, 1998, 2(1), 1–1.

Pinthong, P.; Das Gupta, A.; Babel, M. S.; Weesakul, S. Improved reservoir operation using hybrid genetic algorithm and neurofuzzy computing, Water Resour. Manage., 2009. 23(4), 697– 720.

Prasanchum, H.; Kangrang, A. Optimal reservoir rule curves under climatic and land use changes for Lampao Dam using Genetic Algorithm. KSCE Journal of Civil Engineering, 22(1), 2017, 351–364.

Rakwatin, P., Sansena, T., Marjang, N., and Rungsipanich, A.: Using multi-temporal remote-sensing data to estimate 2011 flood area and volume over Chao Phraya River basin, Thailand, Remote Sensing Letters, Vol. 4, No. 3, pp.243-250, DOI: 10.1080/2150704X.2012.723833, 2013.

Robock, A.; Vinnikov, K. Y.; Schlosser, C. A.; Speranskaya, N. A.; Xue, Y. Use of Midlatitude Soil Moisture and Meteorological Observations to Validate Soil Moisture Simulations with Biosphere and Bucket Models. Journal of Climate, 1995, 8(1), 15–35.

Schaake, J. C.; Hamill, T. M.; Buizza, R.; Clark, M. HEPEX: The Hydrological Ensemble Prediction Experiment. Bulletin of the American Meteorological Society, 2007, 88(10), 1541–1548.

Schaake, J. C.; Hamill, T. M.; Buizza, R.; Clark, M. HEPEX: The Hydrological Ensemble Prediction Experiment. Bulletin of the American Meteorological Society, 2007, 88(10), 1541–1548.

Stephanie, J., Ferranti, L, Magdalena, B., Molteni, F., Li-nus, M., Tietsche, S., Decremer, D., Weisheimer, A., Bal-samo, G., Keeley, S., Mogensen, K., Zuo, H., Monge-Sanz, B.: SEAS5: the new ECMWF seasonal forecast system, Geosci. Model Dev., Vol. 12, pp. 1087-1117, 2019.

Suiadee, W.; Tingsanchali, T. A combined simulation - genetic algorithm optimization for optimal rule curves of a reservoir: A case study of the Nam Oon Irrigation Project, Thailand, Hydrol. Processes, 2007, 21(23), 3211- 3225.

Tasseff, B.; Bent, R.; Van Hentenryck, P. Optimization of structural flood mitigation strategies. Water Resources Research, 2019, 55, 1490– 1509.

Tebakari, T., Yoshitani, J., and Suvanpimol, P. : Impact of large-scale reservoir operation on flow regime in the Chao Phraya River basin, Thailand. Hydrological Processes, Vol. 26, No.16, pp. 2411-2420. doi:10.1002/hyp.9345, 2012.

Thaiwater. Available online: https://www.thaiwater.net/web/attachments/25basins/10-chaopraya.pdf (accessed on 3 October 2020).

Themeßl, M. J.; Gobiet, A.; Heinrich, G. Empirical-statistical downscaling and error correction of regional climate models and its impact on the climate change signal. Climatic Change, 2011, 112(2), 449–468.

Viel, C.; Beaulant, A.-L.; Soubeyroux, J.-M.; Céron, J.-P. How seasonal forecast could help a decision maker: an example of climate service for water resource management. Advances in Science and Research, 2016, 13, 51–55.

Voisin, N.; Hamlet, A. F.; Graham, L. P.; Pierce, D. W.; Barnett, T. P.; Lettenmaier, D. P. The Role of Climate Forecasts in Western U.S. Power Planning. Journal of Applied Meteorology and Climatology, 2006, 45(5), 653-673.

Wichakul, S.; Tachikawa, Y.; Shiiba, M.; Yorozu, K. Developing a regional distributed hydrological model for water resources assessment and its application to the Chao Phraya River Basin, J. Jpn. Soc. Civ. Eng., 2013a, 69(4), I_43– I_48.

Wichakul, S.; Tachikawa, Y.; Shiiba, M.; Yorozu, K. Development of a flow routing model including inundation effect for the extreme flood in the Chao Phraya River Basin, Thailand 2011, J. of Disaster Res., 2013b, 8(3), 415– 423.

World bank. Available online: https://www.economist.com/economic-and-financial-indicators/2013/10/11/natural-disasters (accessed on 11 November 2020).

Yoshimura, K.; Sakimura, T.; Oki, T.; Kanae, S.; Seto, S. Toward flood risk prediction: a statistical approach using a 29-year river discharge simulation over Japan. Hydrological Research Letters, 2008, 2, 22–26.